Oligonucleotide Analogues with Integrated Bases and Backbone

Part 13[1])

Synthesis and Association of Ethynylene-Linked Self-Complementary Dimers

by **Xiaomin Zhang**, **Bruno Bernet**, and **Andrea Vasella***

Laboratorium für Organische Chemie, ETH Zürich, Wolfgang Pauli-Strasse 10, CH-8093 Zürich
(e-mail: vasella@org.chem.ethz.ch)

The self-complementary UA and AU dinucleotide analogues **41**–**45**, **47**, **48**, and **51**–**60** were prepared by *Sonogashira* coupling of 6-iodouridines with *C(5′)*-ethynylated adenosines and of 8-iodoadenosines with *C(5′)*-ethynylated uridines. The dinucleotide analogues associate in $CDCl_3$ solution. The *C(6/I)*-unsubstituted AU dimers **51** and **54** prefer an *anti*-oriented uracilyl group and form stretched linear duplexes. The UA propargyl alcohols **41** and **43**–**45** possess a persistent intramolecular O(5′/I)–H···N(3/I) H-bond and, thus, a *syn*-oriented adeninyl and a *gt*- or *tg*-oriented ethynyl moiety; they form corrugated linear duplexes. All other dimers form cyclic duplexes characterized by *syn*-oriented nucleobases. The preferred orientation of the ethynyl moiety (the C(4′),C(5′) torsion angle) defines a conformation between *gg* and one where the ethynyl group eclipses O(4′/I). The UA dimers **42**, **47**, and **48** form *Watson–Crick* H-bonds, the AU dimers **56** and **58**–**60** H-bonds of the *Watson–Crick*-type, the AU dimers **53** and **55** reverse-*Hoogsteen*, and **57** *Hoogsteen* H-bonds. The pairing mode depends on the substituent of C(5′/I) (H, OSi^iPr_3; OH) and on the H-bonds of HO–C(5′/I) in the AU dimers. Association constants were derived from the concentration-dependent chemical shift for HN(3) of the uracilyl moiety; they vary from 45–104 M^{-1} for linear duplexes to 197–2307 M^{-1} for cyclic duplexes. The thermodynamic parameters were determined by *van't Hoff* analysis of the temperature-dependence of the (concentration-dependent) chemical shift for HN(3) of the uracilyl moiety. Neglecting stacking energies, one finds an average energy of 3.5–4.0 kcal/mol per intermolecular H-bond. Base stacking is evidenced by the temperature-dependent CD spectra. The crystal structure of **54** shows two antiparallel chains of dimers connected by *Watson-Crick* H-bonds. The chains are bridged by a strong H-bond between the propargylic OH and O=C(4) and by weak reverse A·A *Hoogsteen* H-bonds.

1. Introduction. – Oligoribonucleoside analogues that integrate nucleobases and backbone[2]) differ from all known oligonucleotide analogues by their architecture, and were designed to explore the extent to which such a fundamental structural change is compatible with sequence-selective pairing, base stacking, and the formation of secondary structural elements. Among the first analogues to be synthesised are the ethynylene-linked dimers and oligomers of type **I** [1–5] (*Fig. 1*). Ethynylene-linked adenosine dimers AA of type **I** (X = OH) adopt almost exclusively the *syn*-conformation of the nucleobases, as favoured by the substituent at C(8) and a persistent intramolecular

[1]) Part 12: [1].

[2]) We suggest the shorthand designation 'ONIB' for 'OligoNucleosides with Integrated Bases and backbone'.

H-bond from the propargylic HO–C(5′) to N(3) of the same nucleoside unit [6] (see also [7]). The design of these analogues, however, implied that the *anti* conformers pair. This suggested, on the one hand, to design oligonucleotide analogues that pair with their bases in a *syn* conformation, and, on the other hand, to remove the propargylic OH group. Ether-linked, 2′,3′-*O*-isopropylidene-protected dimers of type **II** [8] (X = O), designed to pair with the bases in a *syn*-conformation, indeed associate in $CHCl_3$ solution [9]. The synthesis of partially protected, self-complementary, ethynylene-linked dinucleotide analogues of type **I**, their triisopropylsilyl ethers, C(5′)-epimers, and C(5′)-deoxy analogues, and the extent and nature of their association should allow us to evaluate the role of the intramolecular C(5′)–OH···N(3) H-bond in controlling the *syn* conformation, the dependence of the H-bond on the configuration of the propargylic centre, and the requirement of an *anti* conformation for the pairing of such dimers.

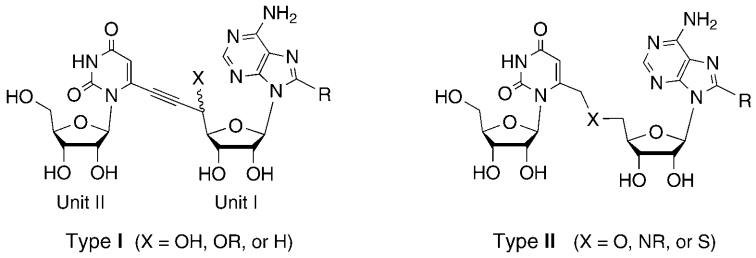

Fig. 1. *Types* **I** *and* **II** *for the connection between the nucleobase and C(5′) of the adjacent unit* (illustrated for UA dimers)

We thus aimed at the synthesis of the (2′,3′-*O*-isopropylidenated) dinucleotide analogues U*[c_y]A$^{(*)}$ and A*[c_y]U$^{(*)}$[3]) shown in *Schemes 3* and *4* to study the sequence selectivity of pairing, and the effect of the configuration of C(5′/I)OR and of its deoxygenation.

2. Results and Discussion. – 2.1. *Synthesis of the U$^{(*)}$ and A$^{(*)}$ Monomeric Building Blocks.* The synthesis of the desired dinucleotide analogues requires the 6-iodouridine **38**, the 8-iodoadenosines **24**–**26**, the adenosine derived alkynes **28**, **34**, **35**, **37**, **39**, **40**, and **46**, and the uridine derived alkynes **2**, **6**, **8**, **10**, **18**, **49**, and **50** (*cf. Schemes 3* and *4*).

C-Desilylation of the propargyl alcohol **1** [2] gave **2** that was transformed to the triisopropylsilyl ether **3** (88% from **1**; *Scheme 1*). *Barton–McCombie* deoxygenation [10] of the D-*allo*-configured propargylic alcohol **4** [2] led in 81% to the 5′-deoxy derivative **5**. It was desilylated by treatment with $Bu_4NF \cdot 3\ H_2O$ in THF to yield 96% of the alkyne **6**. The alcohol **4** was hydroxymethylated at C(6) by formylation followed by reduction

[3]) *Conventions for abbreviated notation:* The substitution at C(6) of pyrimidines and C(8) of purines is denoted by an asterisk (*); for example U* and A* for hydroxymethylated uridine and adenosine derivatives, respectively. The moiety linking C(6)CH_2 or C(8)CH_2 and C(5′) of the previous unit is indicated in square brackets, such as [c] for a carbon atom. The indices y, e, and a indicate a triple, double, or single bond, respectively.

[9] to provide the diol **7** (60%). Similarly, **1** was transformed in a yield of 54% into the epimeric diol **9**, and both **7** and **9** were *C*-desilylated with $Bu_4NF \cdot 3\ H_2O$, and then selectively *O*-silylated with ^{t}BuPh$_2$SiCl to afford the propargyl alcohols **8** (81%) and **10** (85%), respectively.

To obtain the *C(5′)*-deoxygenated and *C(6)*-silyloxymethylated uridine derivative **18**, we explored the inverse sequence of transformations that were used to prepare **7**–**9**, *i.e.*, hydroxymethylation followed by oxidation and ethynylation, starting with 2′,3′-*O*-isopropylideneuridine (**11** [11]; *Scheme 1*)[4]). Silylation of **11** to **12**, followed by formylation and reduction, gave **13** (76% from **11**). Silylation with ^{t}BuPh$_2$SiCl (→ **14**), followed by selective removal of the ^{t}BuMe$_2$Si group with H_2SiF_6 in MeCN/^{t}BuOH/H_2O at 0° [12] yielded 99% of the alcohol **15**. It was oxidized according to *Pfitzner–Moffatt* [13], and the resulting aldehyde was directly treated with (triethylsilyl)ethynylmagnesium bromide in THF at −15° to yield 51% of a 1:1 mixture of the epimeric propargylic alcohols **16**. The isomers proved difficult to separate[5]). An attempted diastereoselective alkynylation with (trimethylsilyl)acetylene in the presence of $Zn(OTf)_2$, (+)-*N*-methylephedrine, and Et_3N in toluene [14] for 3 h at 80° led only to recovered starting material, while heating to 90° for 12 h resulted in a complex mixture. The deoxygenated monomer **17** was thus prepared from the epimeric mixture **16**, similarly as described for the synthesis of **5**. The selective *C*-desilylation of the monomer **17** failed. It proved resistant to H_2SiF_6 in MeCN/^{t}BuOH/H_2O, while desilylation with $Bu_4NF \cdot 3\ H_2O$ in THF at −18° removed only the *O*-Si^{t}BuPh$_2$ group. The desired terminal alkyne **18** was thus prepared by complete desilylation of **17** with $Bu_4NF \cdot 3\ H_2O$ at 25° followed by *O*-silylation to yield 88% of **18**.

The A$^{(*)}$ monomeric building blocks were obtained from N^6-benzoyl-2′,3′-*O*-isopropylideneadenosine (**19** [15]; *Scheme 2*). The (*tert*-butyl)diphenylsilyl ether **20** (87%) and the (*tert*-butyl)dimethylsilyl ether **22** (88%) were prepared similarly to the known triisopropylsilyl ether **21** [9]. Iodination [7] of **20** followed by debenzoylation provided the 8-iodoadenosine **25** (77%), and iodination of **21** gave **26** (76%), while debenzoylation of the 8-iodoadenosine **23** [7] gave the iodo alcohol **24**. Debenzoylation and desilylation of the alkyne **27** [7] provided the propargyl alcohol **28** (72%). Hydroxymethylation of the silyl ether **22** yielded 83% of **29** that was protected as the (*tert*-butyl)diphenylsilyl ether **30**. Selective removal of the C(5′)-*O*Si^{t}BuMe$_2$ group with H_2SiF_6 in MeCN/^{t}BuOH/H_2O led to **31** (79% besides 16% of starting material), and *Pfitzner–Moffatt* oxidation of **31** gave the corresponding aldehyde. The crude aldehyde reacted with (trimethylsilyl)ethynylmagnesium bromide to provide the epimeric propargylic alcohols **32** (42%) and **33** (21%). *C*-Desilylation of **32** (K_2CO_3 in MeOH at 0°) and *N*-debenzoylation ($MeNH_2$ in THF/EtOH) yielded 72% of the monosilylated propargylic alcohol **34**, while the same conditions led to complete desilylation of the epimeric alcohol **33**. The desired product **35** was obtained in 80% by desilylating **33** at −20°, followed by debenzoylation. *Barton–McCombie* deoxygenation of a 2:1

---

[4]) The inverse sequence has the advantage that the mixture of diasteroisomers is obtained in a later step, without necessarily facilitating their separation.

[5]) A combination of different protecting groups, including the *C*-SiMe$_3$ and *C*-SiEt$_3$ groups, and a combination of them with several *O*-silyl groups did not facilitate separation.

Scheme 1

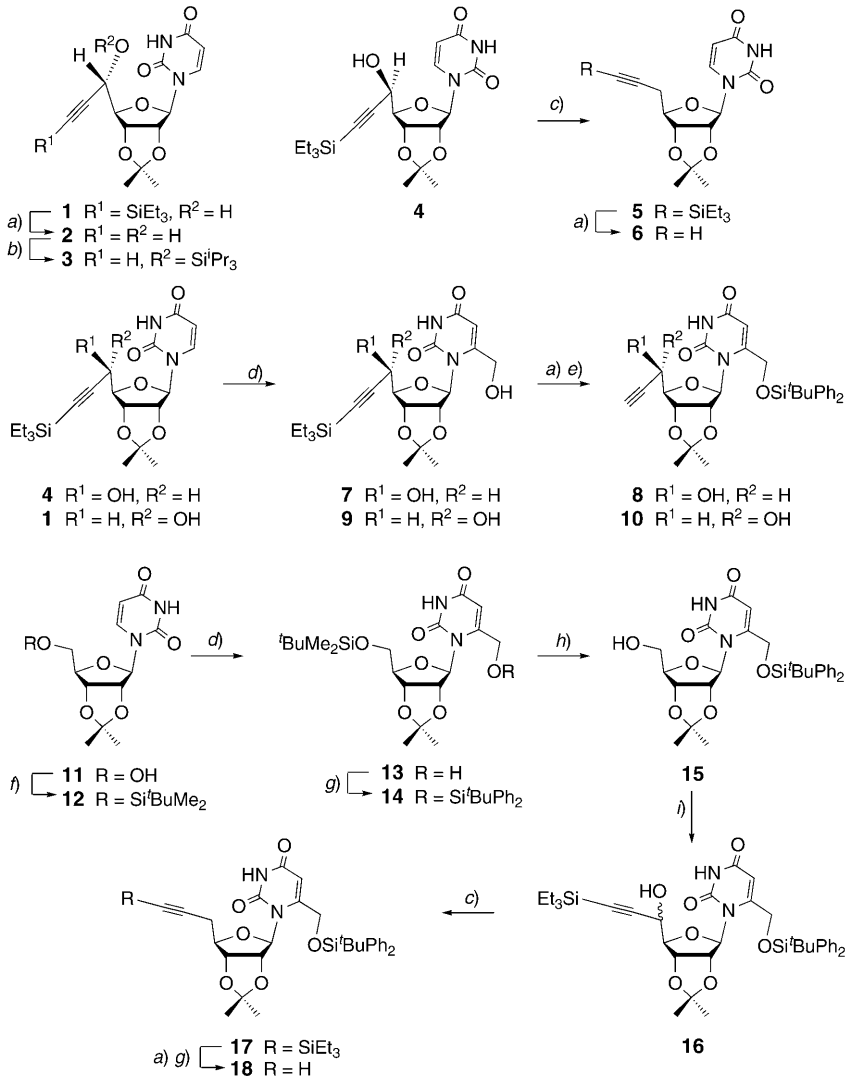

a) $Bu_4NF \cdot 3\,H_2O$, THF; 96% of **2**; 96% of **6**. *b*) $^iPr_3SiCl$ (TIPSCl), 1*H*-imidazole, DMF; 92%. *c*) 1. (Thiocarbonyl)diimidazole, CH_2Cl_2. 2. Bu_3SnH, 'α,α-azoisobutyronitrile' (AIBN), toluene; 81% of **5**; 59% of **17**. *d*) 1. Lithium diisopropylamide (LDA), THF, $-76°$, then DMF, then AcOH. 2. $NaBH_4$, EtOH; 60% of **7**; 54% of **9**; 85% of **13**. *e*) ^{t}BuPh$_2$SiCl, 1*H*-imidazole, DMF; 81% of **8**; 85% of **10**. *f*) ^{t}BuMe$_2$SiCl, 4-(dimethylamino)pyridine (DMAP), 1*H*-imidazole, CH_2Cl_2; 90%. *g*) ^{t}BuPh$_2$SiCl, DMAP, 1*H*-imidazole, CH_2Cl_2; 59% of **14**; 88% of **18**. *h*) H_2SiF_6, MeCN/^{t}BuOH/H_2O; 99%. *i*) 1. *N*,*N*′-Dicyclohexylcarbodiimide (DCC), $CHCl_2CO_2H$, DMSO. 2. (Triethylsilyl)acetylene, EtMgBr, THF; 51% of **16** (D-*allo*/L-*talo* 1:1).

Scheme 2

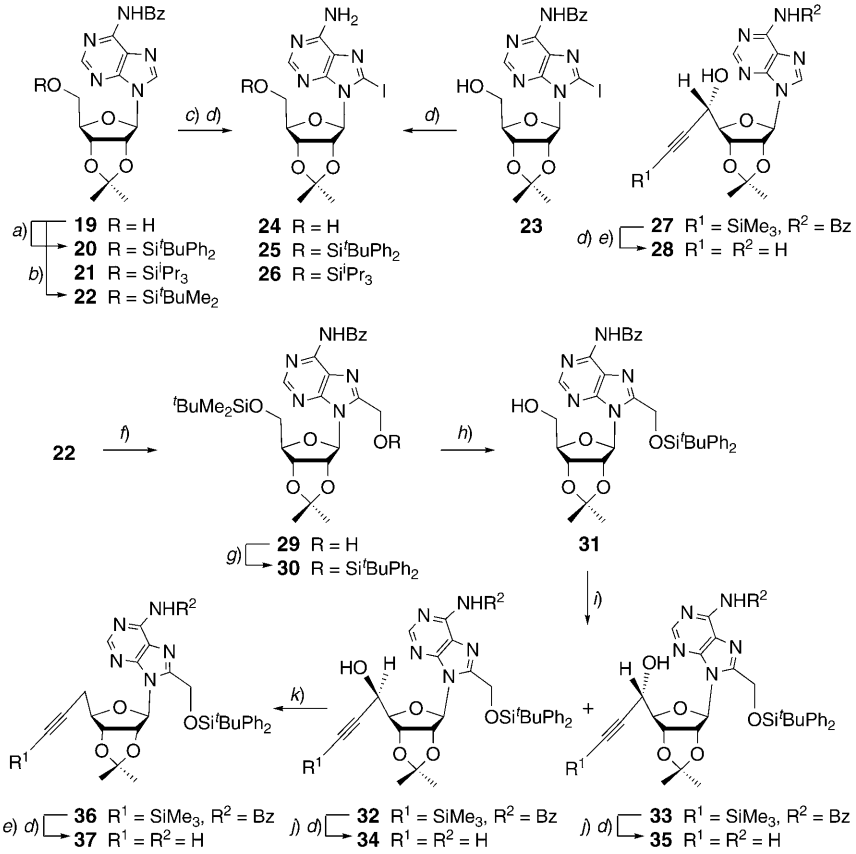

a) ^{t}BuPh$_2$SiCl, 1*H*-imidazole, DMF; 87%. *b*) ^{t}BuMe$_2$SiCl, DMAP, 1*H*-imidazole, CH_2Cl_2; 88%. *c*) LDA, THF, −76°, then *N*-iodosuccinimide (NIS). *d*) $MeNH_2$, THF/EtOH; 84% of **24** from **23**; 77% of **25** from **20**; 76% of **26** from **21**; 72% of **34**; 80% of **35**; 77% of **37**. *e)* $Bu_4NF \cdot 3\,H_2O$, THF; 72% of **28**. *f*) 1. LDA, THF, −76°, then DMF, then AcOH. 2. $NaBH_4$, EtOH; 83%. *g*) ^{t}BuPh$_2$SiCl, DMAP, 1*H*-imidazole, CH_2Cl_2; 89%. *h*) H_2SiF_6, MeCN/^{t}BuOH/H_2O; 79%. *i*) 1. DCC, $CHCl_2CO_2H$, DMSO. 2. (Trimethylsilyl)acetylene, EtMgBr, THF; 42% of **32** and 21% of **33**. *j*) K_2CO_3, MeOH, 0° (**32**) or −20° (**33**). *k*) 1. (Thiocarbonyl)diimidazole, CH_2Cl_2. 2. Bu_3SnH, AIBN, toluene; 65%.

mixture of **32** and **33** provided the 5′-deoxy derivative **36** (65%) that was *C*-desilylated and *N*-debenzoylated to yield 77% of the D-*ribo*-configured monomer **37**.

2.2. *Conformation of the A$^{(*)}$ and U$^{(*)}$ Monomers.* Investigation of the duplex formation of A*[c$_y$]U$^{(*)}$ and U*[c$_y$]A$^{(*)}$ dimers requires a detailed conformational analysis of the A$^{(*)}$ and U$^{(*)}$ building blocks, and particularly of the *syn*/*anti* equilibrium, the C(4′),C(5′) torsion angle, the conformation of the ribofuranose ring, and the dependence of the conformation on the intramolecular H-bond to N(3) and on the substituent at C(6) or C(8). This information is derived from ^{1}H-NMR parameters, such as δ(H−C(2′)) (*syn*/*anti* equilibrium), J(4′,5′) (C(4′),C(5′) torsion angle), J(1′,2′)/J(3′,4′)

(conformation of the ribofuranose ring), and δ(HO–C(5′)) and J(5′,OH) (H-bonding of the propargylic OH group).

2.2.1. *Conformation of the A(*) Monomers.* In $CDCl_3$, 8-unsubstituted and *O(5′)*-protected adenosine-derived propargyl alcohols and the corresponding 5′-deoxy analogues adopt an *anti* orientation of the adeninyl moiety, and show a *ca.* 1:1 northern/southern (*N*/*S*) equilibrium of the furanose ring. The A(*) propargyl alcohols possess an intramolecular O(5′)–H···N(3) H-bond, establishing the *syn* orientation of the adeninyl moiety and an (*S*) conformation of the furanose ring. Due to steric interactions between the nucleobase and the substituent at C(4), 8-substituted A* derivatives adopt a *syn*-orientation of the adeninyl moiety and prefer a (*N*) conformation of the furanose ring.

The 8-unsubstituted, *O(5′)*-protected adenosines adopt an *anti* conformation and the 8-substituted *O(5′)*-protected adenosines a *syn* conformation. This is revealed by the chemical shift of H–C(2′), the *syn* conformers being characterized by a downfield shift of 0.4–0.7 ppm (see [7] and refs. cited there). H–C(2′) of the *anti* conformers of 2′,3′-*O*-isopropylidenated, *O(5′)*-protected adenosines in $CDCl_3$ resonates typically at 5.20–5.25 ppm [7]. A small downfield shift for H–C(2′) of the 8-unsubstituted and *O(5′)*-silylated adenosines **20** and **22** resonating at 5.29–5.36 ppm (*Table 12* in the *Exper. Part*) reveals a strong preference for an *anti*-conformation. The 8-substituted and *O(5′)*-silylated adenosines **25**, **26**, and **30**, and the C(5′)-deoxy analogues **36** and **37** (δ(H–C(2′)) = 5.76, 5.85, 5.80, 5.78, and 5.70 ppm, resp.) adopt (almost) completely a *syn* conformation. The upfield shift for H–C(2′) of the alcohol **29** (δ 5.60 ppm) is probably due to an intramolecular H-bond of the OH group to N(9), as suggested by the downfield shift of the OH signal (δ 4.59 ppm).

The adenosine-derived propargyl alcohols **31**–**35** possess a completely persistent intramolecular H-bond of HO–C(5′) to N(3). It is evidenced by the downfield shift of the HO–C(5′) signal (**31**: δ 5.81 ppm; **32**–**35**: 6.35–7.77 ppm) and by characteristic large and small J(5′,OH) values ($\geq$10.5 and $\leq$1.5 Hz for the D-*ribo*-configured **31**, $\geq$10.5 Hz for the L-*talo*-configured **33** and **35**; and $\geq$1.5 Hz for the D-*allo*-configured **32** and **34**) [7]. The δ(HO–C(5′)) values show that the propargylic OH group of **32**–**35** is more highly acidic than HO–C(5′) of **31** and thus a better H-bond donor [16]. The *gg* orientation of HO–C(5′) of these alcohols is revealed by small J(4′,5′) couplings ($\leq$2.1 Hz). Despite the *syn* conformation, H–C(2′) of these intramolecularly H-bonded alcohols resonate upfield at 5.18–5.26 ppm, in agreement with earlier observations [7][9]. The O(5′)–H···N(3) H-bond of **24** and **28** is completely persistent even in $CDCl_3/CD_3OD$, as evidenced by the upfield shift of the H–C(2′) signal (5.13–5.23 ppm) and by small J(4′,5′) values ($\leq$1.8 Hz). The *gg* conformation of the *syn*-oriented adenosines **25**, **26**, **29**, **30**, **36**, and **37** is destabilized by a steric interaction between the adenosyl moiety and either R_3SiO–C(5′) or RC$\equiv$C–C(5′). This is reflected by J(4′,5′) values of 6.0–6.9 Hz for the silyl ethers and of 6.3–8.1 Hz for the alkynes, evidencing a *ca.* 1:1 mixture of *gt* and *tg* conformers. The destabilizing steric interaction between an *anti*-oriented adenosyl moiety and the substituent at C(5′) should be distinctly weaker. Indeed, J(4′,5′a) and J(4′,5′b) values of 4.5–5.1 and 3.6–3.9 Hz of the (*tert*-butyl)diphenylsilyl ether **20** and the (*tert*-butyl)dimethylsilyl ether **21** evidence *gg*/*gt*/*tg* equilibria of *ca.* 1:1:1 and 2:1:1, respectively, also in keeping with the relative steric demand of the two silyl substituents.

According to the $J(1',2')$ and $J(3',4')$ values (*Table 12* in the *Exper. Part*), the *anti*-oriented **20** and **22** are *ca.* 1:1 mixtures of (*N*) and (*S*) conformers, whereas the *syn*-oriented *O(5′)*-silyl ethers **25**, **26**, **29**, and **30**, and the *syn*-oriented *O(5′)*-deoxy acetylenes **36** and **37** prefer the (*N*) conformation. The (*S*) conformation is strongly preferred by the intramolecularly H-bonded alcohols **24**, **28**, and **31**–**35**, corroborating earlier observations about the change of ring conformation upon deprotection of HO–C(5′) [7]. Interestingly, the desilylated and debenzoylated amino diol derived from **31** [9] also adopts an (*S*) conformation in $CDCl_3$ solution, but a northern (E_4)-conformation in the crystalline state.

The ^{13}C-NMR spectra of the adenosine monomers show the expected chemical shifts (*Table 13* in the *Exper. Part*). Iodination induces a strong upfield shift of C(8) ($\Delta\delta \approx 40$ ppm), and hydroxymethylation a downfield shift ($\Delta\delta \approx 11$ ppm). The CH_2–C(8) *t* of **29**–**37** resonates at 58.1–60.1 ppm, and the C(6) *s* of the amines appears *ca.* 4 ppm downfield to that of the corresponding benzamides.

2.2.2. *Conformation of the U(*) Monomers.* In $CDCl_3$, 6-unsubstituted and *O(5′)*-protected uridine-derived propargyl alcohols and their *C(5′)*-deoxy analogues adopt completely an *anti* orientation of the uracilyl moiety. The intramolecular O(5′)–H···O=C(2) H-bond of the 6-unsubstituted U propargyl alcohols is weak, and leads to a minor population only of a *syn* conformation, whereas the corresponding 6-substituted U* analogues adopt completely a *syn*-conformation. The *anti* conformers form a *ca.* 1:1 equilibrium of the (*N/S*)-conformers, whereas the (*N/S*) equilibrium of the *syn* conformers depends upon the configuration and substitution of C(5′) (*ca.* 1:1 for D-*allo* and *ca.* 2:1 for L-*talo* and D-*ribo* derivatives).

That 6-unsubstituted and *O(5′)*-protected, 2′,3′-*O*-isopropylidenated uridines prefer an *anti*, and the corresponding 6-substituted analogues a *syn* conformation is revealed by typical chemical shifts of H–C(2′), *viz. ca.* 4.70 ppm for the former and 5.20–5.30 for the latter in $CDCl_3$ [2]. Thus, the 6-unsubstituted, *O(5′)*-silylated uridines **3** and **5** (δ(H–C(2′)) = 4.76–4.79 ppm; *Table 10* in the *Exper. Part*) adopt an *anti*-conformation, while the 6-substituted *O(5′)*-silyl ethers **13** and **14**, and the 6-substituted, *O(5′)*-deoxygenated acetylenes **17** and **18** (δ(H–C(2′)) = 5.18–5.25 ppm) prefer a *syn* conformation. Since the 6-hydroxymethyl group of **13** does not form a persistent intramolecular H-bond, in contradistinction to the corresponding 8-hydroxymethyl adenosine, its protection, as in **14**, leads only to a small shift ($\Delta\delta = 0.03$ ppm) of the H–C(2′) signal. Subtle factors influence the *syn*/*anti* equilibrium. Thus, *C*-desilylation of **5** leads to substantial amounts of a *syn*-conformer of **6**, as evidenced by the downfield shift of the H–C(2′) signal ($\Delta\delta = 0.14$ ppm) and a decreased population of the *gg* conformer (*gg*/*gt*/*tg* 1:2:2 for **6** and *ca.* 1:1:1 for **5**, as deduced from $J(4',5')$ values of 5.7/5.7 and 5.4/4.5 Hz, resp.). The *gg*/*gt*/*tg* 1:2:2 ratio of the (*t*-butyl)dimethylsilyl ether **12** ($J(4',5') = 5.7$ and 5.7 Hz) reflects the steric repulsion between the bulky silyl group and even an *anti*-oriented uracilyl unit.

Although the intramolecular O(5′)–H···O=C(2) H-bond of uridines is much less persistent than the O(5′)–H···N(3) H-bond of adenosines (see [2] and refs. cit. there), the *C*-desilylated propargyl alcohol derived from the uridine **4** [2] and the diol derived from **13** by desilylation [9] possess an intramolecular O(5′)–H···O=C(2) H-bond in the solid state. The orientation of the hydroxymethyl group of these two crystalline uridines is very similar to that of the desilylated and debenzoylated diol

derived from the adenosine **31** [9] (*gg* orientation; torsion angles H–O–C(5′)–H_a of −67 to −86° and H–O–C(5′)–R (R = H_b or C≡CH) of 155–173°). Therefore, O(5′)–H···O=C(2) H-bonded uridines should be easily identified by large and/or small *J*(5′,OH) couplings depending upon the configuration at C(5′). HO–C(5′) of the 6-substituted uridine **15** resonates at 3.11 ppm as a sharp *dd* with *J*(5′a,OH) = 3.9 and *J*(5′b,OH) = 8.1 Hz. Calculations[6]) suggest a *ca.* 40% persistence of the O(5′)–H···O=C(2) H-bond. This agrees well with the *ca.* 1:1 ratio of the *gg*, and the sum of *gt* and *tg* conformers that is deduced from *J*(4′,5′a) = 3.3 and *J*(4′,5′b) = 4.2 Hz. HO–C(5′) of the 6-substituted propargyl alcohols **7**–**9** resonates as broad *s*s at 3.71–4.11 ppm, evidencing a fast OH exchange (*Table 10* in the *Exper. Part*). Only the H–C(5′) signal of **8** shows a *J*(5′,OH) coupling. In the D-*allo* and L-*talo* pairs **7**/**8** and **9**/**10**, respectively, the rotamer distribution should correlate with differences between the H-bonding. Of the staggered conformers depicted in *Fig. 2*, only the rotamers **A** can form an intramolecular H-bond. As the rotamers **C** are disfavoured by the steric interaction between the ethynyl and the *syn*-oriented uracilyl group, one expects mainly an equilibrium between rotamers **A** and **B**. In the L-*talo* series, rotamer **B** is disfavoured by the *gauche* orientation of the *C*-substituents; hence, the L-*talo* conformer **A** should predominate. In the D-*allo* series, rotamer **A** is disfavoured by the *gauche* orientation of the *C*-substituents, and rotamer **B** lacks the *gauche* orientation of the *O*-substituents; an equilibrium D-*allo*-**A**/D-*allo*-**B** *ca.* 1:1 is expected. This means that the L-*talo* uridines **9**/**10** are expected to possess a more strongly persistent H-bond than the D-*allo* analogues **7**/**8**. Calculations suggest a L-*talo*-**A**/L-*talo*-**B** equilibrium of 8:2 for **7** (*J*(4′,5′) = 3.3 Hz) and 7:3 for **8** (*J*(4′,5′) = 4.2 Hz), and a D-*allo*-**A**/D-*allo*-**B** equilibrium of *ca.* 1:1 for **9** and **10** (*J*(4′,5′) = 6.0–6.3 Hz), assuming typical coupling constants of 1.5 Hz for *gauche*-oriented H-atoms and of 10.5 Hz for antiperiplanar H-atoms. Thus, at best 50% of the D-*allo* alcohols and 70–80% of the L-*talo* epimers possess an intramolecular H-bond. *J*(5′,OH) of **8** (2.7 Hz) indicates that only half of the L-*talo*-**A** conformers are engaged in intramolecular H-bonding. H–C(2′) of **7**–**9** and **15** resonates at a similar position (5.14–5.26 ppm) as H–C(2′) of the *O(5′)*-silyl ethers **13** and **14**, evidencing a negligible influence of the intramolecular H-bond on δ(H–C(2′)). Also the 8-unsubstituted propargyl alcohol **2** in CD_3OD shows a *ca.* 1:1 equilibrium of the L-*talo*-**A** and L-*talo*-**B** conformers, evidencing that the L-*talo*-**C** conformer is also disfavoured in such *anti*-oriented uridines.

The 6-unsubstituted uridines exist as *ca.* 1:1 mixtures of the (*S*) and (*N*) conformers; only **6** (*J*(1′,2′)/*J*(3′/4′) = 0.6) shows a preference for the (*N*) conformation, in agreement with the higher proportion of a *syn* conformer. There is a strong correlation between the *syn* orientation of 6-substituted uridines and the (*N*) conformation (*J*(1′,2′)/*J*(3′/4′) ≤ 0.45), with the exception of the D-*allo*-propargyl alcohols **7** and **8** which exist each as a *ca.* 1:1 (*S*/*N*) equilibrium.

The ^{13}C-NMR spectra of the U and U* momomers show the expected chemical shifts (*Table 11* in the *Exper. Part*). Thus, C(4′) resonates between 90.8 and 84.4 ppm; both 5-deoxygenation, and the change of the *syn* to *anti* orientation lead to an upfield shift of 2–3 ppm. Characteristic chemical shifts are also observed for the silylated and

---

[6]) Using 0.5 and 11.5 Hz [7] as limiting *J*(5′,OH) values, and *J*(H,OH) = 5.8 and 4.5 Hz [17] for completely solvated primary and secondary OH groups.

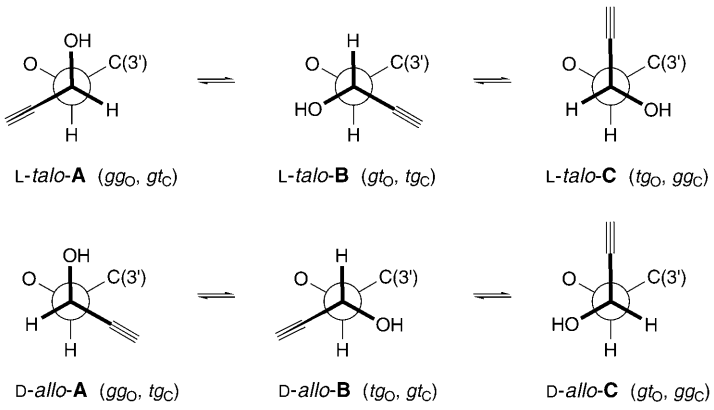

Fig. 2. Newman *projections of the staggered rotamers around the C(5′)–C(4′) bond of the* L-talo- *and* D-allo-*configured propargyl alcohols*

desilylated C≡C moiety (102.5–103.8 and 83.6–88.7 *vs.* 82.7–79.7 and 75.8–69.9 ppm); deoxygenation at C(5′) leads to an upfield shift of C(7′) by *ca.* 5 ppm. Hydroxymethylation induces a downfield shift of the C(6) signal by 15 ppm and the subsequent *O*-silylation an upfield shift of 1–2 ppm for C(6) and a downfield shift of 2 ppm for CH_2–C(6).

2.3. *Synthesis of the Dinucleoside Analogues.* The nucleoside dimers were prepared by *Sonogashira* cross-coupling under previously optimized conditions [3]. The U*[c_y]A dimers **41**, **42**, **44**, and **47** were prepared by coupling the 6-iodouridine **38** [2] with the alkynes **39** [6], **40** [5], **28**, and **46** [3], and the U*[c_y]A* analogues **43**, **45**, and **48** by coupling **38** with **34**, **35**, and **37** (*Scheme 3*). The dimer **44** derived from the L-*talo*-configured propargyl alcohol **28** was obtained in higher yields (84%) than the dimer **41** (70%) derived from the D-*allo* isomer **39**. Lower yields resulted also from coupling **38** with the propargyl silyl ethers **40** to **42** (70%). The same dependence of the yield upon the presence or absence of the propargylic OH group and its configuration was observed in the synthesis of the U*[c_y]A* dimers **43** (68%), **45** (90%), and **48** (73%), and, similarly, in the synthesis of the A*[c_y]U$^{(*)}$ dimers **51** (92%), **54** (90%), **52** (86%), **56** (99%), **58** (91%), **53** (89%), **55** (83%), **57** (98%), **59** (80%), and **60** (80%) that were obtained by cross-coupling the 8-iodoadenosines **24**–**26** with the alkynes **2**, **6**, **8**, **10**, **18**, **49** [2], and **50** [2], respectively (*Scheme 4*).

2.4. *Association of the U*[c_y]A$^{(*)}$ and A*[c_y]U$^{(*)}$ Dinucleosides. A priori*, the U*[c_y]A$^{(*)}$ and A*[c_y]U$^{(*)}$ dinucleosides may form linear duplexes and higher associates and/or cyclic duplexes. The formation of cyclic duplexes is mainly influenced by structural parameters of unit I. These are *1*) the orientation of the nucleobase, as specified by the χ angle and strongly influenced by R^2, *2*) the furanose ring conformation, *3*) the orientation of the ethynyl moiety, as described by the torsional angle ϕ_{CO} (C(6′/I)–C(5′/I)–C(4′/I)–O(4′/I)), and *4*) the nature of the propargylic substituent X and the configuration at C(5′/I) (X≠H; *Fig. 3*, *a*). Possible steric interactions between the ribosyl units in all dinucleosides and a co-operativity between the intramolecular O(5′/II)–H···N(3/II) H-bond and intermolecular H-bonds of the adeninyl unit of A*[c_y]U$^{(*)}$

Scheme 3

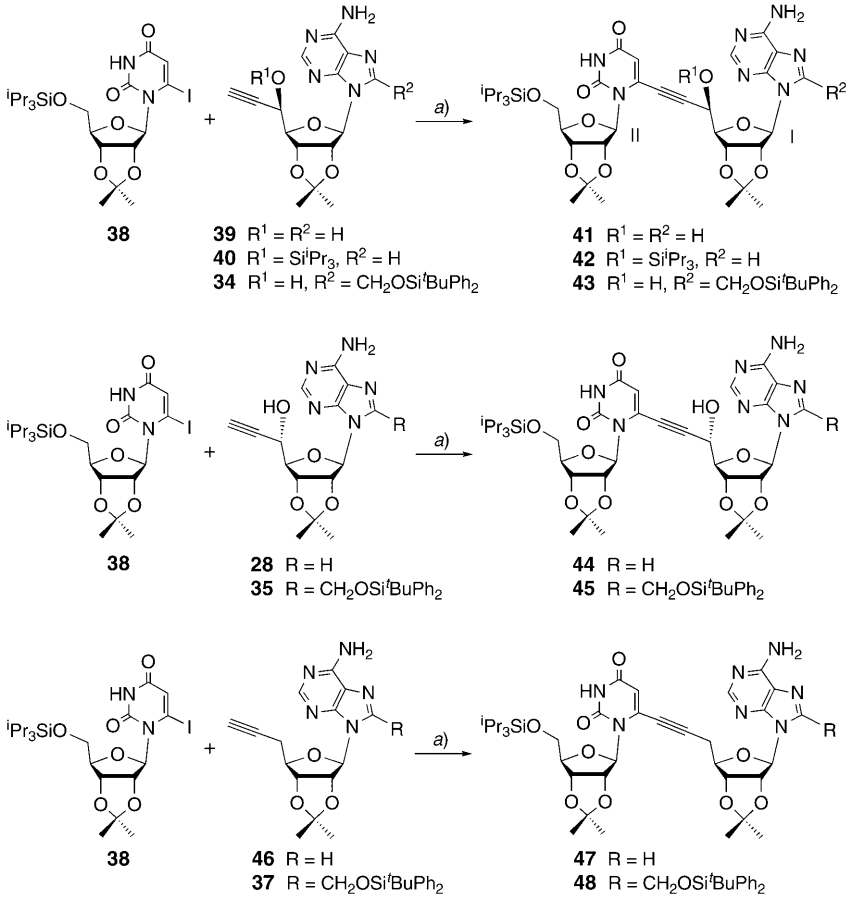

a) $[Pd_2(dba)_3]$, CuI, $P(fur)_3$, toluene/Et_3N 1:1; 70% of **41**; 70% of **42**; 68% of **43**; 84% of **44**; 90% of **45**; 76% of **47**; 73% of **48**.

dinucleosides ($R^1 = H$) must be also taken into consideration. *Maruzen* models indicate that cyclic duplexes of both U*[c_y]A$^{(*)}$ and A*[c_y]U$^{(*)}$ dinucleosides can accommodate *Watson–Crick*, reverse-*Watson–Crick*, *Hoogsteen*, or reverse-*Hoogsteen* H-bonds, but only in a restricted range of the χ and ϕ_{CO} angles, *viz.* -80 to $+125°$ for the χ angle, specifying a *syn*-type orientation of the nucleobase, and $+30$ to $-125°$ for the ϕ_{CO} angle, corresponding to a *gg*-type orientation of the ethynyl group (*Fig. 3*, *b*). Hence, U*[c_y]A$^{(*)}$ and A*[c_y]U$^{(*)}$ dinucleosides with an *anti*-oriented nucleobase, or a *gg*- or *tg*-oriented ethynyl moiety can only form linear duplexes and higher (linear or cyclic) associates, but not cyclic duplexes.

The association of the U*[c_y]A$^{(*)}$ and A*[c_y]U$^{(*)}$ dinucleosides in $CHCl_3$ solution was investigated by vapour-pressure osmometry (VPO) [18], and by NMR and CD spectroscopy. A doubling of the molecular mass at higher concentration, as shown by VPO measurements, evidences cyclic duplexes, whereas other values for the apparent

Scheme 4

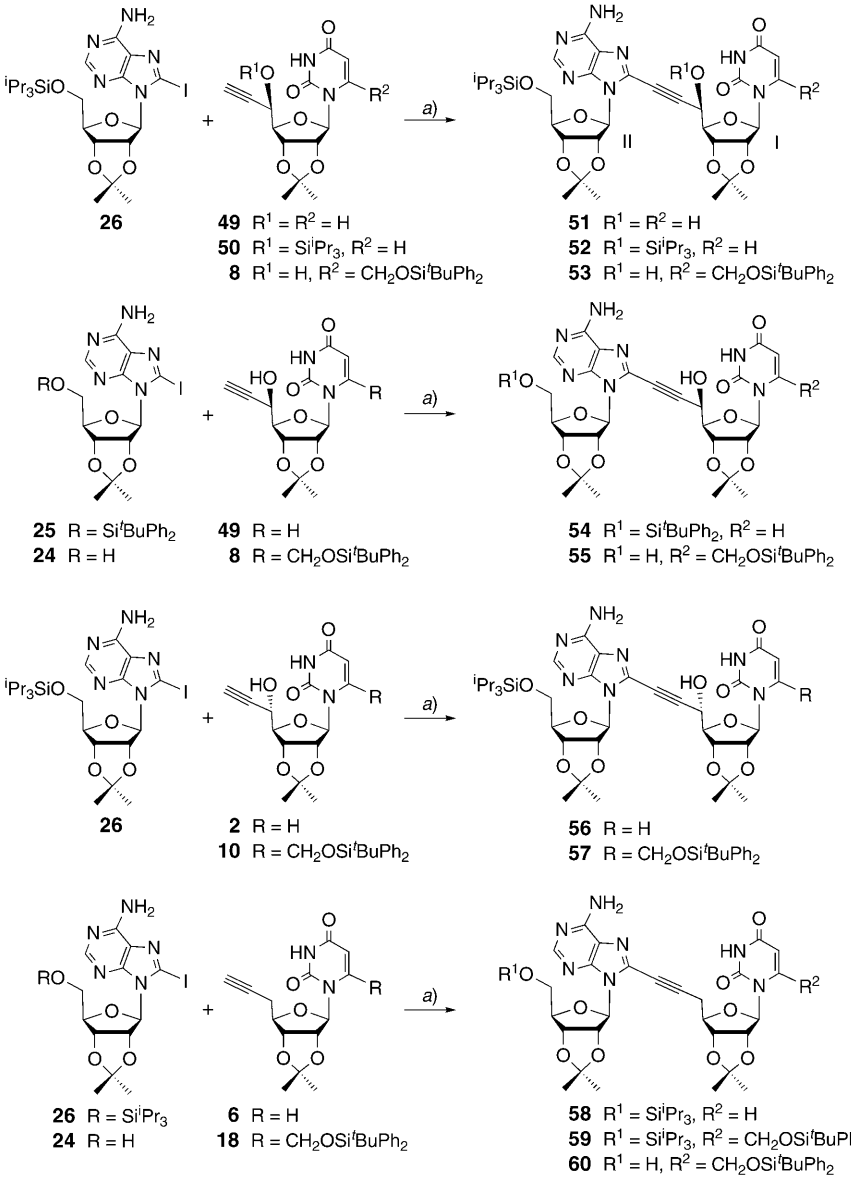

a) $[Pd_2(dba)_3]$, CuI, $P(fur)_3$, toluene/Et_3N 1:1; 92% of **51**; 86% of **52**; 89% of **53**; 90% of **54**; 83% of **55**; 99% of **56**; 98% of **57**; 91% of **58**; 80% of **59**; 80% of **60**.

molecular mass and its concentration dependence even at higher concentration evidence linear duplexes and higher associates. The association is also revealed by the concentration dependence of ^{1}H-NMR signals, and best quantified by analysing the concentration dependence of δ(HN(3)) of the uracilyl moiety (easily assigned, large δ

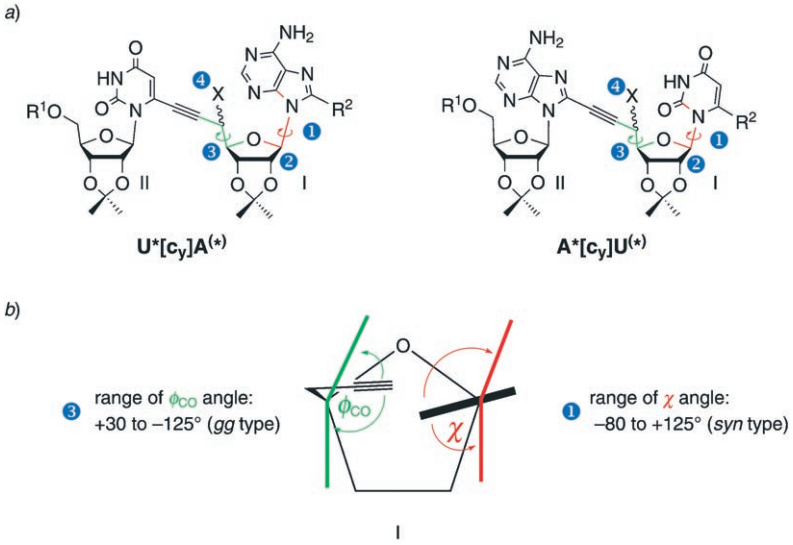

Fig. 3. a) *Factors of unit I influencing the formation of cyclic duplexes and* b) *ranges of the* ϕ_{CO} *and* χ *angles of unit I*

range, no overlapping with other signals). A large $\Delta\delta$ value between simplex (extrapolation to $c = 0$ mM) and duplex(es) ($c > 20$ mM), a strong bending of the curve at low concentration, and the reaching of a plateau a high concentration evidences the formation of cyclic duplexes, whereas a distinctly smaller $\Delta\delta$ value between simplex and duplex, a moderate bending of the curve at low concentration, and an increasing downfield shift with increasing higher concentration evidences linear duplexes and higher associates. The temperature dependence of δ(HN(3)) (*van't Hoff* plot) allows to calculate the thermodynamic parameters. A thorough analysis of the ^{1}H- and ^{13}C-NMR spectra (recorded at a concentration where *ca.* 80% of the dinucleosides are in the form of duplexes), a comparison of these data with those of the monomeric precursors, and the concentration dependence of additional ^{1}H-NMR parameters (such as δ(H–C(2′/I)) and J(4′,5′/I)) should allow to determine the conformation of duplexes. ROESY and CD spectroscopy will give information about the type of the base pairing and π-stacking. Cross-peaks between the signals of HN(3) of the uracilyl moiety and H–C(2) of the adeninyl moiety evidence *Watson–Crick*-type base pairing. The absence of these cross-peaks, and cross-peaks between the signals of HN(3) of the uracilyl moiety and H–C(8) of the adeninyl moiety (only possible in U*[c$_y$]A dimers) evidence *Hoogsteen*-type base pairing. The ROESY spectra do not allow to discriminate between *Watson–Crick* and reverse-*Watson–Crick*, nor between *Hoogsteen* and reverse-*Hoogsteen* H-bonds[7]). The stabilisation of nucleoside base pairs by π-stacking in aqueous solutions is estimated to

[7]) *A priori*, HMBC cross-peaks between H_2N–C(6) of adenosines and either O=C(2) or O=C(4) of uridines would provide this information, as would ^{15}N-labelled isotopomers (intermolecular ^2J(N,N) or ^3J(N,C) couplings [19][20]). However, such HMBC cross-peaks are only visible when H_2N–C(6) resonates as a sharp signal which is usually not the case.

be 0.5–1.8 kcal/mol (see [21] and refs. cit. there); it is expected to be significantly weaker in $CHCl_3$. As a rule, base stacking is evidenced by positive and negative bands in CD spectra that decrease in intensity with increasing temperature [22–24]. Finally, the restrictions resulting from these analyses should allow to generate appropriate *Maruzen* and AMBER* models of the cyclic duplexes.

In the following, observations valid for all A*[c_y]U$^{(*)}$ and U*[c_y]A$^{(*)}$ dimers will be discussed first. Subsets of U*[c_y]A$^{(*)}$ and A*[c_y]U$^{(*)}$ dinucleosides will then be analysed according to the procedure described in the previous paragraph. In the U*[c_y]A$^{(*)}$ series, there are two subsets (one with and one without intramolecular H-bond), and in the A*[c_y]U$^{(*)}$ series there are four subsets, according to the strong influence both of the substituents at C(8/I) and C(5′/I), and of the configuration at C(5′/I).

2.4.1. *Discussion of NMR Parameters Relevant to Both the U*[c_y]A$^{(*)}$ and the A*[c_y]U$^{(*)}$ Dimers.* The concentration dependence of the ^{1}H-NMR signals of the U*[c_y]A$^{(*)}$ and A*[c_y]U$^{(*)}$ dimers was determined at two or three different concentration ranges (30–60, *ca.* 10, and 1.2 mM); the chemical shifts of the most sensitive H-atoms at the highest concentration and the relative shifts at the lower concentrations are listed in *Tables 1* and *2*. As expected, the strongest shift dependence is observed for the H-atoms directly involved in base pairing. HN(3) of U*[c_y]A$^{(*)}$ dimers (*ca.* 10 and 1–2 mM solutions) displays $\Delta\delta$ values of 1.3–2.5 ppm, and HN(3) of A*[c_y]U$^{(*)}$ dimers displays $\Delta\delta$ values of 1.0–1.8 ppm, with the exception of **55** ($\Delta\delta$ of only 0.28 ppm). The H_2N–C(6) signals show a similar concentration dependence, with $\Delta\delta$ values of 0.3–0.6 ppm for *ca.* 10 and 1–2 mM solutions. The chemical shift of the HN(3) and H_2N–C(6) signals depends not only on the type and persistence of the base pairing, but also on intramolecular H-bonds, the substituents at C(6) and C(8), and the orientation of the nucleobases (see *Sect. 2.4.8*). Still, the downfield shift of the HN(3) and H_2N–C(6) signals in the duplexes should qualitatively correlate with the strength of the base pairing. Since A·U heteropairing is much stronger than U·U and A·A homopairing, a stronger downfield shift is expected for HN(3) and H_2N–C(6) of the self-complementary UA and AU dimers than for HN(3) and H_2N–C(6) of the corresponding monomers and of UU and AA homodimers. Indeed, HN(3/II) of **41**–**45**, **47**, and **48**, and HN(3/I) of **52**, **53**, and **55**–**60** ($\geq$10 mM solutions; *Tables 1* and *2*) resonate at 10.3–13.8 ppm, clearly downfield to HN(3) of the U$^{(*)}$ monomers **5**–**10**, **12**–**15**, **17**, and **18** (8.95–10.35 ppm), and of the corresponding U*[c_y]U$^{(*)}$ homodimers (8.90–10.40 ppm [2][5]). Similarly, H_2N–C(6/I) of **41**–**45**, **47**, and **48**, and H_2N–C(6/II) of **52**, **53**, and **55**–**60** resonate at 6.15–7.9 ppm, downfield to the H_2N–C(6) signal of the A$^{(*)}$ monomers **25**, **26**, **34**, **35**, and **37** (5.7–6.25 ppm), and of the corresponding A*[c_y]A$^{(*)}$ homodimers (5.95–6.8 ppm [1][3][4]). Usually, the NH_2 signal appears as a single broad *s*, with the exception of **48** and **60** that show two signals at a concentration of 1 mM.

Smaller shifts (up to 0.18 ppm) are observed for H–C(5) and CH_2–C(6) of the uracilyl group, H–C(2) and CH_2–C(8) of the adeninyl group, and H–C(1′–3′) of both ribosyl units (*Tables 1* and *2*). The H–C(2′/II) signal is shifted upfield upon dilution of the dimers where it resonates at rather low field at high concentration. This is the case for the U*[c_y]A$^{(*)}$ dimers **42**, **47**, and **48** (δ = 5.15–5.38 ppm) and the *O(5′/II)*-protected A*[c_y]U* dimer **59** (δ = 5.79 ppm at c = 83.5 mM). In contradistinction, the H–C(2′/II) signal is shifted downfield upon dilution of those dimers where it resonates

Table 1. *Concentration Dependence of the ^{1}H-NMR Chemical Shifts* [ppm] *of the U*[c$_y$]A$^{(*)}$ Dimers* **41**–**45**, **47**, *and* **48** *in* $CDCl_3$ (highest concentration: δ value [ppm]; lower concentrations: $\Delta\delta$ values [ppm] relative to the highest concentration)[a]).

	41		**42**			**43**			**44**			**45**			**47**			**48**		
Conc. [mM]	10.5	0.9	95	9	0.5	86.5	9	1.2	99	10.5	1.6	92.5	9.5	1.5	60	5	0.5	50	11	1.0
Uridine unit (II)																				
HN(3)	10.32	−2.30	13.76	−1.05	−3.51	11.48	−2.12	[b])	12.37	−1.65	−3.69	11.32	−1.89	−3.17	13.55	−1.11	−3.19	12.91	−0.61	−2.66
H–C(5)	6.02	−0.01	5.67	−0.24	−0.07	6.01	0	+0.01	5.79	0	0	5.77	0	+0.01	5.52	−0.02	+0.14	5.26	−0.02	+0.06
H–C(1′)	5.89	−0.01	5.96	+0.01	+0.08	6.25	0	+0.01	6.16	0	−0.01	6.19	+0.01	+0.02	6.15	+0.01	+0.04	6.57	0	+0.01
H–C(2′)	5.24	−0.02	5.30	−0.06	−0.11	[c])	[c])	[c])	5.15	−0.02	−0.02	5.05	+0.04	+0.07	5.33	−0.04	−0.09	5.38	+0.03	−0.04
Adenosine unit (I)																				
H_2N–C(6)	6.18	−0.44	7.07	−0.53	−1.07	6.51	−0.60	−0.90	6.81	−0.49	−1.00	6.44	−0.55	−0.87	7.02	−0.52	−0.99	6.7	−0.3	[d])
H–C(8)	7.92	−0.06	8.06	+0.03	−0.05	–	–	–	7.92	−0.03	−0.07	–	–	–	8.06	−0.02	−0.08	–	–	–
CH_a–C(8)	–	–	–	–	–	5.06	−0.05	−0.07	–	–	–	5.04	−0.03	−0.05	–	–	–	5.04	−0.01	−0.03
CH_b–C(8)	–	–	–	–	–	4.93	−0.03	−0.04	–	–	–	4.92	−0.01	−0.02	–	–	–	4.98	−0.03	−0.05
H–C(1′)	6.24	−0.01	6.15	+0.01	−0.01	6.52	+0.01	+0.01	5.89	0	+0.01	6.50	0	+0.01	6.14	+0.01	−0.02	6.23	0	+0.01
H–C(2′)	5.17	−0.02	5.98	−0.04	−0.23	[c])	[c])	[c])	5.16	−0.01	−0.07	5.21	−0.03	−0.05	5.92	−0.04	−0.18	5.94	−0.01	−0.14
H–C(3′)	5.19	−0.01	5.11	−0.02	+0.05	[c])	[c])	[c])	5.06	0	0	5.14	−0.03	−0.04	5.16	−0.02	−0.03	5.32	0	−0.03
HO–C(5′)	8.14	+0.01	–	–	–	8.06	+0.02	+0.06	8.27	+0.05	+0.06	7.91	+0.09	+0.14	–	–	–	–	–	–

[a]) $\Delta\delta > 0.03$ ppm between the highest and the lowest concentration are also observed for H–C(2/I) of **42** (+0.04 ppm) and **43** (−0.04 ppm), H–C(4′/I) of **42** (−0.05 ppm) and **48** (+0.05 ppm), H–C(5′/I) of **45** (−0.04 ppm), and H_a–C(5′/I) of **48** (+0.05 ppm). [b]) NH Signal not visible. [c]) Overlapping signals at 5.26–5.15 ppm (no concentration dependence). [d]) Two signals with the intensity ratio of 2:1 at 5.98 and 5.48 ppm ($\Delta\delta = 0.72$ and 1.22 ppm).

Table 2. *Concentration Dependence of the ^{1}H-NMR Chemical Shifts* [ppm] *of the A*[c$_y$]U$^{(*)}$ Dimers* **52**, **53**, *and* **55**–**60** *in* $CDCl_3$ (highest concentration: δ value [ppm]; lower concentrations: $\Delta\delta$ values [ppm] relative to the highest concentration)[a]).

	52			**53**			**55**		**56**		**57**			**58**			**59**		**60**	
Conc. [mM]	85	8.5	1.3	55	10	1.2	50	1.2	30	1.0	80	11	1.7	114	8.5	1.3	83.5	1.5	50	1.0
Adenosine unit (II)																				
H_2N–C(6)	7.12	−0.56	−1.23	6.84	−0.35	−0.76	[b])	[b])	7.2	−0.63	7.5	−0.15	−0.6	7.4	−0.6	−1.15	[b])	−0.65	7.87	[c])
H–C(2)	8.31	−0.02	−0.02	8.11	+0.01	+0.08	7.99	+0.03	8.31	−0.01	8.19	+0.06	+0.09	8.29	+0.02	+0.02	8.21	+0.04	8.30	+0.01
H–C(1′)	6.18	−0.04	+0.01	6.32	0	+0.02	6.29	+0.01	6.29	0	6.32	−0.01	−0.01	6.29	0	+0.01	6.32	+0.02	6.24	0
H–C(2′)	5.63	−0.01	+0.06	5.76	+0.02	0	5.84	−0.04[d])	5.71	+0.01	5.73	+0.02	+0.02	5.74	+0.01	0	5.79	−0.03	5.27	−0.04
Uridine unit (I)																				
HN(3)	11.48	−1.10	−2.92	11.68	−0.60	−1.72	11.90	−0.28	11.71	−1.45	12.10	−0.49	−1.37	11.81	−1.36	−2.38	12.50	−1.24	12.80	−2.85
H–C(5)	5.72	+0.02	+0.01	5.46	0	+0.07	5.19	+0.04[d])	5.68	+0.04	5.66	+0.04	+0.05	5.67	+0.04	+0.06	5.41	+0.03	5.98	−0.05
CH_a–C(6)	–	–	–	4.58	−0.03	−0.05	4.46	0	–	–	4.63	−0.02	−0.04	–	–	–	4.68	−0.03	4.60	−0.01
CH_b–C(6)	–	–	–	4.33	−0.01	+0.02	4.11	+0.02	–	–	4.44	0	0	–	–	–	4.42	−0.02	4.40	−0.01
H–C(1′)	5.91	−0.09	−0.09	5.96	−0.03	−0.09	5.97	−0.02	5.85	−0.05	6.05	−0.05	−0.10	5.68	−0.04	−0.02	6.01	−0.04	5.62	−0.02
H–C(2′)	5.04	−0.08	−0.09	5.31	−0.02	−0.03	5.28	−0.01	5.07	−0.02	[e])	[e])	[e])	5.18	−0.03	−0.08	[f])	[f])	5.33	−0.04
H–C(3′)	4.99	−0.10	−0.08	5.24	[g])	[g])	4.94	+0.01	5.12	0	[e])	[e])	[e])	5.08	−0.01	−0.07	[f])	[f])	5.33	−0.20
HO–C(5′)	–	–	–	4.96	−0.34	−0.74	5.34	[b])	5.05	−0.72	4.41	−0.58	−0.74	–	–	–	–	–	–	–

[a]) $\Delta\delta > 0.03$ ppm between the highest and the lowest concentration are also observed for H–C(5′/I) of **57** (−0.05 ppm), H_a–C(5′/II) of **53** (+0.06 ppm), and H_b–C(5′/II) of **53** (+0.06 ppm). [b]) Not determined. [c]) Two broad *s* at 6.52 (+1.35) and 6.49 (+1.38 ppm). [d]) Broad signal. [e]) *AB* System at 5.28–5.24 ppm. [f]) *AB* System at 5.34–5.27 ppm. [g]) Overlapping with H–C(3′/II) at 5.22–5.15 ppm.

at rather high field at high concentration, *viz*. the U*[c_y]A* dimer **45** ($\delta = 5.05$ ppm at $c = 92.5$ mM) and the *O(5′/II)*-protected A*[c_y]U dimer **52** ($\delta = 5.63$ ppm at $c = 85$ mM). This suggests differently *syn*-oriented nucleobases of unit II in the cyclic duplexes of **42**/**47**/**48**/**59** ($\chi = 90-120°$; high-*syn*) and **45**/**52** ($\chi = 0-30°$; low-*syn*). The H–C(2′/I) signal is always shifted upfield upon dilution. The highest upfield shifts of H–C(2′/I) are observed for the U*[c_y]A dimers **42** (0.23 ppm) and **47** (0.18 ppm), and for the U*[c_y]A dimer **48** (0.14 ppm), evidencing a similar orientation of the adeninyl moiety in the duplex **48**·**48** and in the duplex **59**·**59**. H–C(2′/I) of the A*[c_y]U dimers **52** and **58** shows a stronger upfield shift ($\Delta\delta = 0.08-0.09$ ppm) than H–C(2′/I) of the A*[c_y]U$^{(*)}$ dimers **53**, **55**, **56**, and **60** ($\Delta\delta \leq 0.04$ ppm). This evidences a subtle influence of the substituents at C(6/I) and C(5′/I).

The concentration dependence of the chemical shift for HN(3) of the U*[c_y]A$^{(*)}$ and A*[c_y]U$^{(*)}$ dimers was determined for 1 to 50 mM solutions in $CDCl_3$. It is expressed by the dilution curves in *Fig. 4* that are qualitatively discussed in the sections dealing with the subsets of the dimers. The curves were analysed graphically [25] and by linear least-squares fitting [26] to derive the equilibrium constant K, and to calculate δ(HN(3)) of the simplex and duplex (or an averaged δ(HN(3)) of several duplexes; *Table 3*). The chemical shift for HN(3) of the simplex may be slightly influenced by the substituents at C(6) and C(5′) of the uridinyl moiety. The calculated δ(HN(3)) values of the U*[c_y]A$^{(*)}$ **41**–**43** and **45** (7.58–7.97 ppm) are indeed similar to each other, whereas the calculated δ(HN(3)) values of the A*[c_y]U$^{(*)}$ simplexes differ more strongly (7.98–8.71 ppm). A fast H/H exchange between NH and H_2O at low concentrations (ratio dimer/$H_2O \leq 1$) may result in too small $\delta(NH_{simplex})$, as it is probably the case for **44** and **48** (7.13 and 7.26 ppm, resp.). The $\delta(NH_{simplex})$ value of **47** (8.68 ppm) is surprisingly high, for unknown reasons.

Thermodynamic parameters were determined by *van't Hoff* analysis of ^{1}H-NMR spectra recorded of 3–5 mM solutions in $CDCl_3$ in 10° intervals and in the temperature range of 0 to 50° (*Table 3*). The results are discussed in the following sections. They evidence an enthalpy/entropy compensation [27][28], as expressed by a good linear correlation coefficient of ΔH and $T\Delta S$ [29] with a slope of 0.79 and an intercept of 0.77, resulting in similar ΔG values of -2.0 to -4.6 kcal/mol. Enthalpy/entropy compensation is very common in host–guest complexes [30][31] and nucleic acid duplexes [29][32][33] with the entropy increase resulting from the loss of translational (position) and rotational (orientation) freedom upon duplex formation [34]; the correlation may also be the result of a so-called extra-thermodynamic relation [35].

The formation of cyclic duplexes may require an orientation of the ethynyl moiety that differs from the one of the simplex. Such a conformational change is best followed by analysing the J(4′,5′/I) couplings. Since also non-staggered conformers have to be considered for cyclic duplexes, the energy and the J(4′,5′) values for the conformers resulting from rotation about the C(4)–C(5) bond were calculated by force-field modelling of the monomeric uridine derivative **61** (MM3* implemented in Macromodel V. 6 [36]), varying ϕ_{CO} (torsion angle C(6′)–C(5′)–C(4′)–O(4′)) in steps of 10° (*Fig. 5*). The yellow bar between the diagrams in *Fig. 5* indicates the range of ϕ_{CO} compatible with the formation of a cyclic duplex (see *Fig. 3*). The ϕ_{CO} torsion angles of the *C(5′/I)*-deoxy compounds are deduced from two J(4′,5′/I) values, and the rotameric equilibrium is thus more easily deduced. The experimental J(4′,5′/I) values were determined at

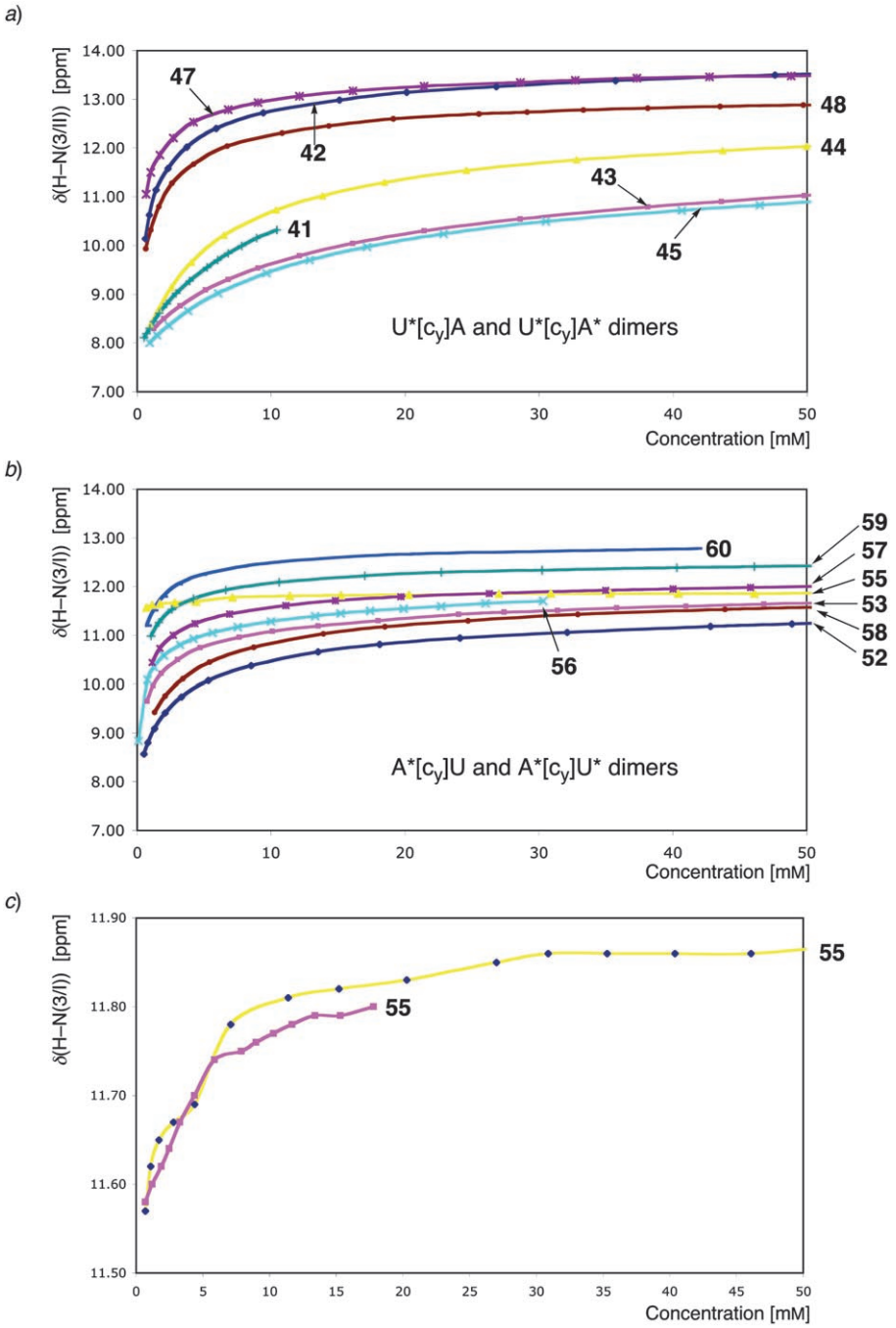

Fig. 4. *Concentration dependence of* a) *δ(HN(3/II)) of the U*[c$_y$]A$^{(*)}$ dimers* **41**–**45**, **47**, *and* **48**, b) *δ(HN(3/I)) of the A*[c$_y$]U$^{(*)}$ dimers* **52**, **53**, *and* **55**–**60**, *and* c) *expanded δ(HN(3/I)) of the A*[c$_y$]U* dimer* **55** *in CDCl$_3$ solution* (two measurements)

Table 3. *Association Constant* K *and* δ(NH) *of the Simplex and the Duplex as Calculated from the Concentration Dependence of δ(HN(3)) in $CDCl_3$ at 295 K for the Dimers* **41**–**45**, **47**, **48**, **52**, **53**, *and* **56**–**60**, *and Determination of the Thermodynamic Parameters by* van't Hoff *Analysis of the Temperature Dependence of δ(HN(3)) for 3–5 mM Solutions in $CDCl_3$ at 0–50°* (in 10° steps)

Dimer	K [M^{-1}]	$\delta(NH_{simplex})$ [ppm]	$\delta(NH_{duplex})$ [ppm]	ΔG_{298} [kcal/mol]	ΔH [kcal/mol]	ΔS [e.u.]
U*[c_y]A$^{(*)}$ series						
41	45	7.82	14.71	−2.2	−6.2	−13.4
43	39	7.87	13.22	−2.0	−6.7	−16.1
44	104	7.13	13.54	−2.7	−8.4	−19.4
45	46	7.58	13.07	−1.8	−6.8	−16.8
42	702	7.97	14.23	−3.9	−14.0	−34.3
47	1159	8.68	13.96	−4.0	−15.0	−37.3
48	973	7.26	13.51	−4.1	−15.7	−39.2
A*[c_y]U$^{(*)}$ series						
52	197	7.98	12.09	−3.3	−15.9	−42.9
53	364	8.71	12.16	−3.2	−11.4	−27.8
56	930	8.34	12.10	−4.0	−14.0	−33.9
57	995	8.39	12.38	−4.0	−13.8	−33.2
58	277	8.02	12.32	−3.6	−14.2	−36.0
59	1793	8.42	12.74	−3.8	−13.4	−32.5
60	2307	8.56	13.10	−4.6	−18.4	−46.9

Table 4. *Concentration Dependence of* J*(4′,5′/I) of the U*[c_y]A$^{(*)}$ Dimers* **42**, **47**, *and* **48**, *and of the A*[c_y]U$^{(*)}$ Dimers* **52** *and* **57**–**60** *in $CDCl_3$*

Compound	Conc. [mM]	J(4′,5′a/I) [Hz]	J(4′,5′b/I) [Hz]	Compound	Conc. [mM]	J(4′,5′a/I) [Hz]	J(4′,5′b/I) [Hz]
42	0.5	5.7	–	**56**	1.0	3.0	–
	9	4.5	–		30	3.3	–
	95	4.2	–	**57**	1.7	5.4	–
47	0.5	5.7	5.1		11	5.4	–
	5	4.8	4.5		80	5.4	–
	60	4.5	4.2	**58**	1.3	6.0	6.0
48	1.0	6.6	4.8		114	6.0	6.0
	11	5.4	4.2	**59**	1.5	[a])	[a])
	50	5.1	4.2		10	5.7	5.4
52	1.3	4.5	–		83.5	5.4	5.4
	8.5	4.8	–	**60**	1.0	6.3	6.3
	85	5.1	–		50	6.9	6.3

[a]) Not determined (too strong noise).

three different concentrations (1–2, 5–10, and 50–114 mM), listed in *Table 4*, and discussed in the following sections.

As mentioned above, the ^{1}H- and ^{13}C-NMR spectra in $CDCl_3$ of the U*[c_y]A$^{(*)}$ and A*[c_y]U$^{(*)}$ dinucleosides were recorded at a sufficiently high concentration to guarantee a high proportion of the duplex; *i.e.*, of 60 mM solutions of **42**–**45**, **47**, **48**, **52**, **53**, and **57**–**59**, of 50 mM solutions of **55** and **60**, of a 30 mM solution of **56**, and of a 10 mM sol-

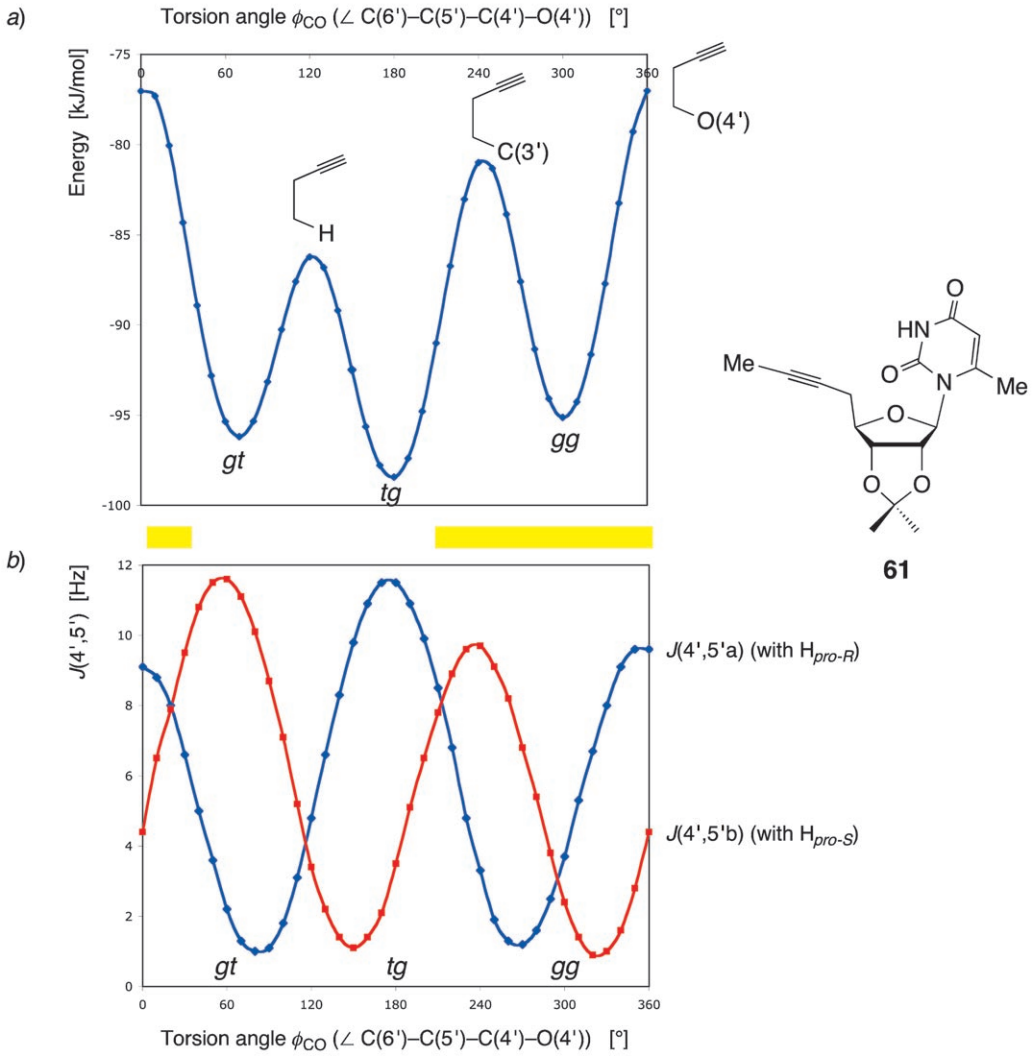

Fig. 5. *MM3*-Calculated energy and* J*(4′,5′) couplings for the rotamers of* **61** *obtained by rotation in 10° steps around the C(4′)–C(5′) bond.* The yellow bar indicates the range of ϕ_{CO} compatible with the formation of a cyclic duplex.

ution of **41**. The ^{1}H- and ^{13}C-NMR assignments are based on selective homodecoupling experiments, on DQF-COSY and HSQC spectra of **43**, **45**, **47**, **53**, **58**, and on HMBC spectra of **48**, **55**, and **60** (*Tables 14–18* in the *Exper. Part*). The relevant parameters of unit I are strongly influenced by the duplex formation and discussed in the following sections, while the NMR parameters of unit II and the ^{13}C-NMR data are usually weakly influenced by the duplex formation and discussed here below. The surprisingly strong downfield shift of H–C(2′/II) or **55** is discussed in *Sect. 2.4.6*.

The *syn* conformation of the uridinyl unit (unit II) of the U*[c_y]A$^{(*)}$ dimers **41**–**45**, **47**, and **48** is evidenced by the downfield shift of H–C(2′/II) (**41**–**44**: 5.14–5.27, **45**: 5.07, **47**: 5.33, **48**: 5.42 ppm; *Table 14* in the *Exper. Part*). The stronger downfield shift for **47** and **48** suggests that the cyclic duplex of **47** and **48** is characterized by a different *syn* orientation of the uridinyl unit than the linear duplex of **41**–**45**. The two H–C(5′/II) of **41**–**45**, **47**, and **48** resonate as a *s* at 3.81–3.88 ppm. *J*(4′,5′/II) of 6.2–6.9 Hz, and the *J*(1′,2′/II)/*J*(3′,4′/II) ratio $\leq$0.42 evidences a *gt*/*tg* 1:1 equilibrium for the silyloxymethyl group and a strong preference for the (*N*) conformation, as it was observed for the *O(5′)*-silylated U* monomers **13** and **14**. The ^{13}C-NMR spectra of **41**–**48** show the expected chemical shifts (*Table 15* in the *Exper. Part*). C(6′/I), C(7′/I), and C(6/II) resonate at 98.5–100.6, 73.3–76.6, and 136.6–137.7 ppm, respectively.

The *syn* conformation of the adenosyl unit of the A*[c_y]U$^{(*)}$ dimers **52**, **53** and **56**–**59** is evidenced by the downfield shift of H–C(2′/II) (5.62–5.79 ppm; *Table 18* in the *Exper. Part*). H_a–C(5′/II) and H_b–C(5′/II) of these dimers resonate as two *dd*s at 3.61–3.82 ppm. *J*(4′,5′a/II) and *J*(4′,5′b/II) of 6.5–7.8 Hz and *J*(1′,2′/II)/*J*(3′,4′/II) = 0.4–0.6 evidence a *gt*/*tg* ratio of *ca.* 1:1 for the silyloxymethyl group and a preference of the (*N*) conformation, as it was observed for the *O(5)*-silylated A* monomers **25**, **26**, **29**, and **30**. HO–C(5′/II) of the alcohols **55** and **60** forms a H-bond to N(3/II), as revealed by the downfield shift of the OH signal (6.77 and 6.51 ppm, resp.), the small *J*(4′,5′a/II), *J*(4′,5′b/II), and *J*(5′a,OH/II) values (all $<$1.5 Hz), the large *J*(5′b,OH/II) value ($\geq$9.9 Hz), and the (*S*) conformation (*J*(1′,2′/II)/*J*(3′,4′/II) $\approx$ 6). The ^{13}C-NMR spectra of **51**–**60** show the expected chemical shifts (*Table 17* in the *Exper. Part*). C(6′/I), C(7′/I), and C(8/II) resonate at 93.4–95.6, 71.5–75.4, and 133.2–134.9 ppm, respectively.

2.4.2. *Association of the U*[c_y]A$^{(*)}$ Propargyl Alcohols* **41** *and* **43**–**45***: Formation of Linear Duplexes.* These propargyl alcohols form a persistent intramolecular H-bond to N(3/I) (see below) leading to a *gt*-oriented ethynyl moiety. This conformation prevents the formation of cyclic duplexes. Vapour pressure osmometry (VPO) determinations of the apparent molecular mass for $CHCl_3$ solutions of **43** show a concentration-dependent low degree of association, as expressed by the ratio of the apparent and the simplex-related molecular mass (1.13, 1.28, and 1.46 at concentrations of 7, 14, and 28 mM, resp.; *Table 5*). This agrees well with an equilibrium between simplex, linear duplexes, and perhaps small amounts of higher associates.

The concentration dependence of δ(HN(3)) was determined for 1 to 50 mM solutions in $CDCl_3$ of **43**–**45**, and for 1 to 10 mM solutions of the much less soluble **41** (*Fig. 4*,*a*). The curves show a progression typical of linear duplexes and higher associ-

Table 5. *Determination of the Association of the U*[c_y]A Dimers* **42**, **43**, *and* **47**, *and of the U*[c_y]A$^{(*)}$ Dimers* **52**, **56**, *and* **58** *in $CHCl_3$ by Vapour Pressure Osmometry*

	43			**52**	**42**	**47**	**56**	**58**
Molecular mass	1038.3			926.3	926.3	753.9	769.9	753.9
Concentration [mM]	7	14	28	30	30	30	20	30
Experimental mass	1179.1	1329.5	1515.8	1499.6	1736.5	1545.2	1489.5	1480.5
Degree of association	1.13	1.28	1.46	1.62	1.87	2.05	1.93	1.96

ates; *i.e.*, a moderate chemical-shift difference between simplex and duplex ($\Delta\delta$(HN(3/II)) = 2.5–4.0 ppm), a weak bending of the curve at concentrations of 1 to 10 mM, and a continued increase of the downfield shift with increasing concentration. Due to the formation of higher associates, calculations result in too large values for $\delta(HN(3)_{duplex})$ and, hence, in too small K values. Weak associations (K = 39–104 M^{-1}; *Table 3*) were calculated for **41** and **43**–**45**. The ΔH values of −6.2 to −8.4 kcal/mol evidence the formation of linear duplexes, with an average energy of 3–4 kcal/mol per intermolecular H-bond; as discussed below there is only negligible stacking of the nucleobases.

The intramolecular H-bond to N(3/I) of the propargyl alcohols **41** and **43**–**45** is evidenced by the downfield shift of HO–C(5′/I) (7.88–8.28 ppm; *Table 14* in the *Exper. Part*), the small J(5′,OH/I) value (< 1.0 Hz) of the D-*allo*-configured alcohols **41** and **43**, the large J(5′,OH/I) (≥ 10.4 Hz) value of the L-*talo*-configured epimers **44** and **45**, the small J(4′,5′/I) values (≤ 1.5 Hz), and the (*S*) conformation. The stronger downfield shift of HO–C(5′/I) of all these dimers, as compared to the corresponding *C*-silylated or *C*-unsubstituted monomers **32**–**34** (6.35–7.77 ppm), is rationalized by the increased acidity of the *C*-uridinylated propargyl alcohols. This intramolecular H-bond restricts the rotation about the C(4′/I)–C(5′/I) bond, and results in a *gg* conformation (relative to HO–C(5′)). The orientation of the ethynyl group depends on the configuration at C(5′/I), and is best described by the C(4′/I),C(5′/I) torsion angle (relative to this group) as specified by a *tg* conformation of **41** and **43**, and a *gt* conformation of **44** and **45**. H–C(2′/I) of **41**, **43**, **44**, and **45** resonates at the field strength that is characteristic of such intramolecularly H-bonded adenosines (5.14–5.25 ppm).

ROESY Cross-peaks of similar intensity between the signals of HN(3/II) of the uridinyl moiety, and both the H–C(2/I) and H–C(8/I) signals of the adeninyl moiety of a 18.5 mM solution of **44** in $CDCl_3$ evidence an equal proportion of *Watson–Crick*- and *Hoogsteen*-type base-paired duplexes. The *syn* orientation of the adeninyl group of **44** is corroborated by a strong cross-peak between the signals of H–C(1′/I) and H–C(8/I) and a weak cross-peak between the signals of H–C(2′/I) and H–C(8/I). The former cross-peak allows to unambiguously assign the H–C(2/I) signal, resonating downfield to that of H–C(8/I). The ROESY spectrum of **44** suggests that **41**–**45** form *ca.* 1:1 mixtures of the corrugated *Watson–Crick*-type base-paired and the stretched *Hoogsteen*-type base-paired linear duplexes.

The CD spectrum of a 2 mM solution of **41** in $CHCl_3$, recorded in the interval of −10 to 50° in 10° steps, shows a very weak molar ellipticity and a weak dependence on the temperature (*Fig. 6*), evidencing the absence of π-stacking. This agrees well with the expectation that the linear duplexes of **41**–**45** are not π-stacked.

2.4.3. *Association of the U*[c_y]A$^{(*)}$ Dimers* **42**, **47**, *and* **48**: *Formation of Cyclic,* Watson–Crick *H-Bonded Duplexes.* VPO Measurements for 30 mM solutions of **42** and **47** in $CHCl_3$ show a degree of association of 1.87 and 2.05, respectively (*Table 5*) evidencing the formation of cyclic duplexes.

The concentration dependence of δ(HN(3)) for 1 to 50 mM solutions of **42**, **47**, and **48** in $CDCl_3$ shows the typical curve progression of cyclic duplexes; *i.e.*, a large chemical shift difference between simplex and duplex ($\Delta\delta$(HN(3/II)) = 5–6 ppm), a strong bending of the curve at concentrations of 1 to 10 mM, and a curve linearity (plateau) at higher concentrations (*Fig. 4*, *a*). Thus, the disilyl ether **42** and the *C(5′/I)*-deoxy compounds **47** and **48** show a dilution curve that evidences a simplex/duplex equilibrium

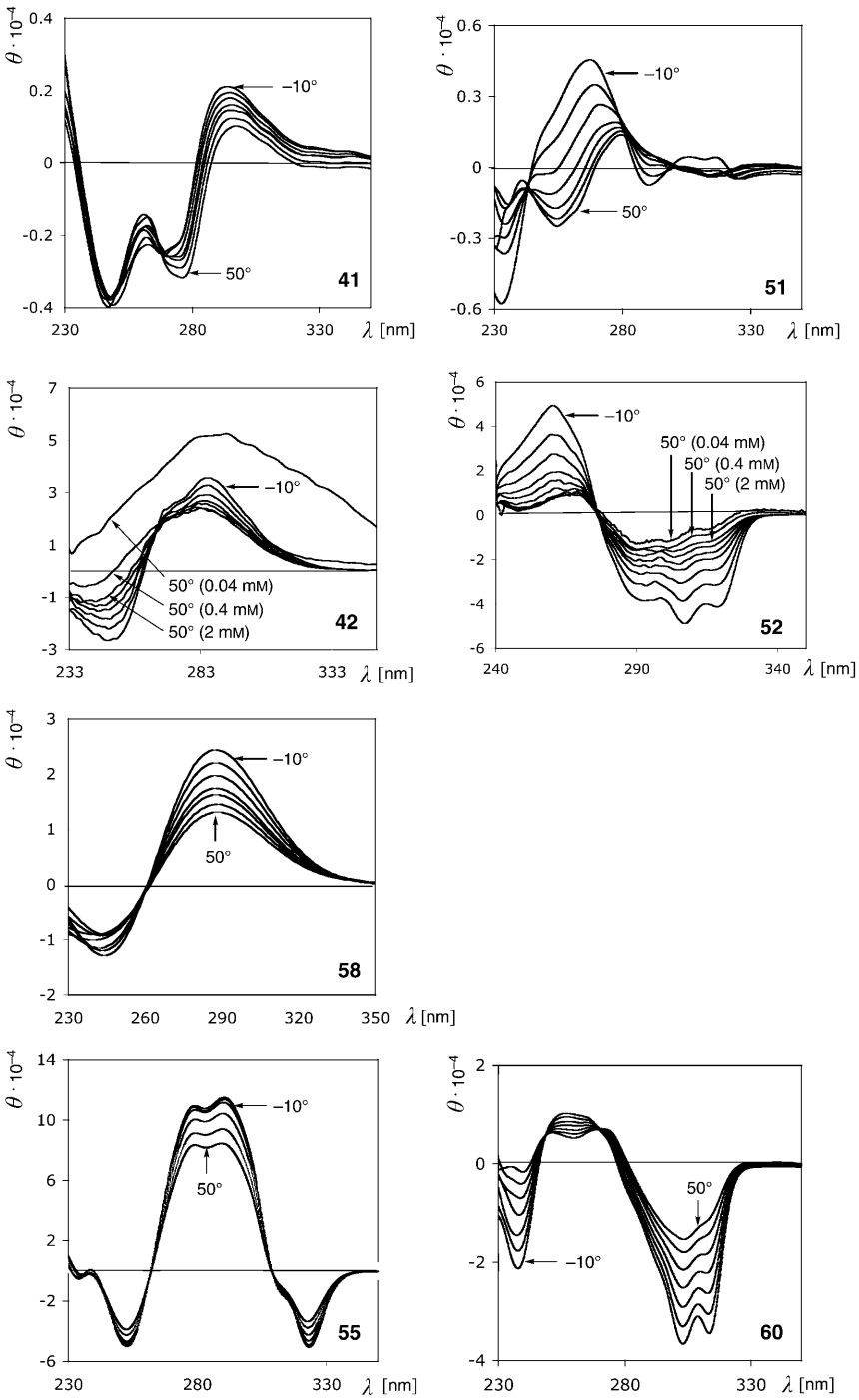

Fig. 6. *CD Spectra recorded in 10° steps from −10 to 50° for 2* mM *solutions of* **41**, **42**, **51**, **52**, *and* **58**, *and for 1* mM *solutions of* **55** *and* **60** (**42** and **59**: with two additional curves recorded for 0.4 and 0.04 mM solutions at 50°)

at concentrations up to 10 mM, and the essentially complete formation of one or several cyclic duplexes at higher concentrations. The cyclic duplexes of **42**, **47**, and **48** show a 10–30-times stronger association ($K = 702–1159$ M^{-1}; *Table 3*) than the linear duplexes of **41** and **43**–**45**, evidencing the co-operative formation of the two base pairs. The ΔH values of -14.0 to -15.7 kcal/mol suggest an energy gain of 3.5–4 kcal/mol per intermolecular H-bond, assuming a small contribution only of stacking in the non-polar solvent, as discussed below.

Upon increasing the concentration, the *C(5′/I)*-deoxygenated dimers **47** and **48** show a parallel decrease of $J(4',5'a/I)$ and $J(4',5'b/I)$ values, evidencing an increasing relative population of the *gg* conformation (*Table 4*). This observation agrees well with the progressive shift of the equilibrium towards a duplex possessing the *gg* conformation. Similarly, the $J(4',5'/I)$ value of the D-*allo*-configured A*[c$_y$]U disilyl ether **42** decreases from 5.7 to 4.2 Hz with increasing concentration. Considering only staggered conformations, these values reflect the $gt_C : (gg_C + tg_C)$ ratio (see *Fig. 2*). The decreasing population of the gt_C conformation of **42** agrees with an increasing proportion of a duplex possessing the gg_C conformation.

The downfield shift of H–C(2′/I) of **42**, **47**, and **48** (5.92–5.97 ppm for 60 mM solutions in $CDCl_3$; *Table 14* in the *Exper. Part*) evidences a s*yn* orientation of the adeninyl moiety. The *syn* conformation of the U*[c$_y$]A dimers **42** and **47**, and a stronger downfield shift for H–C(2′/I) of **42**, **47**, and **48** than for H–C(2′) of the *O(5′)*-silylated A* monomers **25**, **26**, and **30** ($\Delta\delta \approx 0.1$ ppm) is due to the formation of cyclic duplexes.

ROESY Spectra were recorded for 30, 22, and 15 mM solutions of **42**, **47**, and **48** in $CDCl_3$. H–C(2/I) and H–C(8/I) of the U*[c$_y$]A dimers are identified on the basis of strong ROESY cross-peaks between the signals of H–C(1′/I) and H–C(8/I) of **42** and **47**; the assignment is corroborated by the HSQC spectrum of **47** (C(8) is typically found at *ca.* 140 and C(2) at 152–153 ppm). This shows that H–C(2/I) resonates at lower field than H–C(8/I). ROESY Cross-peaks between the signals of HN(3/II) and H–C(2/I) of **42**, **47**, and **48** evidence *Watson–Crick*-type base pairing that appears to be characteristic of the cyclic duplexes of **42**, **47**, and **48**. The *Hoogsteen*-type H-bonds that are evidenced by a weak ROESY cross-peak between the signals of HN(3/II) and H–C(8/I) of **47** belong presumably to minor amounts of a linear duplex.

The CD spectrum of a 2 mM solution of **42** in $CHCl_3$, recorded at -10 to 50° in 10° steps, shows a medium molar ellipticity. This observation and the temperature dependence (*Fig. 6*) evidence a moderate degree of π-stacking, presumably due to partial π-stacking of the base pairs of the cyclic duplexes of **42**, **47**, and **48**. No π-stacking is observed for the simplex of **42** that is exclusively present in 0.4 and 0.04 mM solutions at 50°.

Modelling of the structure of the cyclic duplexes is complicated by the fact that three different structures have to be considered for each pairing system, *i.e.*, two C_2- and one C_1-symmetric duplex. Since the NMR data were obtained of rapidly equilibrating mixtures, C_1-symmetric duplexes cannot be excluded *a priori*. As shown by the ROESY spectra of **42** and **47**, modelling of the U*[c$_y$]A$^{(*)}$ duplexes **42**·**42**, **47**·**47**, and **48**·**48** can be restricted to duplexes possessing *Watson–Crick*-type base pairing. The six possible U*[c$_y$]A$^{(*)}$ duplexes **UA1**–**UA6** possessing *Watson–Crick* and reverse-*Watson–Crick* base pairing were constructed with *Maruzen* models. The schematic representation of these duplexes (*Fig. 7*) indicates the orientation of the adeninyl

and ethynyl moieties, and the destabilizing intramolecular nonbonding interactions between the two ribosyl moieties (marked with *). These nonbonding interactions may be alleviated if the duplex adopts a larger roll angle. In the χ^{+120} (high *syn* [37–40])[8]) and in the χ^{-60} (high *anti*) conformers, the adeninyl moiety is orthogonal to the C(1′/I)–O(4′/I) bond, and the resulting $\pi \rightarrow \sigma^{*}_{C-O}$ interaction stabilizes both conformers. The χ^{+120} conformer is probably also stabilized by a C(2′/I)–H···N(3/I) H-bond [37], while the χ^{-60} conformer is destabilized by the steric interaction of H–C(2′/I) with the substituent at C(8) (**42** and **47**: H, **48**: $CH_2OSi^tBuPh_2$; the interactions are marked with ★ in *Fig. 7*). Only the C_2-symmetric duplexes **UA1** and **UA5** possess the required *gg* orientation of both ethynyl moieties, and are compatible with the bulky silyl substituents of **42** and **48**. The *Watson–Crick* base-paired duplex **UA1** ($\chi \approx 120°$)

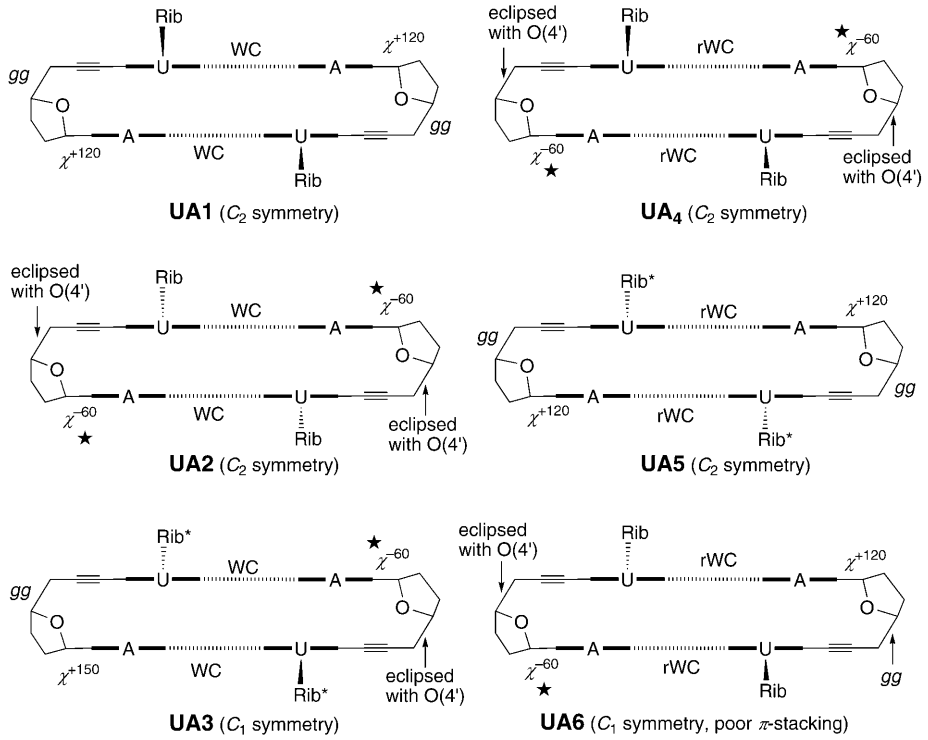

Fig. 7. Maruzen-*modelled cyclic duplexes of U*[c$_y$]A$^{(*)}$ dimers connected by* Watson–Crick (*WC*) *and reverse*-Watson–Crick (r*WC*) *base pairing: schematic representations showing the orientation of the adeninyl and ethynyl moieties, the symmetry, and destabilizing steric interactions* (marked with * or ★)

[8]) The χ angles for unit I of the cyclic duplexes deviate strongly from those typical of *syn*- and *anti*-configured nucleosides ($\chi = +45 \pm 30$ and $-135 \pm 30°$, resp.). To unambiguously characterise the corresponding conformations, we use indexed χ values with the index corresponding to a range of $\pm 15°$. χ^{+150} and χ^{-30} are two additional minima usually not observed in solution. For nucleosides possessing a χ^{+150} orientation of the nucleobase in the solid state, see [41].

is favoured over the reverse-*Watson–Crick* base-paired duplex **UA5**, since the latter is severely destabilized by steric interactions between the two ribosyl moieties.

The *Watson–Crick* H-bonded **UA1** duplex of **48**·**48** was modelled with Macromodel v. 6.0 (AMBER* force field, gas phase; *cf. Fig. 10*). The *gg* orientation of the ethynyl moiety is favoured throughout ($\phi_{CO} = -52°$, *Table 7*), whereas an eclipsing orientation of the adeninyl unit with the C(1′/I)–C(2′/I) bond is disfavoured by the AMBER* calculations; the χ angle is increased to 142°. The representation of **48**·**48** in *Fig. 10* involves partially π-stacked base pairs, in agreement with the CD spectra.

Characteristic inter-unit ROESY cross-peaks are expected for the differently H-bonded duplexes. *Watson–Crick* base pairing of **48** is ascertained by the intramolecular inter-unit cross-peaks H–C(1′/II)/H–C(3′/I), H–C(1′/II)/H_2C(5′/I), H–C(2′/II)/H–C(2/I), and H–C(3′/II)/H–C(2/I) (indicated in *Fig. 10* by double-headed arrows); the additional inter-unit cross-peak H–C(1′/II)/H–C(4′/I) is not a true ROE cross-peak. The ROESY spectra of **42** and **47** show too many cross-peak artefacts (*e.g.*, 8–9 cross peaks with both H–C(2/I) and H–C(8/I) for a confirmation of the *Watson–Crick* H-bonding.

2.4.4. *Association of the* D-allo-*Configured A*[c_y]U Propargyl Alcohols* **51** *and* **54**: Formation of *Linear Duplexes*. The 6-unsubstituted propargyl alcohol **51** forms an organogel in $CDCl_3$ at concentrations above 12 mM. The analogue **54** possessing a more lipophilic silyl protecting group (Si^tBuPh_2 *vs.* Si^iPr_3) is slightly more soluble. The ^{1}H-NMR spectra of 1–2 mM solutions of **51** and **54** in $CDCl_3$ show broadened signals for the uridinyl unit hinting at slowly (NMR time scale) equilibrating mixtures. The upfield shift of H–C(2′/I) at *ca*. 5.00 ppm evidences a predominantly *anti* orientation of the uracilyl moiety that prevents the formation of cyclic duplexes. Hence, an equilibrating mixture of simplex and linear duplexes appears highly probable. Severe line broadening prevents the determination of the concentration dependence of δ(HN(3/I)) and of the thermodynamic parameters by *van't Hoff* analysis.

Due to the poor solubility of **51** and **54** in $CDCl_3$, NMR spectra of **51** and **54** were recorded in (D_6)DMSO and $CDCl_3$/CD_3OD 9:1, respectively (*Tables 16–18* in the *Exper. Part*). δ(HN(3/I)) = 11.5 and δ(H_2N–C(6/II)) = 7.6 ppm indicate that **51** is only present as solvated simplex. The downfield shift of H–C(2′/II) (5.62–5.64 ppm) evidences a *syn* orientation of the adeninyl moiety, and the upfield shift of H–C(2′/I) a predominant *anti* orientation of the uridinyl moiety[9]).

A similar conformation, including the *anti* orientation of the uracilyl moiety, is adopted by **54** in solution and in the solid state. Crystallization of **54** from MeOH gave crystals suitable for X-ray analysis[10])[11]). The crystals are orthorhombic ($P2_12_12_1$ space group). The unit cell contains two molecules of **54**, two ordered molecules of

---

[9]) δ(H–C(2′/I)) of **51** = 5.06 ppm. This has to be compared to 5.26 ppm of the A*[c_y]U* dimer **60**, where the substituted U* moiety is *syn*-oriented and to 4.9–5.02 ppm of monomeric uridines in (D_6)DMSO [42][43].

[10]) The crystallographic data have been deposited with the *Cambridge Crystallographic Data Centre* as deposition No. CCDC-603314. These data can be obtained free of charge *via* http://www.ccdc.cam.ac.uk/cgi-bin/catreq.cgi (or from the *Cambridge Crystallographic Data Centre*, 12 Union Road, Cambridge CB2 1EZ (fax: +441223336033; e-mail: deposit@ccdc.cam.ac.uk)).

[11]) All attempts failed to obtain crystals suitable for X-ray analysis of the U*[c_y]A* and A*[c_y]U* dimers possessing exclusively *syn*-oriented nucleobases.

MeOH, and highly disordered molecules of MeOH (indicated by holes in the structure). The adenosyl unit possesses a *syn*-oriented adeninyl and a *gg*-oriented silyloxymethyl group, and adopts a flattened ^1E conformation (see *Fig. 8,a*, and *Table 6*). The uridinyl unit adopts a ^2E conformation and is further characterized by an *anti*-oriented uracilyl, a *gg*-oriented OH, and a *tg*-oriented ethynyl group. In the crystal, **54** forms two antiparallel strands (*Fig. 8,b*) that are connected by *Watson–Crick* H-bonds (N···H distances: 2.04–2.05 Å). In addition, O=C(4) of the uridine unit accepts a H-bond from the propargylic HO–C(5′) of the other strand (O···H distance: 1.91 Å). Reverse-*Hoogsteen* base pairing connects the adeninyl units of the two strands. The weakness of these reverse A·A *Hoogsteen* H-bonds[12]) is evidenced by the rather large N···H distances of 2.35 and 2.41 Å, and by a buckle twist of 34.5°. To the best of our knowledge, this is the first crystal structure of a dinucleoside analogue possessing both *Watson–Crick* and reverse A·A *Hoogsteen* H-bonds [46]. Intramolecular π-stacking is observed between the adeninyl and one Ph group.

Table 6. *Selected Torsion Angles* [°] *of* **54**·*MeOH in the Crystalline State*

Torsion angle	Mol. A	Mol. B	Torsion angle	Mol. A	Mol. B
Adenosyl unit			Uridinyl unit		
O(4′)–C(1′)–N(7)–C(4) (χ)	76.5	74.7	O(4′)–C(1′)–N(1)–C(2) (χ)	−123.1	−117.4
C(3′)–C(2′)–C(1′)–N(7)	107.7	115.4	C(3′)–C(2′)–C(1′)–N(1)	134.9	142.1
O(2′)–C(2′)–C(1′)–N(7)	−141.2	−130.7	O(2′)–C(2′)–C(1′)–N(1)	−112.6	−105.2
C(1′)–C(2′)–C(3′)–C(4′)	11.0	1.6	C(1′)–C(2′)–C(3′)–C(4′)	−16.0	−24.2
C(2′)–C(3′)–C(4′)–O(4′)	−3.9	4.2	C(2′)–C(3′)–C(4′)–O(4′)	10.1	16.9
C(2′)–C(3′)–C(4′)–C(5′)	−125.0	−118.7	C(2′)–C(3′)–C(4′)–C(5′)	−109.9	−102.4
O(3′)–C(3′)–C(4′)–C(5′)	120.6	126.7	O(3′)–C(3′)–C(4′)–C(5′)	139.4	147.3
C(3′)–C(4′)–C(5′)–O(5′) (ϕ_{OC})	−177.9	−169.4	C(3′)–C(4′)–C(5′)–O(5′) (ϕ_{OC})	43.9	46.5
O(4′)–C(4′)–C(5′)–O(5′) (ϕ_{OO})	62.9	69.9	O(4′)–C(4′)–C(5′)–O(5′) (ϕ_{OO})	−75.4	−71.5
			C(3′)–C(4′)–C(5′)–C(6′) (ϕ_{CC})	−76.0	−74.5
			O(4′)–C(4′)–C(5′)–C(6′) (ϕ_{CO})	164.7	167.5

The CD spectrum of a 2 mM solution of **51** in $CHCl_3$, recorded at −10 to 50° in 10° steps, shows a very small molar ellipticity and a weak temperature dependence (*Fig. 6*), evidencing at best a very weak π-stacking, in agreement with the expectation that the stretched linear duplexes of **51** and **54** are hardly π-stacked. In the solid state structure of **54**·MeOH, there is indeed only intramolecular π-stacking between the adeninyl moiety and a Ph group of the silyl protecting group (see above and *Fig. 8*).

2.4.5. *Association of the A*[c$_y$]U$^{(*)}$ Dimers* **52** *and* **58**–**60**: *Formation of Cyclic* Watson–Crick *H-Bonded Duplexes.* VPO Measurements for a 30 mM solution of **58** in $CHCl_3$ show a degree of association of 1.96 (*Table 5*), evidencing the formation of cyclic duplexes. VPO for the A*[c$_y$]U dimer **52** indicates a lower degree of association of 1.62, suggesting an equilibrium of the simplex with linear and cyclic duplexes. The striking difference between **52** and **58** is rationalized by the destabilisation of the *syn* conformer

[12]) For reverse-*Hoogsteen* A·A base pairing of homo-DNA oligoadenylates, see [44], and for the homopairing of adenine, see [45] and refs. cit. there.

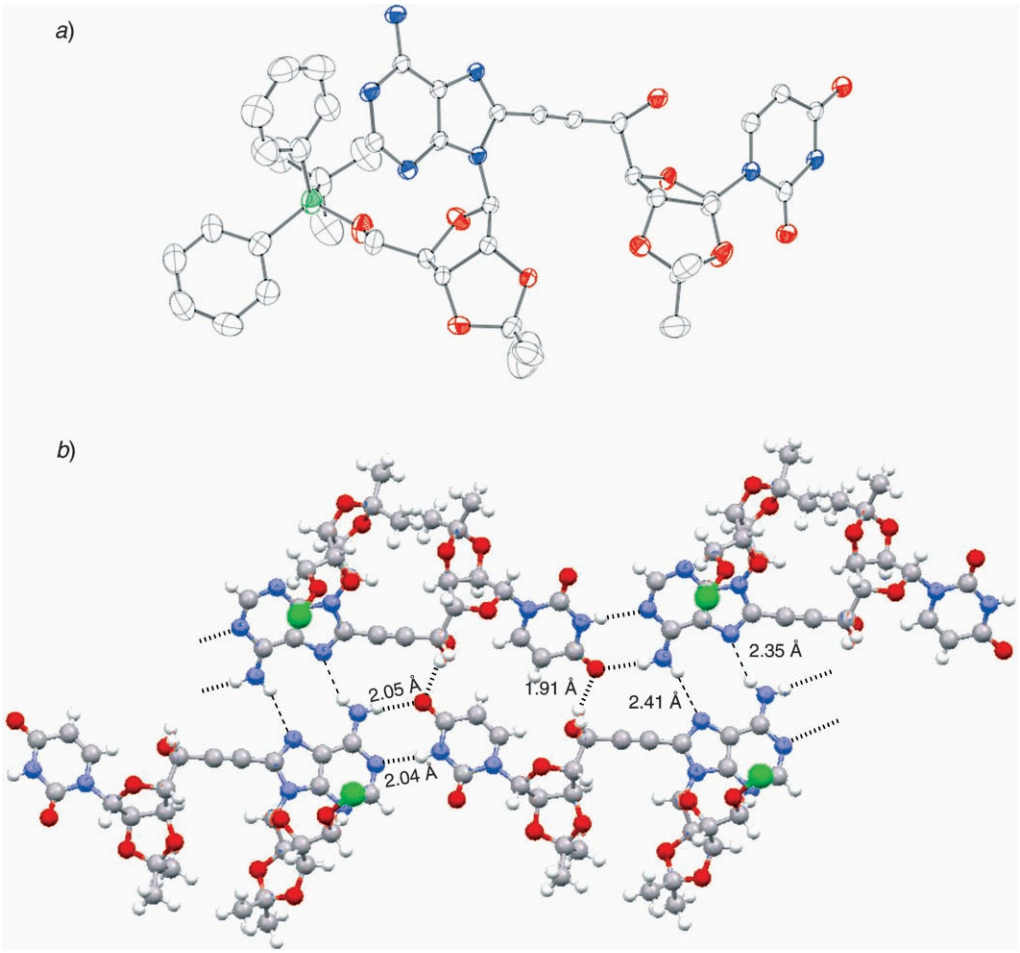

Fig. 8. *Crystal structure of* (**54**·MeOH)$_2$: a) *ORTEP representation* (heavy atoms only) *of one molecule of* **54** *and* b) *intermolecular H-bonding of* **54** (MeOH and substituents at the Si-atoms omitted to enhance clarity)

of **52** by the sterically demanding propargylic $^{i}Pr_3SiO$ group. The *anti* conformers can only form linear duplexes and higher associates.

The concentration dependence of δ(HN(3)) for 1 to 50 mM solutions of **52** and **58**–**60** in $CDCl_3$ shows the typical curve progression of cyclic duplexes (*Fig. 4*, *b*). A slight continued concentration dependence, expressed by the curves of the A*[c$_y$]U dimers **52** and **58** at higher concentrations, suggests the formation of minor amounts of linear duplexes and higher associates, probably derived from the disfavoured conformer of the simplex possessing an *anti*-oriented uracilyl moiety. The weak association of the A*[c$_y$]U dimers **52** and **58** ($K = 197–277$ M^{-1}; *Table 3*) and the 6.5 times stronger association of the A*[c$_y$]U* dimer **59** ($K = 1793$ M^{-1}) agree well with this conclusion. The ΔH values of **52**, **58**, and **59** (-13.4 to -15.5 kcal/mol) evidence an average energy

of 3.5–4 kcal/mol per intermolecular H-bond. The strong association of the alcohol **60** ($K = 2307\ M^{-1}$) suggests that co-operativity between the intra- and the intermolecular H-bonds results in a stronger base pairing, as expressed by a ΔH value of -18.4 kcal/mol.

The $J(4',5'a/I)$ and $J(4',5'b/I)$ values of the *C(5′/I)*-deoxygenated dimers **58**–**60** remain constant over the whole concentration range (1 up to 114 mM for **58**; *Table 4*). The value of these coupling constants suggests a *gg*/*gt*/*tg* equilibrium of *ca.* 1:1:1 for the simplex of **59**, and a *gg*/*gt*/*tg* equilibrium of *ca.* 0.6:1.2:1.2 for the simplex of **58** and **60**. These rotameric equilibria are clearly different from those of duplexes that possess a (staggered) *gg*-oriented ethynyl group. Hence, duplexes possessing non-staggered ethynyl groups that are more or less eclipsed with either O(4′/I) or C(3′/I) must also be taken into account. There are two regions of ϕ_{CO} (*ca.* 20 and 210°; *Fig. 5*) correlating with $J(4',5'a)$ and $J(4',5'b)$ values that agree well with the (large) experimental values for **58**–**60**. These two conformers are within the range of rotamers capable of forming cyclic duplexes, as indicated by the yellow bar below the energy diagram. The destabilisation of the corresponding rotamers (20° rotamer: 3.6 kcal/mol, 210° rotamer: 1 kcal/mol) should be easily compensated by the energy gained upon formation of the second base pair.

In contradistinction to the above discussed concentration-indifferent $J(4',5'/I)$ values of **58**–**60**, those of the D-*allo*-configured U*[c_y]A disilyl ether **52** increase from 4.5 to 5.1 Hz with increasing concentration. This reveals the formation of a duplex possessing an ethynyl group that is more or less eclipsed with either O(4′/I) or C(3′/I); the relative energy of the rotamers expressed by the red curve in *Fig. 5*, *b* is again in favour of the rotamers with a ϕ_{CO} torsion angle of *ca.* 20 and 210°.

The chemical shift for H–C(2′/I) of the *C(5′/I)*-deoxygenated dimers **58**–**60** (5.17–5.35 ppm; *Table 18* in the *Exper. Part*) evidences that the *syn* conformers dominate almost completely. The upfield shift for H–C(2′/I) of the disilyl ether **52** (5.00 ppm) reveals a *ca.* 1:1 s*yn*/*anti* equilibrium, in keeping with the VPO measurement which evidences a mixture of linear and cyclic duplexes. Steric interactions between the *C(5′/I)*-silyloxy and the uracilyl group are responsible for the stronger preference for the *anti* conformer of **52** than of **58**.

ROESY Spectra were recorded of 13, 44, and 15 mM solutions of **52**, **58**, and **60** in $CDCl_3$. Strong ROESY cross-peaks between the signals of HN(3/I) and H–C(2/II) evidence *Watson–Crick*-type base-paired duplexes. Hence, exclusive *Watson–Crick*-type base pairing is assumed for **52** and **58**–**60**, although *Hoogsteen*-type base pairing could not be observed directly, as these dimers lack H–C(8/II). A *syn*/*anti* equilibrium of the uridinyl unit of **52** and **58** is suggested by cross-peaks between the signal of H–C(6/I) and the signals of H–C(1′/I), H–C(2′/I), and H–C(3′/I).

The CD spectra of 2 mM solutions of **52** and **58**, and of a 1 mM solution of **60** in $CHCl_3$, recorded at -10 to 50° in 10° steps, show a similar medium molar ellipticity as for **42**. This observation, and the temperature dependence (*Fig. 6*) evidence a moderate degree of π-stacking that is reduced for 0.4 and 0.04 mM solutions of **52** at 50°. The CD spectra thus suggest a partial π-stacking of the base pairs of the cyclic duplexes of **52** and **58**–**60**.

The C_1-symmetric duplex structures **UA3** and **UA6** in *Fig. 7* show both orientations of the ethynyl moiety, as observed for the corresponding C_2-symmetric duplexes **UA1**,

UA2, **UA4**, and **UA5**, respectively. Hence, the unfavourable steric interactions in a C_2-symmetric duplex will also be present in the corresponding C_1-symmetric duplex, so that modelling of the A*[c_y]U$^{(*)}$ dimers can be restricted to the C_2-symmetric duplexes. The A*[c_y]U$^{(*)}$ dimers **52** and **58**–**60** show *Watson–Crick*-type base pairing and an orientation of the ethynyl moiety that deviates from an optimal *gg* conformation. *Maruzen* modelling suggests that the *Watson–Crick* base-paired duplex **AU1** and the reverse-*Watson–Crick* base-paired duplex **AU4** are equally favoured over **AU2** and **AU3** (*Fig. 9*). The preferred duplexes show the expected distorted *gg* conformation of the

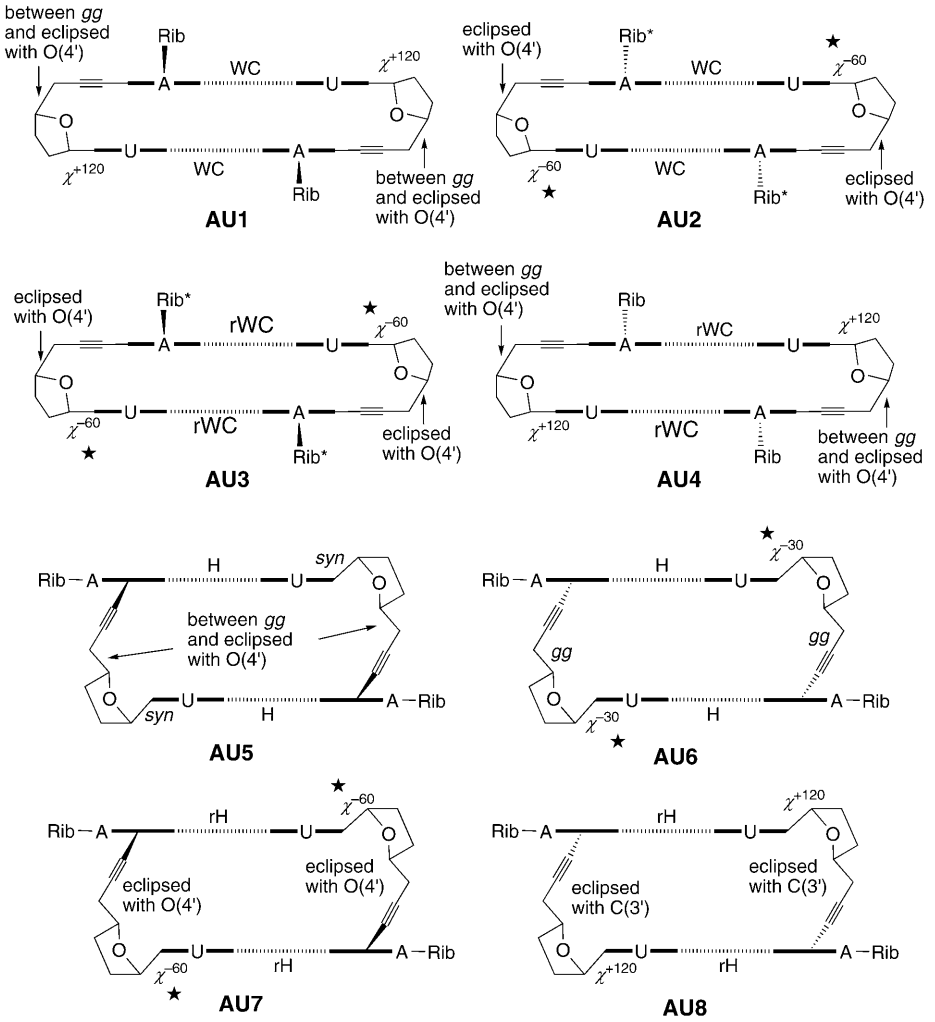

Fig. 9. Maruzen-*modelled* C_2-*symmetric cyclic duplexes of A*[c_y]U$^{(*)}$ dimers connected by* Watson–Crick (*WC*), *reverse*-Watson–Crick (r*WC*), Hoogsteen (*H*), *and reverse*-Hoogsteen (r*H*) *base pairing: schematic representations showing the orientation of the uracilyl and ethynyl moieties, the symmetry, and destabilizing steric interactions* (marked with * or ★)

ethynyl moiety, and are compatible with the sterically demanding substituent at C(6/I) of **59** and **60**.

The *Watson–Crick* H-bonded duplex **AU1** and the reverse-*Watson–Crick* H-bonded duplex **AU4** of **60**·**60** were modelled with Macromodel (*Fig. 10*). The eclipsing arrangement of the uridinyl moiety with the C(1′/I)–C(2′/I) bond ($\chi \approx 120°$ by *Maruzen* modelling) is changed to a *syn* orientation ($\chi = 58–84°$, *Table 7*). The torsional strain associated with the distorted *gg* orientation of the ethynyl moiety (ϕ_{CO} of *ca.* $-30°$ by *Maruzen* modelling) is alleviated by Amber* modelling ($\phi_{CO} = -47$ to $-52°$). Both structures of **60**·**60** (*Fig. 10*) show π-stacking of the purine bases only, in agreement with the CD spectra. The *Watson–Crick* H-bonded duplex of **60**·**60** may be slightly favoured over the reverse-*Watson–Crick* H-bonded duplex, as suggested by smaller propeller twist angles (3 and 12 *vs.* 23–25°).

Table 7. *Selected Distances* [Å] *and Torsion Angles* [°] *for Unit I of the Duplexes Connected by* Watson–Crick (**48**·**48**, **56**·**56**, **60**·**60**), *reverse*-Watson–Crick (**60**·**60**), Hoogsteen (**57**·**57**), *and reverse*-Hoogsteen (**55**·**55**) *H-Bonds*

	48·**48** (*WC*)	**56**·**56** (*WC*)	**60**·**60** (*WC*)	**60**·**60** (r*WC*)	**57**·**57** (*H*)	**55**·**55** (r*H*)
Distance N(3)H···N(1 or 7)	1.75	1.79	1.80	1.79	1.81	1.80
Distance NH···O=C(4 or 2)	1.75	1.73	1.72	1.70	1.74	1.73
Distance O(5′)H···O=C(2 or 4)	–	–	–	–	1.80	1.77
Distance O(5′)H···O(4′)	–	2.31	–	–	–	–
Distance between base pairs	3.41	3.2	3.45	3.35	3.4	3.4–3.6
χ of unit I	142	80, 87	70, 84	58, 73	65, 75	60, 79
ϕ_{CO} of unit I	−52	−55	−48, −52	−47	−23, −28	−58
Propeller twist	−17	2, 5	3, 12	23, 25	20, 22	22, 27

The ROESY spectrum of the A*[c_y]U* dimer **60** shows intramolecular inter-unit ROESY cross-peaks H–C(1′/II)/H–C(3′/I), H–C(1′/II)/H–C(5′/I), Me_{endo}/II/H–C(3′/I), and Me_{endo}/II/H–C(5′/I), as indicated in *Fig. 10* by double-headed arrows. The cross-peaks confirm the *Watson–Crick* base pairing; there are no cross-peaks to suggest reverse-*Watson–Crick* base pairing. The ROESY spectra of **52** and **58** also show the expected H–C(1′/II)/H–C(3′/I) and H–C(1′/II)/H–C(5′/I) cross-peaks, corroborating the *Watson–Crick* H-bonding. They also show several other inter-unit cross-peaks presumably originating from minor amounts of linear duplexes.

2.4.6. *Association of the* D-allo-*Configured A*[c_y]U* Propargyl Alcohols* **53** *and* **55**: *Formation of Cyclic Reverse*-Hoogsteen *H-Bonded Duplexes.* The concentration dependence of δ(HN(3)) for 1 to 50 mM solutions of **53** in $CDCl_3$ shows the typical curve progression of cyclic duplexes, whereas the curve of **55** lacks the characteristic bending at low concentrations (*Fig. 4*, *b*). Extrapolation of the curve for **55** leads to a δ(HN(3/I)) at 0 mM of *ca.* 11.5 ppm (*Fig. 4*, *c*; compare with *ca.* 8.0 of **53**). Repetition of the measurement showed that the sigmoidal progression at low concentrations is a consequence of the small shift differences. The different curve progression for **53** and **55** evidences a simplex/duplex equilibrium of **53** and a linear duplex/cyclic duplex equilibrium of **55**. A comparison of **55** with the 5′-deoxy analogue **60** evidences that the propargylic OH group of **55** is responsible for the enhanced stability of the duplexes.

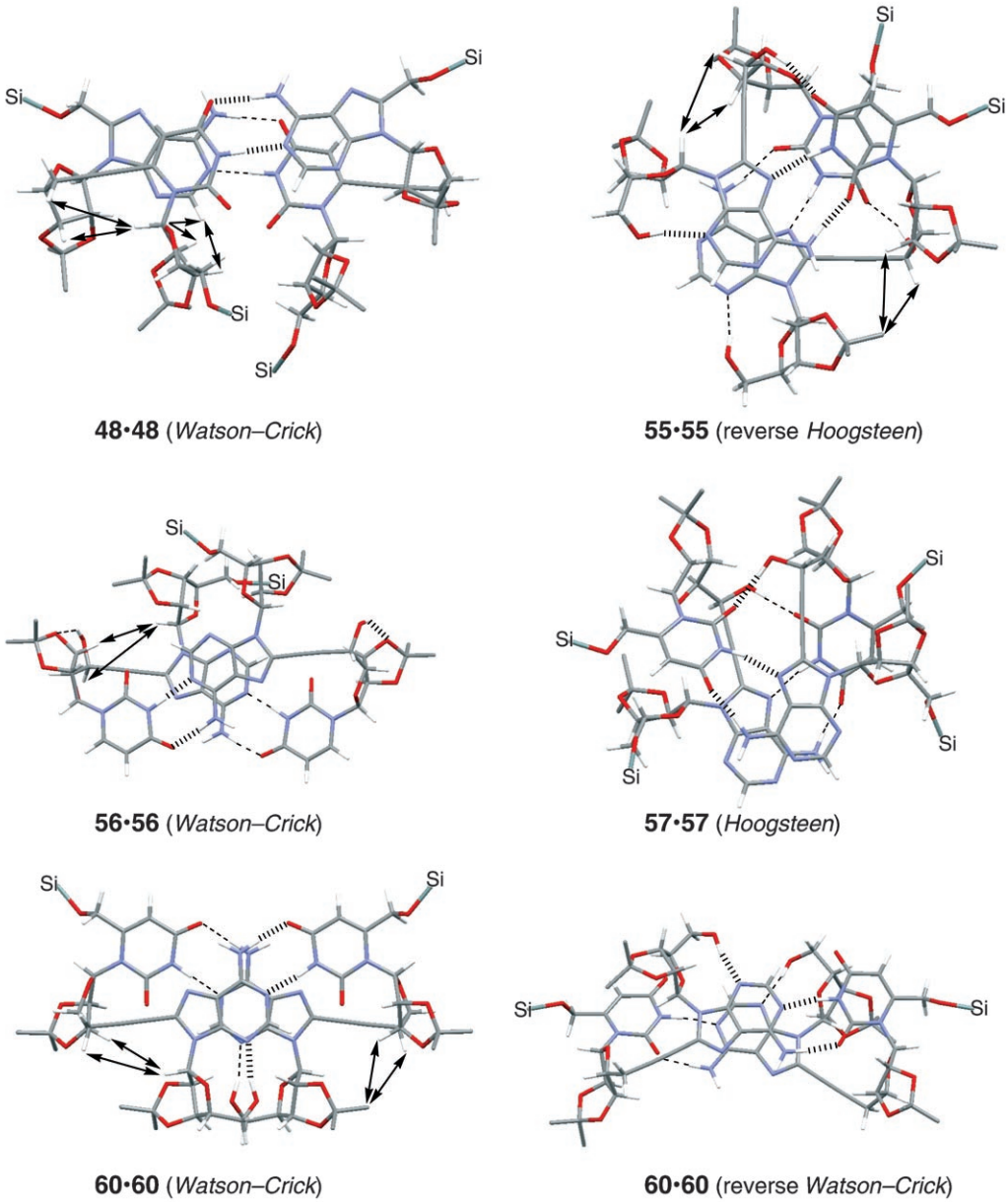

Fig. 10. *AMBER*-Modelled cyclic duplexes connected by* Watson–Crick (**48**·**48**, **56**·**56**, and **60**·**60**), Hoogsteen (**57**·**57**), *and reverse*-Hoogsteen (**55**·**55**) *base pairing: H-bonds marked with hashed* (base pair in the foreground) *and dashed* (base pair in the background) *bonds* (for enhanced visibility, the substituents at Si- and the isopropylidene H-atoms are omitted). Inter-unit interactions (ROEs) are indicated by double-headed arrows.

The monoalcohol **53** associates rather weakly ($K = 364\ M^{-1}$; *Table 3*), and the energy of the association, -11.4 kcal/mol, is rather small. The different ΔH values of **53** and **52**/**58**–**60** may be due to the different types of base pairing. Since the δ(HN(3/I))/Δc curve of **55** reflects the equilibrium between linear and cyclic duplexes, the equilibrium between simplex and duplexes, and the corresponding thermodynamic parameters cannot be determined. The high stability of the duplexes of **55**, however, evidences that the association is even stronger than the one of the deoxy analogue **60** ($K = 2307\ M^{-1}$).

Line broadening of the H–C(4′/I) and H–C(5′/I) signals precludes a determination of the concentration dependence of J(4′,5′/I) values of **53** and **55**.

The downfield shift of H–C(2′/I) (5.28–5.31 ppm; *Table 18* in the *Exper. Part*) and J(1′,2′/I)/J(3′,4′/I) ≤ 0.2 of **53** and **55** evidences a *syn* orientation of the uridinyl moiety and an (*N*) conformation of the furanose ring. HO–C(5′/I) of **53** and **55** resonates as broad *s* at 5.11 to 5.34 ppm; the absence of J(5′,OH/I) couplings does not allow to determine the persistence of the intramolecular O(5′/I)–H···O=C(2/I) H-bond.

Surprisingly, H–C(2′/II) of the diol **55** is strongly shifted downfield to 5.84 ppm, whereas H–C(2′/II) of the corresponding mono-alcohol **60** resonates at the expected position (5.27 ppm). This chemical shift and the strong upfield shift of H–C(5/I) of **55** (5.19 *vs.* 5.98 ppm for **60**) evidence that **55** and **60** form a differently base-paired cyclic duplex; anisotropy effects must be responsible for the surprising shifts of H–C(2′/II) and H–C(5/I) of **55**. Since weak duplexes dissociate to a large extent in DMSO solution, the striking differences between the ^{1}H-NMR spectra of the diol **55** and the monoalcohol **60** in $CDCl_3$ should disappear for solutions in (D_6)DMSO. The spectra of **55** and **60** in (D_6)DMSO are indeed very similar ($\Delta\delta$(H–C(2′/II)) = 0.02 and $\Delta\delta$(H(5/I) = 0.03 ppm; *Table 16* in the *Exper. Part*). The OH groups of **55** and **60** are completely solvated (δ(HO–C(5′/II) = 5.26–5.27 ppm, J(5′,OH/II) = 5.4–6.3 Hz; δ(HO–C(5′/I) = 6.38–6.59 ppm; J(5′,OH/I) = 6.2–6.9 Hz). H–C(2′/II) of **55** and **60** is shifted upfield to 5.46–5.48 ppm, evidencing that also the intermolecularly H-bonded HO–C(5′/II) induces an upfield shift. H–C(2′/I) of the 6-substituted dimer **55** and **60** resonates at the expected position for a *syn*-oriented uridinyl unit (5.25–5.26 ppm).

Hoogsteen-type base-paired duplexes of **55** are evidenced by the absence of a cross-peak between the signals of HN(3/I) and H–C(2/II) in the ROESY spectrum (15 mM in $CDCl_3$); the same type of base pairing is also assumed for **53**.

The CD spectrum of a 1 mM solution of **55** in $CHCl_3$, recorded at -10 to 50° in 10° steps, shows a large, temperature-dependent molar ellipticity (*Fig. 6*) and evidences extensive π-stacking, presumably involving the purine and pyrimidine bases of **53** and **55**.

The propargylic HO–C(5′/I) of **53** and **55** may have a significant effect upon the type of duplex that is formed, and the H-bonding of this OH group in the duplexes must be analysed. The ROESY spectrum of **55** evidences *Hoogsteen*-type base pairing. The *Hoogsteen* H-bonded duplex **AU5** and the reverse-*Hoogsteen* H-bonded duplex **AU8** are clearly favoured over **AU6** and **AU7** (*Fig. 9*). In **AU8**, HO–C(5′/I) of the D-*allo*-configured **53** and **55** can form an intermolecular H-bond to O=C(4/I), whereas neither an intra- nor an intermolecular H-bond can be formed in the *Hoogsteen* H-bonded duplex **AU5**. Hence, one expects reverse-*Hoogsteen* base pairing for **53** and **55**.

AMBER* Modelling of the reverse-*Hoogsteen* H-bonded duplex **AU8** of **55** shows that the intermolecular H-bond of HO–C(5′/I) is maintained. The eclipsing orientation

of the uracilyl and the ethynyl moieties is converted to a *syn* and a *gg* conformation ($\chi = 60-79°$, $\phi_{CO} = -58°$; *Table 7*) at the expense of pronounced propeller twisting (22–27°). The representation in *Fig. 10* evidences that there is favourable π-stacking of the purine and pyrimidine bases, in agreement with the large molar ellipticity in the CD spectrum.

The reverse-*Hoogsteen* base pairing of the duplex **55**·**55** is confirmed by the intramolecular inter-unit ROESY cross-peaks H–C(1′/II)/H–C(3′/I), H–C(1′/II)/H–C(5′/I), Me_{endo}/II/H–C(3′/I), and Me_{endo}/II/H–C(5′/I) indicated in *Fig. 10* by double-headed arrows. The additional inter-unit cross-peaks H–C(1′/II)/H–C(4′/I) and Me_{endo}/II/H–C(4′/I) cannot be true ROE cross-peaks.

The surprising downfield shift of H–C(2′/II) of **55** in $CDCl_3$ (5.84 ppm; **60**: 5.27 ppm) is rationalised in the following way. In both the reverse-*Hoogsteen* H-bonded duplex **55**·**55** and the *Watson–Crick* H-bonded duplex **60**·**60**, H–C(2′/II) of **55**·**55** is located in the plane midway between the planes of the base pairs at the intersection with a second, orthogonal plane going through the σ-lone pairs of $N(3/II_{intra})$ and $N(1/II_{inter})$ but moved slightly away from the π-stacked adeninyl moieties, whereas H–C(2′/II) of **60**·**60** is shifted laterally away from the orthogonal plane going through the σ-lone pairs of $N(3/II_{intra})$ and $N(1/II_{inter})$. The proximity of H–C(2′/II) and these two σ-lone pairs of **55**·**55** (bifurcated H-bond?) is responsible for the downfield shift. The upfield shift of H–C(5/I) of **55** (5.19 ppm; **60**: 5.62 ppm) is rationalised by the π-stacking of the uridinyl groups in **55**·**55**, but not in **60**·**60** (see *Fig. 10*).

2.4.7. *Association of the* L-talo-*Configured A*[c_y]U$^{(*)}$ Propargyl Alcohols* **56** *and* **57**: *Formation of Cyclic* Watson–Crick *and* Hoogsteen *H-Bonded Duplexes.* VPO Measurements for a 20 mM solution of **56** in $CHCl_3$ show a degree of association of 1.93 (*Table 5*), evidencing the formation of a cyclic duplex.

The concentration dependence of δ(HN(3)) for 1 to 30 mM solutions of **56** and **57** in $CDCl_3$ shows the typical curve progression of cyclic duplexes. Although **56** and **57** associate by a different type of H-bonding, their association constants K (930 *vs.* 995 M^{-1}; *Table 3*) and ΔH values (−14.0 *vs.* −13.8 kcal/mol) are nearly identical.

The J(4′,5′/I) value of the L-*talo* dimers **56** (3.0–3.3 Hz) and **57** (5.4 Hz) does not depend on the concentration (1–30 mM for **56** and 1–80 mM for **57**; *Table 4*). The different J(4′,5′/I) values evidence a different duplex type of **56** and **57**. The small J(4′,5′/I) value of the duplex of **56** agrees with a conformation close to a staggered gg_C (*Fig. 2*), whereas the larger J(4′,5′/I) coupling of the duplex of **57** suggests a conformation deviating more strongly from the staggered gg_C; the blue curve in *Fig. 5*, *b*, suggests a ϕ_{CO} torsion angle of *ca.* 320°.

The downfield shift for H–C(2′/I) of **57** (5.25–5.31 ppm; *Table 18* in the *Exper. Part*) evidences a *syn* orientation of the uridinyl moiety, whereas the upfield shift of H–C(2′/I) of **56** (5.13 ppm) suggests a *syn*/*anti* equilibrium. Alternatively, however, the shift difference may be due to a different type of base pairing. J(1′,2′/I)/J(3′,4′/I) ≤ 0.7 evidences an (*N*) conformation for **56** and **57**. HO–C(5′/I) resonates as a broad signal at 5.05 (**56**) and at 4.41–4.46 ppm (**57**); the absence of J(5′,OH/I) couplings does not allow to determine the persistence of the intramolecular O(5′/I)–H···O=C(2/I) H-bond.

ROESY Spectra were recorded of a 30 mM solution of **56** and an 11 mM solution of **57** in $CDCl_3$. A ROESY cross-peak between the signals of HN(3/I) and H–C(2/II) in

the spectrum of **56** and its absence in the spectrum of **57** evidence *Watson–Crick*- and *Hoogsteen*-type base pairing for the cyclic duplexes of **56** and **57**, respectively.

Duplex structures **AU1** to **AU8** are depicted schematically in *Fig. 9*. In **AU1** and **AU4**, HO–C(5′/I) of the L-*talo*-configured **56** and **57** can form an intramolecular H-bond to O(4′/I); in **AU5**, it can form an intermolecular H-bond to O=C(2/I), whereas neither an intra- nor an intermolecular H-bond can be formed in **AU8**. Hence, *Watson–Crick* base pairing is expected for **56**, and *Hoogsteen* base pairing for **57**. This surprising difference in H-bonding evidences that the intramolecular H-bonding of HO–C(5′/I) in **AU1** may counterbalance the intermolecular H-bond in **AU5**. An additional factor, possibly intramolecular π-stacking between the adeninyl moiety and a Ph group of the silyl protecting group (similarly as in solid state structure of **54**·MeOH), must be responsible for the preference of **57**·**57** for *Hoogsteen* base pairing.

The intra- and the intermolecular H-bonds of HO–C(5′/I) are maintained during AMBER* modelling of the *Watson–Crick* H-bonded duplex **AU1** of **56** and the *Hoogsteen* H-bonded duplex **AU5** of **57**. The eclipsing orientation of the uracilyl moiety of **56** is converted to a *syn* conformation ($\chi = 80–87°$; *Table 7*), whereas the *syn* conformation of **57** was already present in the *Maruzen*-modelled duplex. The non-staggered conformation of the duplex of **56** was converted to a *gg* conformation ($\phi_{CO} = -55°$), but maintained for the duplex of **57** ($\phi_{CO} = -23$ to $-28°$) that also shows a propeller twisting of 20–22°. These two factors destabilize the *Hoogsteen* H-bonded duplex and may be responsible for the preference for *Watson–Crick* base pairing of **56**.

The ROESY spectrum of **56** shows the H–C(1′/II)/H–C(3′/I) and H–C(1′/II)/H–C(5′/I) cross-peaks expected for a *Watson–Crick* H-bonded duplex. The cross-peaks are indicated in *Fig. 10* by double-headed arrows. The spectrum shows also several other inter-unit cross-peaks, presumably stemming from minor amounts of linear duplexes. The shortest contacts between H-atoms of the A and U units of the *Hoogsteen* base-paired **AU5** duplex **57**·**57** are observed between H–C(3′/II) and CH_2–C(6/I) (3.6–3.8 Å), but the expected cross-peaks H–C(3′/II)/CH_2–C(6/I) are missing. The observed cross peaks H–C(1′/II)/(H–C(2′/I) + H–C(3′/I)), H–C(1′/II)/(H–C(4′/I), and H–C(1′/II)/(H–C(5′/I) suggest a *Watson–Crick* base-paired duplex, but the characteristic HN(3/I)/H–C(2/II) cross-peak is missing. Presumably, **57** prefers *Hoogsteen* base pairing, while also forming small amounts of a *Watson–Crick* base-paired duplex.

2.4.8. *Influence of the Substitution at C(6/I) and C(8/I), and the H-Bonding Type on the Chemical Shift of HN(3).* The chemical shift for HN(3) of the U*[c_y]A$^{(*)}$ and A*[c_y]U$^{(*)}$ cyclic duplexes was measured for 30 mM solutions in $CDCl_3$ containing a high proportion of duplexes (*Table 8*). The U*[c_y]A$^{(*)}$ cyclic duplexes **42**·**42**, **47**·**47**, and **48**·**48** display *Watson–Crick*-type base pairing. HN(3) of the U*[c_y]A cyclic duplexes **42**·**42** and **47**·**47** resonates at 13.30–13.37 ppm, whereas HN(3) of the U*[c_y]A* cyclic duplex **48**·**48** appears upfield at 12.75 ppm; hence, substitution at C(8/I) induces an upfield shift of *ca.* 0.6 ppm. HN(3) of the A*[c_y]U* cyclic duplex **60**·**60** and the A*[c_y]U cyclic duplexes **56**·**56**, **58**·**58**, and **52**·**52** resonates at 12.72, 11.71, 11.40, and 11.03 ppm, respectively. A lower downfield shift for HN(3) of the A*[c_y]U cyclic duplexes is expected considering the formation of small amounts of linear duplexes. As these duplexes are also pairing in a *Watson–Crick* mode, the δ values suggest that substitution at C(6/I) induces a downfield shift of *ca.* 1 ppm. HN(3) of the *Hoogsteen*-type pairing A*[c_y]U* duplexes **53**·**53**, **55**·**55**, and **57**·**57** resonates at

11.50–11.89 ppm. As compared with δ(HN(3)) of **60·60**, these values suggest an upfield shift of *ca.* 1 ppm upon changing the H-bonding from a *Watson–Crick* to a *Hoogsteen* type, corroborating a similar upfield shift ($\Delta\delta = 0.8$ ppm) observed by *Weisz* and co-workers [20].

Table 8. *H-Bonding Type and* δ(HN(3)) *of the Cyclic Duplexes Derived from the Dimers* **42**, **47**, **48**, **52**, **53**, *and* **55**–**60** (30 mM in $CHCl_3$)

Duplex	6/I- or 8/I-substitution	H-bonding type	δ(HN(3)) [ppm]
U*[c_y]A$^{(*)}$ series			
47·47	no	*Watson–Crick*	13.37
42·42	no	*Watson–Crick*	13.30
48·48	yes	*Watson–Crick*	12.75
A*[c_y]U$^{(*)}$ series			
60·60	yes	*Watson–Crick*	12.72
59·59	yes	*Watson–Crick*	12.34
57·57	yes	*Hoogsteen*	11.89
55·55	yes	reverse-*Hoogsteen*	11.86
53·53	yes	reverse-*Hoogsteen*	11.50
56·56	no	*Watson–Crick*	11.71[a])
58·58	no	*Watson–Crick*	11.40[a])
52·52	no	*Watson–Crick*	11.03[a])

[a]) Minor amounts of linear duplexes are partially responsible for the upfield shift.

2.4.9. *Investigation of the Cyclic Duplexes* **55·55** *and* **60·60** *at Low Temperature.* To answer the question if the most stable duplexes **55·55** and **60·60** prefer a single H-bonding type, we measured low-temperature ^{1}H-NMR spectra for 4 mM solutions in CH_2Cl_2 at 20 to $-60°$ (*Table 9*). At room temperature, HN(3/I) of **55** and **60** resonates as a broad *s* at 11.76 and 11.84 ppm, and H_2N–C(6/II) as a very broad *s* at 7.5–7.9 and 7.2–7.6 ppm, respectively. At $-10°$, H_2N–C(6/II) appear as two signals (**55**: 7.88/7.6, **60**: 8.32/7.77 ppm). Whereas the NH signals of **55** become sharp at $-40°$ (similar to CH signals), those of **60** become broader with decreasing temperature. Broadening was also observed for the CH signals of unit I and for H–C(2′/II) of **60**; at $-60°$, the CH signals of the ribosyl unit I are broad and those of the ribosyl unit II (except H–C(2′/II)) sharp. These observations evidence a simplex/duplex equilibrium at room temperature for both **55** and **60** (unsplit NH_2 signal), and the presence of a single rigid cyclic duplex **55·55** and a single flexible cyclic duplex **60·60** at temperatures below $-10°$. The presence of several cyclic duplexes of **60** at low temperature cannot be excluded, although the low coalescence temperature (estimated *ca.* $-80°$) speaks in favour of a single flexible duplex.

3. Conclusions. – The self-complementary ethynylene-linked dinucleotide analogues associate in a sequence-dependent fashion. Their mode of association depends upon several structural parameters, the most important one being the propargylic OH group of the U*[c_y]A$^{(*)}$ dimers that prevents formation of a cyclic duplex. Cyclic duplexes form *Watson–Crick*- or *Hoogsteen*-type H-bonds and show various degrees

Table 9. *Temperature-Dependent ^{1}H-NMR Chemical Shifts* [ppm] *and Coupling Constants* [Hz] *for 4 mM Solutions of the A*[c_y]U* Dimers* **55** *and* **60** *in CD_2Cl_2* (*: broadened signal, **: broad signal).

	55			**60**			
	20°	−10°	−40°	20°	−10°	−40°	−60°
Adenosine unit (II)							
H_2N–C(6)	7.7**	7.88*	7.92	7.4**	8.32**	8.71**	8.95**
		7.6**	5.99		7.77*	8.05**	8.29**
H–C(2)	7.95	7.93	7.92	8.22	8.22	8.23*	8.29**
H–C(1′)	6.30	6.27	6.26	6.24	6.22	6.20	6.19
H–C(2′)	5.85*	5.88*	5.89	5.24	5.22	5.20	5.18*
H–C(3′)	5.08	5.06	5.04	5.04	5.01	4.99	4.98
H–C(4′)	4.55	4.55	4.55	4.48	4.49	4.50	4.51
H_a–C(5′)	3.88	3.86	3.84	3.90	3.89	3.87	3.87
H_b–C(5′)	3.74	3.72	3.72	3.72	3.71	3.71	3.71
HO–C(5′)	6.49	6.62	6.72	6.24	6.48	6.69	6.82
J(1′,2′)	6.0	6.0	6.3	5.1	5.5	6.0	5.7
J(2′,3′)	5.4	5.1	5.1	5.7	5.4	5.4	6.0
J(3′,4′)	<1.0	<1.0	<1.0	<1.0	<1.0	<1.0	<1.0
J(4′,5′a)	<1.0	<1.0	<1.0	<1.0	<1.0	<1.0	<1.0
J(4′,5′b)	<1.0	<1.0	<1.0	<1.0	<1.0	<1.0	<1.0
J(5′a,5′b)	12.6	12.6	12.6	12.6	12.6	12.6	12.6
J(5′a,OH)	1.5	1.5	<1.5	<1.5	<1.5	<1.5	<1.5
J(5′b,OH)	11.4	11.4	11.4	11.5	12.3	10.8	10.8
Uridine unit (I)							
HN(3)	11.76*	12.02*	12.12	11.84*	12.88*	13.48**	13.87**
H–C(5)	5.20*	5.16*	5.13	5.97	5.91	5.81	5.70*
CH_a–C(6)	4.49	4.45	4.42	4.64	4.62	4.59	4.58*
CH_b–C(6)	4.13	4.05	3.98	4.43	4.42	4.42	4.42*
H–C(1′)	6.00	5.98	5.97	5.59	5.64	5.72**	5.88**
H–C(2′)	5.30	5.25	5.23	5.33	[a])	[b])	[c])
H–C(3′)	4.91	4.85	4.80	5.27	[a])	[b])	[c])
H–C(4′)	4.12	4.09	4.08	4.34	4.35	4.35**	4.39**
H_a–C(5′)	4.72	4.69	4.67	3.06	3.07	3.07*	3.06**
H_b–C(5′)	–	–	–	2.99	2.98	2.95*	2.94**
HO–C(5′)	5.20*	5.37*	5.43	–	–	–	–
J(H_a,H_b)	12.9	12.6	12.6	13.8	13.8	14.4	12.3
J(1′,2′)	0.6	0.6	<1.0	1.8	1.8	[d])	[d])
J(2′,3′)	6.3	6.3	6.3	6.9	[d])	[d])	[d])
J(3′,4′)	6.9	6.9	6.9	3.9	3.9	[d])	[d])
J(4′,5′a)	3.0	3.0	2.7	6.3	6.6	5.4	[d])
J(4′,5′b)	–	–	–	6.6	6.6	5.7	[d])
J(5′a,5′b)	10.2[e])	10.8[e])	10.8[e])	17.4	17.4	17.4	[d])

[a]) *AB* System at 5.34–5.30. [b]) 5.52** (0.25 H) and 5.4–5.2 (1.75 H). [c]) 5.57* (0.25 H), 5.38** (0.75 H), and 5.35–5.2 (1 H). [d]) Not determined. [e]) *J*(5′a,OH).

of π-stacking. The formation of cyclic duplexes requires a *syn* orientation of the nucleobase of unit I, and a *gg* conformation or one between *gg* and eclipsing of O(4′) by the ethynyl moiety. The originally assumed requirement of an *anti* conformation is – not

surprisingly – the result of the (over)simplified original model-building, and can be abandoned. The results of this work allow to predict the relative propensity for the formation of cyclic duplexes of analogous, self-complementary ethynylene-linked tetramers and will be used for the analysis of their association.

We thank the ETH Zürich and *F. Hoffmann-La Roche AG*, Basel, for generous support, Mrs. *B. Brandenberg* for recording the 2D-NMR spectra, Mr. *M. Schneider* for the VPO measurements, and Prof. *B. Jaun* for helpful discussions.

Experimental Part

General. See [5]. THF and toluene were distilled from Na/benzophenone, and CH_2Cl_2, pyridine, and diisopropylamine ($^iPr_2NH$) from CaH_2. For NMR titrations, NMR spectra were recorded at 295 K on a *Varian Gemini 300* spectrometer (300 MHz) in $CDCl_3$ passed through basic aluminum oxide immediately prior to use. Experiments started at the highest indicated concentration with stepwise replacement of 0.1, 0.2, 0.3 ml of the 0.8-ml soln. with same amount of pure $CDCl_3$. The data were analyzed graphically [25] and by linear least-squares fitting [26]. Thermodynamic parameters were determined by *van't Hoff* analysis. The uracilyl δ(HN(3)) was monitored between 0 and 50° at a fixed concentration (between 20–80% of saturation). MS: Matrix-assisted laser desorption ionization time-of-flight mass spectrometry (MALDI-TOF) with 0.05M indole-3-acrylic acid (IAA) in THF or 0.05M α-cyano-4-hydroxycinnamic acid (CCA) in MeCN/EtOH/H_2O, and high-resolution (HR) MALDI-MS with 0.05M 2,5-dihydroxybenzoic acid (DHB) in THF.

*1-(6,7-Dideoxy-2,3-*O*-isopropylidene-α-*L*-talo-hept-6-ynofuranosyl)uracil* (**2**). A soln. of **1** [2] (1 g, 2.37 mmol) in THF (10 ml) was treated with $Bu_4NF \cdot 3\,H_2O$ (1.2 g, 3.56 mmol), stirred for 3 h at 25°, and evaporated. FC (AcOEt/cyclohexane 2:1) gave **2** (700 mg, 96%). White solid. R_f (AcOEt/cyclohexane 2:1) 0.14. M.p. 182–184°. $[\alpha]_D^{25} = +1.9$ ($c = 0.2$, $CHCl_3$). UV ($CHCl_3$): 258 (10800). IR ($CHCl_3$): 3387*w*, 3304*w*, 3014*w*, 2180*w*, 1696*s*, 1455*w*, 1384*w*, 1260*w*, 1156*w*, 1114*w*, 1083*w*, 808*w*. ^{1}H-NMR (300 MHz, CD_3OD): see *Table 10*; additionally, 1.54, 1.34 (2*s*, Me_2C). ^{13}C-NMR (75 MHz, CD_3OD): see *Table 11*; additionally, 114.90 (*s*, Me_2C); 27.47, 25.48 (2*q*, Me_2C). HR-MALDI-MS: 331.0904 ($[M+Na]^+$, $C_{14}H_{16}N_2NaO_6^+$; calc. 331.0906). Anal. calc. for $C_{14}H_{16}N_2O_6$ (308.29): C 54.54, H 5.23, N 9.09; found: C 54.36, H 5.30, N 9.06.

*1-[6,7-Dideoxy-2,3-*O*-isopropylidene-5′-*O*-(triisopropylsilyl)-α-*L*-talo-hept-6-ynofuranosyl]uracil* (**3**). A soln. of **2** (85 mg, 0.28 mmol) and 1*H*-imidazole (56 mg, 0.82 mmol) in DMF (3 ml) was treated dropwise with $^iPr_3SiCl$ (TIPSCl; 75 µl, 0.35 mmol), stirred at 26° for 16 h, diluted with AcOEt (50 ml), washed with H_2O (30 ml) and brine (30 ml), dried (Na_2SO_4), filtered, and evaporated. FC (cyclohexane/AcOEt 2:1) gave **3** (120 mg, 92%). White solid. R_f (cyclohexane/AcOEt 2:1) 0.12. M.p. 117–119°. $[\alpha]_D^{25} = +4.4$ ($c = 1.0$, $CHCl_3$). UV ($CHCl_3$): 260 (8400). IR ($CHCl_3$): 3389*w*, 3303*w*, 2946*m*, 2869*m*, 2190*w*, 1695*s*, 1458*m*, 1385*m*, 1269*m*, 1089*m*, 882*w*, 809*w*. ^{1}H-NMR (300 MHz, $CDCl_3$): see *Table 10*; additionally, 8.96 (br. *s*, NH); 1.59, 1.36 (2*s*, Me_2C); 1.10–1.06 (*m*, $(Me_2CH)_3Si$). ^{13}C-NMR (75 MHz, $CDCl_3$): see *Table 11*; additionally, 114.33 (*s*, Me_2C); 27.24, 25.40 (2*q*, Me_2C); 17.95 (*q*, $(Me_2CH)_3Si$): 12.21 (*d*, $(Me_2CH)_3Si$). HR-MALDI-MS: 487.2229 ($[M+Na]^+$, $C_{23}H_{36}N_2NaO_6Si^+$; calc. 487.2343).

*1-[5,6,7-Trideoxy-2,3-*O*-isopropylidene-7-*C*-(triethylsilyl)-β-*D*-ribo-hept-6-ynofuranosyl]uracil* (**5**). A soln. of **4** [2] (811 mg, 1.92 mmol) in dry CH_2Cl_2 (30 ml) was treated with (thiocarbonyl)diimidazole (685 mg, 3.84 mmol), stirred for 17 h at 24°, and evaporated. FC ($CHCl_3$/AcOEt 2:1) gave 876 mg of the imidazolyl thiocarbamate. It was dissolved in dry toluene (28 ml), treated with α,α-diazoisobutyronitrile (AIBN; 36 mg, 0.22 mmol) and Bu_3SnH (0.89 ml, 3.37 mmol), stirred for 1.5 h at 80°, and evaporated. FC ($CHCl_3$/AcOEt 2:1) gave **5** (630 mg, 81%). White foam. R_f ($CHCl_3$/AcOEt 1:1) 0.36. $[\alpha]_D^{25} = -56.2$ ($c = 0.5$, $CHCl_3$). UV ($CHCl_3$): 260.0 (10100). IR ($CHCl_3$): 3390*w*, 3016*w*, 2174*w*, 1695*s*, 1456*m*, 1385*m*, 1257*w*, 1086*m*, 1046*w*. ^{1}H-NMR (300 MHz, $CDCl_3$): see *Table 10*; additionally, 9.37 (br. *s*, NH); 1.58, 1.34 (2*s*, Me_2C); 0.98 (*t*, $J = 8.1$, $(MeCH_2)_3Si$); 0.58 (*q*, $(MeCH_2)_3Si$). ^{13}C-NMR (75 MHz,

Table 10. *Selected ^{1}H-NMR Chemical Shifts* [ppm] *and Coupling Constants* [Hz] *of the Uridine Monomers* **3**, **5**–**10**, *and* **12**–**15**, **17**, *and* **18** *in $CDCl_3$, and* **2** *in CD_3OD*

	2	**3**	**9**	**10**	**7**	**8**	**5**	**6**	**17**	**18**	**12**	**13**	**14**	**15**
H–C(5)	5.67	5.71	5.70	5.60	5.90	5.74	5.73	5.74	5.73	5.83	5.68	5.79	5.68	5.57
H–C(6)	7.83	7.63	–	–	–	–	7.55	7.41	–	–	7.68	–	–	–
CH_a–C(6)	–	–	4.38	4.55	4.48	4.49	–	–	4.57	4.57	–	4.54	4.58	4.44
CH_b–C(6)	–	–	4.38	3.36	4.48	4.43	–	–	4.41	4.39	–	4.54	4.39	4.33
H–C(1′)	5.83	5.93	5.88	5.85	5.68	5.72	5.87	5.72	5.78	5.73	5.98	5.82	5.80	5.68
H–C(2′)	4.95	4.76	5.21	5.21	5.26	5.24	4.79	4.93	5.25	5.22	4.76	5.18	5.20	5.14
H–C(3′)	4.88	4.92	5.05	5.03	5.13	5.16	4.80	4.82	4.91	4.91	4.68	4.80	4.80	4.88
H–C(4′)	4.18	4.29	4.16	4.22	4.24	4.22	4.26	4.27	4.20	4.21	4.30	4.15	4.13	4.07
H_a–C(5′)	4.54	4.72	4.65	4.66	4.62	4.61	2.77	2.72	2.75	2.70	3.91	3.88	3.81	3.74
H_b–C(5′)	–	–	–	–	–	–	2.67	2.63	2.60	2.59	3.79	3.84	3.81	3.65
HO–C(5′)	–	–	4.07[a])	3.71[a])	[b])		4.11[a])	–	–	–	–	–	–	3.11
H–C(7′)	2.95	2.55	–	2.52	–	2.52	–	2.09	–	2.04	–	–	–	–
J(5,6)	8.1	8.4	–	–	–	–	8.1	8.1	–	–	8.1	–	–	–
^4J(5,NH)	–	0	0	0	0	1.8	0	0	1.8	0	1.8	0	2.1	1.8
$J(H_a,H_b)$	–	–	14.7	14.1	[b])	14.4	–	–	14.1	14.1	–	13.3	13.8	14.1
J(1′,2′)	2.4	3.3	1.8	1.8	3.6	2.7	2.7	2.4	0.9	0.9	2.4	1.4	0.9	2.1
J(2′,3′)	6.3	6.3	6.6	6.6	6.6	6.6	6.9	6.6	6.3	6.6	6.0	6.6	6.3	6.6
J(3′,4′)	2.7	2.7	4.5	4.2	3.0	3.0	3.0	3.9	3.6	3.9	3.0	4.8	4.8	4.5
J(4′,5′a)	6.0	4.8	6.3	6.0	3.3	4.2	5.4	5.7	7.5	7.2	5.7	6.6	6.9	3.3
J(4′,5′b)	–	–	–	–	–	–	4.8	5.7	6.9	7.2	5.7	5.4	6.9	4.2
J(5′,OH)	–	–	[c])	[c])	[c])	2.7	–	–	–	–	–	–	–	3.9, 8.1
J(5′a,5′b)	–	–	–	–	–		17.4	16.8	16.8	16.5	11.7	11.1	[b])	15.0
^4J(5′,7′)	2.1	2.1	–	2.4	–	2.1	–	2.7	–	3.0	–	–	–	–

[a]) Broad OH signal. [b]) Not determined. [c]) No splitting of the H–C(5′) signal by a *J*(5′,OH) coupling.

$CDCl_3$): see *Table 11*; additionally, 114.65 (*s*, Me_2C); 27.15, 25.28 (2*q*, Me_2C); 7.49 (*q*, $(MeCH_2)_3Si$); 4.41 (*t*, $(MeCH_2)_3Si$). HR-MALDI-MS: 429.1822 ($[M+Na]^+$, $C_{20}H_{30}N_2NaO_5Si^+$; calc. 429.1822). Anal. calc. for $C_{20}H_{30}N_2O_5Si$ (406.55): C 59.09, H 7.44, N 6.89; found: C 58.97, H 7.52, N 6.81.

*1-(5,6,7-Trideoxy-2,3-*O*-isopropylidene-β-*D*-*ribo*-hept-6-ynofuranosyl)uracil* (**6**). A soln. of **5** (564 mg, 1.39 mmol) in THF (30 ml) was treated with $Bu_4NF\cdot 3\,H_2O$ (541 mg, 1.66 mmol), stirred at 24° for 2 h, and evaporated. FC (cyclohexane/AcOEt 1:1) gave **6** (391 mg, 96%). White solid. R_f (cyclohexane/AcOEt 1:1) 0.17. M.p. 173–174°. $[\alpha]_D^{25} = -22.4$ ($c = 0.25$, $CHCl_3$). UV ($CHCl_3$): 259.0 (9400). IR ($CHCl_3$): 3388*w*, 3307*w*, 3017*s*, 1696*s*, 1454*m*, 1384*m*, 1257*m*, 1091*m*, 1046*w*. ^{1}H-NMR (300 MHz, $CDCl_3$): see *Table 10*; additionally, 8.97 (br. *s*, NH); 1.58, 1.36 (2*s*, Me_2C). ^{13}C-NMR (75 MHz, $CDCl_3$): see *Table 11*; additionally, 114.70 (*s*, Me_2C); 27.22, 25.41 (2*q*, Me_2C). MALDI-MS: 315.0 ($[M+Na]^+$, $C_{14}H_{16}N_2NaO_5^+$; calc. 315.1). Anal. calc. for $C_{14}H_{16}N_2O_5$ (292.29): C 57.53, H 5.52, N 9.58; found: C 57.46, H 5.68, N 9.36.

*1-[6,7-Dideoxy-2,3-*O*-isopropylidene-7-*C*-(triethylsilyl)-β-*D*-allo-hept-6-ynofuranosyl]-6-(hydroxymethyl)uracil* (**7**). A soln. of ^{i}Pr$_2$NH (2.7 ml, 18.96 mmol) in THF (11 ml) was cooled to −76°, treated dropwise with 1.6M BuLi in hexane (11.9 ml, 18.96 mmol), stirred for 20 min, warmed to 0°, stirred for 15 min, cooled to −76°, treated dropwise with a soln. of **4** (1.0 g, 2.37 mmol) in THF (12 ml), stirred for 3.0 h, treated dropwise with DMF (5.5 ml), stirred for 2.5 h, treated with AcOH (2.6 ml), and allowed to warm to 27°. The mixture was diluted with EtOH (24 ml), treated portionwise with $NaBH_4$ (360 mg, 9.5 mmol), stirred for 2 h, cooled to 0°, and treated with sat. aq. NH_4Cl soln. (7.6 ml). After evaporation, a soln. of the residue in AcOEt (450 ml) was washed with H_2O and brine, dried (Na_2SO_4), and evaporated. FC (cyclohexane/AcOEt 1:2) gave **7** (644 mg, 60%). White solid. R_f (cyclohexane/AcOEt 1:2) 0.18. M.p.

100–102°. $[\alpha]_D^{25} = -57.9$ ($c = 1.0$, $CHCl_3$). UV ($CHCl_3$): 258 (7700). IR ($CHCl_3$): 3607*w*, 3387*w*, 3018*m*, 2958*w*, 2876*w*, 2180*w*, 1699*s*, 1628*w*, 1457*w*, 1384*m*, 1157*w*, 1093*w*, 988*w*, 875*w*, 836*w*. ^{1}H-NMR (300 MHz, $CDCl_3$): see *Table 10*; additionally, 9.80 (br. *s*, NH); 4.48 (br. *s*, *H*OCH$_2$–C(6)); 1.56, 1.34 (2*s*, Me_2C); 0.98 (*t*, *J* = 7.5, (*Me*CH$_2$)$_3$Si); 0.60 (*q*, *J* = 7.5, (MeC*H*$_2$)$_3$Si). ^{13}C-NMR (75 MHz, $CDCl_3$): see *Table 11*; additionally, 113.93 (*s*, Me_2*C*); 27.01, 24.93 (2*q*, *Me*$_2$C); 7.19 (*q*, (*Me*CH$_2$)$_3$Si); 4.20 (*t*, (Me*C*H$_2$)$_3$-Si). HR-MALDI-MS: 475.1864 ([*M* + Na]$^+$, $C_{21}H_{32}N_2NaO_7Si^+$; calc. 475.1876). Anal. calc. for $C_{21}H_{32}N_2O_7Si$ (452.58): C 55.73, H 7.13, N 6.19; found: C 55.57, H 7.12, N 6.08.

*6-[[(*tert*-Butyl)diphenylsilyloxy]methyl]-1-(6,7-dideoxy-2,3-*O*-isopropylidene-β-*D*-*allo*-hept-6-ynofuranosyl)uracil* (**8**). A soln. of **7** (644 mg, 1.42 mmol) in THF (12 ml) was treated with $Bu_4NF \cdot 3\ H_2O$ (541 mg, 1.71 mmol), stirred for 1 h, and evaporated. FC (cyclohexane/AcOEt 1:4) gave the desilylated product (432 mg). A soln. of 324 mg of this crude in DMF (6 ml) was treated with 1*H*-imidazole (136 mg, 2.0 mmol) and ^{t}BuPh$_2$SiCl (TBDPSCl; 0.3 ml, 1.15 mmol), stirred for 3.5 h at 0°, treated with H_2O (50 ml), and extracted with AcOEt (3 × 50 ml). The combined AcOEt extracts were washed with H_2O and brine, dried (Na_2SO_4), and evaporated. FC (cyclohexane/AcOEt 1:1) gave **8** (498 mg, 81%). White solid. R_f (cyclohexane/AcOEt 1:1) 0.22. M.p. 153–154°. $[\alpha]_D^{25} = -36.8$ ($c = 0.25$, $CHCl_3$). UV ($CHCl_3$): 258 (18500). IR ($CHCl_3$): 3386*w*, 3307*w*, 3020*s*, 2861*w*, 2140*w*, 1698*m*, 1385*w*, 1213*s*, 1207*s*, 1113*w*, 841*w*. ^{1}H-NMR (300 MHz, $CDCl_3$): see *Table 10*; additionally, 9.45 (br. *s*, NH); 7.69–7.64 (*m*, 4 arom. H); 7.51–7.34 (*m*, 6 arom. H); 1.45, 1.35 (2*s*, Me_2C); 1.09 (*s*, ^{t}Bu). ^{13}C-NMR (75 MHz, $CDCl_3$): see *Table 11*; additionally, 135.38 (2*d*); 135.34 (2*d*); 131.60, 131.56 (2*s*); 130.27 (2*d*); 127.97 (4*d*); 114.20 (*s*, Me_2*C*); 27.28, 25.27 (2*q*, *Me*$_2$C); 26.65 (*q*, *Me*$_3$C); 19.29 (*s*, Me_3*C*). HR-MALDI-MS: 599.2175 ([*M* + Na]$^+$, $C_{31}H_{36}N_2NaO_7Si^+$; calc. 599.2189). Anal. calc. for $C_{31}H_{36}N_2O_7Si$ (576.72): C 64.56, H 6.29, N 4.86; found: C 64.41, H 6.34, N 4.77.

*1-[6,7-Dideoxy-2,3-*O*-isopropylidene-7-*C*-(triethylsilyl)-α-*L*-talo-hept-6-ynofuranosyl]-6-(hydroxymethyl)uracil* (**9**). A soln. of ^{i}Pr$_2$NH (2.7 ml, 19 mmol) in THF (11 ml) was cooled to −76°, treated dropwise with 1.6M BuLi in hexane (11.9 ml, 19 mmol), and stirred for 20 min. The mixture was warmed to 0°, stirred for 15 min, cooled to −76°, treated dropwise with a soln. of **1** (1.0 g, 2.37 mmol) in THF (12 ml), stirred for 3 h, treated dropwise with DMF (5.5 ml), stirred for 2.5 h, treated with AcOH (2.6 ml), and allowed to warm to 27°. The mixture was diluted with EtOH (24 ml), treated portionwise with $NaBH_4$ (360 mg, 9.5 mmol) for 2 h, cooled to 0°, and treated with sat. aq. NH_4Cl soln. (7.6 ml). After evaporation, a soln. of the residue in AcOEt (450 ml) was washed with H_2O and brine, dried (Na_2SO_4), and evaporated. FC (cyclohexane/AcOEt 1:2) gave **9** (582 mg, 54%). White solid. R_f (cyclohexane/AcOEt 1:1) 0.16. M.p. 195–197°. $[\alpha]_D^{25} = -20.3$ ($c = 0.5$, $CHCl_3$). UV ($CHCl_3$): 258 (8300). IR ($CHCl_3$): 3396*w*, 3018*s*, 2958*w*, 2876*w*, 2190*w*, 1697*s*, 1457*w*, 1384*m*, 1157*w*, 1059*w*, 930*w*, 875*w*, 833*w*. ^{1}H-NMR (300 MHz, $CDCl_3$): see *Table 10*; additionally, 9.18 (br. *s*, NH); 4.45–4.10 (br. *s*, *H*OCH$_2$–C(6)); 1.55, 1.32 (2*s*, Me_2C); 0.97 (*t*, *J* = 7.8, (*Me*CH$_2$)$_3$Si); 0.59 (*q*, *J* = 7.8, (MeC*H*$_2$)$_3$Si). ^{13}C-NMR (75 MHz, $CDCl_3$): see *Table 11*; additionally, 113.82 (*s*, Me_2*C*); 26.78, 24.75 (2*q*, *Me*$_2$C); 7.09 (*q*, (*Me*CH$_2$)$_3$Si); 3.80 (*t*, (Me*C*H$_2$)$_3$Si). HR-MALDI-MS: 475.1864 ([*M* + Na]$^+$, $C_{21}H_{32}N_2NaO_7Si^+$; calc. 475.1876). Anal. calc. for $C_{21}H_{32}N_2O_7Si$ (452.58): C 55.73, H 7.13, N 6.19; found: C 55.66, H 7.13, N 6.14.

*6-[[(*tert*-Butyl)diphenylsilyloxy]methyl]-1-(6,7-dideoxy-2,3-*O*-isopropylidene-α-*L*-talo-hept-6-ynofuranosyl)uracil* (**10**). A soln. of **9** (439 mg, 0.97 mmol) in THF (8 ml) was treated with $Bu_4NF \cdot 3\ H_2O$ (370 mg, 1.17 mmol), stirred for 1 h, and evaporated. FC (cyclohexane/AcOEt 1:6) gave the desilylated product (311 mg). Its soln. in DMF (6 ml) was treated with 1*H*-imidazole (136 mg, 2.0 mmol) and ^{t}BuPh$_2$-SiCl (0.255 ml, 0.98 mmol), stirred for 12 h at 25°, treated with H_2O (50 ml), and extracted with AcOEt (3 × 50 ml). The combined AcOEt extracts were washed with H_2O and brine, dried (Na_2SO_4), and evaporated. FC (cyclohexane/AcOEt 1:1) gave **10** (476 mg, 85%). White solid. R_f (cyclohexane/AcOEt 1:2) 0.42. M.p. 170–172°. $[\alpha]_D^{25} = -8.9$ ($c = 0.2$, $CHCl_3$). UV ($CHCl_3$): 258 (16000). IR ($CHCl_3$): 3387*w*, 3307*w*, 3020*w*, 2933*w*, 2860*w*, 2100*w*, 1698*s*, 1456*w*, 1428*w*, 1384*w*, 1223*s*, 1215*s*, 1209*s*, 1114*m*, 839*w*. ^{1}H-NMR (300 MHz, $CDCl_3$): see *Table 10*; additionally, 9.80 (br. *s*, NH); 7.69–7.63 (*m*, 4 arom. H); 7.50–7.37 (*m*, 6 arom. H); 1.47, 1.33 (2*s*, Me_2C); 1.08 (*s*, ^{t}Bu). ^{13}C-NMR (75 MHz, $CDCl_3$): see *Table 11*; additionally, 135.36 (4*d*); 131.64, 131.59 (2*s*); 130.19, 130.18 (2*d*); 127.91 (2*d*); 127.86 (2*d*); 114.03 (*s*, Me_2*C*); 27.20, 25.28 (2*q*, *Me*$_2$C); 26.64 (*q*, *Me*$_3$C); 19.25 (*s*, Me_3*C*). HR-MALDI-MS: 599.2185 ([*M* + Na]$^+$, $C_{31}H_{36}N_2NaO_7Si^+$; calc. 599.2189). Anal. calc. for $C_{31}H_{36}N_2O_7Si$ (576.72): C 64.56, H 6.29, N 4.86; found: C 64.60, H 6.25, N 4.79.

*5′-O-[(*tert*-Butyl)dimethylsilyl]-2′,3′-O-isopropylideneuridine* (**12**). A soln. of **11** [11] (18 g, 63.3 mmol), 1*H*-imidazole (5.18 g, 76 mmol), and DMAP (0.78 g, 6.2 mmol) in CH_2Cl_2 (240 ml) was treated with a soln. of ^{t}BuMe$_2$SiCl (TBDMSCl; 18 g, 140 mmol) in CH_2Cl_2 (40 ml), stirred for 12 h at 24°, washed with H_2O (50 ml) and brine (40 ml), dried (Na_2SO_4), and evaporated. FC (cyclohexane/AcOEt 2:1) gave **12** (22.7 g, 90%). White solid. R_f (cyclohexane/AcOEt 1:1) 0.28. M.p. 134–135°. $[\alpha]_D^{25} = -24.7$ ($c = 0.5$, $CHCl_3$). UV ($CHCl_3$): 262 (11300). IR ($CHCl_3$): 3389*w*, 3013*w*, 2954*w*, 2931*w*, 2858*w*, 1692*s*, 1458*w*, 1385*w*, 1258*m*, 1214*m*, 1129*w*, 1085*m*, 969*w*, 837*m*. ^{1}H-NMR (300 MHz, $CDCl_3$): see *Table 10*; additionally, 9.35 (br. *s*, NH); 1.58, 1.35 (2*s*, Me$_2$C); 0.89 (*s*, ^{t}Bu); 0.083, 0.077 (2*s*, Me$_2$Si). ^{13}C-NMR (75 MHz, $CDCl_3$): see *Table 11*; additionally, 114.00 (*s*, Me$_2$*C*); 27.33, 25.42 (2*q*, *Me*$_2$C); 25.90 (*q*, *Me*$_3$C); 18.41 (*s*, Me$_3$*C*); −5.32, −5.43 (2*q*, Me$_2$Si). HR-MALDI-MS: 421.1765 ([*M* + Na]$^+$, $C_{18}H_{30}N_2NaO_6Si^+$; calc. 421.1873).

*5′-O-[(*tert*-Butyl)dimethylsilyl]-6-(hydroxymethyl)-2′,3′-O-isopropylideneuridine* (**13**). A soln. of ^{i}Pr$_2$NH (20.35 ml, 144.1 mmol) in THF (80 ml) was cooled to −76°, treated dropwise with 1.6M BuLi in hexane (90.2 ml, 144 mmol), stirred for 20 min, warmed to 0°, stirred for 15 min, cooled to −76°, treated dropwise with a soln. of **12** (9.28 g, 23.28 mmol) in THF (116 ml), stirred for 2.5 h, treated dropwise with DMF (55.7 ml), stirred for 2.5 h, treated with AcOH (20.5 ml), and allowed to warm to 26°. The mixture was diluted with EtOH (220 ml), treated portionwise with $NaBH_4$ (367 mg, 9.7 mmol), stirred for 5.5 h, cooled to 0°, treated with sat. aq. NH_4Cl soln. (80 ml), and evaporated. A soln. of the residue in AcOEt (750 ml) was washed with H_2O and brine, dried (Na_2SO_4), and evaporated. FC (cyclohexane/AcOEt 1:1) gave **13** (8.48 g, 85%). White solid. R_f (cyclohexane/AcOEt 1:2) 0.22. M.p. 89–91°. $[\alpha]_D^{25} = +12.7$ ($c = 0.5$, $CHCl_3$). UV ($CHCl_3$): 260 (9600). IR ($CHCl_3$): 3600*w*, 3387*w*, 3013*w*, 2930*w*, 2857*w*, 1697*s*, 1462*w*, 1383*m*, 1256*w*, 1157*w*, 1081*m*, 973*w*, 877*w*, 837*m*. ^{1}H-NMR (300 MHz, $CDCl_3$): see *Table 10*; additionally, 8.95 (br. *s*, NH); 1.55, 1.34 (2*s*, Me$_2$C); 0.89 (*s*, ^{t}Bu); 0.08, 0.07 (2*s*, Me$_2$Si). ^{13}C-NMR (75 MHz, $CDCl_3$): see *Table 11*; additionally, 113.88 (*s*, Me$_2$*C*); 27.29, 25.38 (2*q*, *Me*$_2$C); 26.00 (*q*, *Me*$_3$C); 18.56 (*s*, Me$_3$*C*); −5.10 (*q*, Me$_2$Si). HR-MALDI-MS: 451.1880 ([*M* + Na]$^+$, $C_{19}H_{32}N_2NaO_7Si^+$; calc. 451.1979).

*5′-O-[(*tert*-Butyl)dimethylsilyl]-6-{[(*tert*-butyl)diphenylsilyloxy]methyl}-2′,3′-O-isopropylideneuridine* (**14**). A soln. of **13** (4.5 g, 10.5 mmol), 1*H*-imidazole (0.86 g, 12.6 mmol), and DMAP (129 mg, 1.06 mmol) in CH_2Cl_2 (100 ml) was treated dropwise with ^{t}BuPh$_2$SiCl (5.44 ml, 21.1 mmol), stirred at 26° for 6 h, washed with H_2O (2 × 30 ml) and brine (30 ml), dried (Na_2SO_4), filtered, and evaporated. FC (cyclohexane/AcOEt 4:1) gave **14** (4.01 g, 59%). White foam. R_f (cyclohexane/AcOEt 2:1) 0.45. $[\alpha]_D^{25} = +6.5$ ($c = 2.0$, $CHCl_3$). UV ($CHCl_3$): 260 (13600). IR ($CHCl_3$): 3600*w*, 3389*w*, 3018*m*, 2932*m*, 2859*m*, 1697*s*, 1627*w*, 1471*m*, 1463*w*, 1428*w*, 1383*m*, 1256*w*, 1113*m*, 1074*m*, 879*w*, 838*s*. ^{1}H-NMR (300 MHz, $CDCl_3$): see *Table 10*; additionally, 9.77 (br. *s*, NH); 7.65–7.71 (*m*, 4 arom. H); 7.39–7.49 (*m*, 6 arom. H); 1.50, 1.32 (2*s*, Me$_2$C); 1.08, 0.88 (2*s*, 2 ^{t}Bu); 0.045, 0.041 (2*s*, Me$_2$Si). ^{13}C-NMR (75 MHz, $CDCl_3$): see *Table 11*; additionally, 135.39 (4*d*); 131.75, 131.72 (2*s*); 130.20 (2*d*); 127.95 (2*d*); 127.91 (2*d*); 113.52 (*s*, Me$_2$*C*); 27.32, 25.47 (2*q*, *Me*$_2$C); 26.67, 26.04 (2*q*, 2 *Me*$_3$C); 19.30, 18.59 (2*s*, 2 Me$_3$*C*); −5.07 (*q*, Me$_2$Si). MALDI-MS: 689.3 ([*M* + Na]$^+$, $C_{35}H_{50}N_2NaO_7Si_2^+$).

*6-{[(*tert*-Butyl)diphenylsilyloxy]methyl}-2′,3′-O-isopropylideneuridine* (**15**). A soln. of **14** (1.55 g, 2.37 mmol) in MeCN/^{t}BuOH 11:1 (24 ml) was cooled to 0°, treated with 20–25% soln. of H_2SiF_6 in H_2O (0.71 ml), stirred for 3 h, diluted with aq. Na_2CO_3 soln. (20 ml), and extracted with AcOEt (3 × 40 ml). The combined org. layers were washed with H_2O (2 × 30 ml) and brine (30 ml), dried (Na_2SO_4), filtered, and evaporated. FC (cyclohexane/AcOEt 1:1) gave **15** (1.29 g, 99%). White solid. R_f (cyclohexane/AcOEt 1:1) 0.14. M.p. 92–94°. $[\alpha]_D^{25} = -19.7$ ($c = 1.0$, $CHCl_3$). UV ($CHCl_3$): 261 (14400). IR ($CHCl_3$): 3389*w*, 3017*m*, 2934*m*, 2861*w*, 1698*s*, 1629*w*, 1455*w*, 1428*w*, 1384*m*, 1343*w*, 1221*s*, 1113*m*, 1072*m*. ^{1}H-NMR (300 MHz, $CDCl_3$): see *Table 10*; additionally, 9.49 (br. *s*, NH); 7.61–7.56 (*m*, 4 arom. H); 7.42–7.30 (*m*, 6 arom. H); 1.38, 1.24 (2*s*, Me$_2$C); 0.99 (*s*, ^{t}Bu). ^{13}C-NMR (75 MHz, $CDCl_3$): see *Table 11*; additionally, 135.38 (4*d*); 131.67, 131.63 (2*s*); 130.25 (2*d*); 127.95 (4*d*); 113.99 (*s*, Me$_2$*C*); 27.34, 25.34 (2*q*, *Me*$_2$C); 26.66 (*q*, *Me*$_3$C); 19.30 (*s*, Me$_3$*C*). MALDI-MS: 575.2 ([*M* + Na]$^+$, $C_{29}H_{36}N_2NaO_7Si^+$). Anal. calc. for $C_{29}H_{36}N_2O_7Si$ (552.70): C 63.02, H 6.56, N 5.07; found: C 62.75, H 6.61, N 4.95.

*6-{[(*tert*-Butyl)diphenylsilyloxy]methyl}-1-[5,6,7-trideoxy-2,3-O-isopropylidene-7-C-(triethylsilyl)-β-*D*-allo/α-*L*-talo-hept-6-ynofuranosyl]uracil* (**16**). A soln. of **15** (1.22 g, 2.26 mmol) and dicyclohexyl carbodiimide (DCC; 1.41 g, 6.8 mmol) in dry DMSO (9 ml) was cooled to 15°, treated dropwise with

$CHCl_2CO_2H$ (93 µl, 1.12 mmol), stirred for 15 min, warmed to 25°, stirred for 3 h, and filtered (washing of the residue with 6 ml of DMSO). The combined filtrate and washing were extracted with hexane (4×120 ml). The DMSO layer was diluted with $CHCl_3$ (300 ml), washed with H_2O (3×150 ml), dried (Na_2SO_4), and evaporated to afford the crude aldehyde (0.97 g).

A soln. of EtMgBr (5.42 mmol) in THF (9 ml) was cooled to 0°, treated dropwise with (triethylsilyl)-acetylene (0.97 ml, 5.42 mmol), stirred for 15 min, warmed to 26°, stirred for 40 min, cooled to −15°, and treated with a soln. of the above crude aldehyde in dry THF (30 ml). The mixture was stirred for 2 h, treated with sat. aq. NH_4Cl soln. (50 ml), and allowed to reach 25°. After separation of the layers, the aq. layer was extracted with AcOEt (2×60 ml). The combined org. layers were washed with H_2O and brine, dried (Na_2SO_4), and evaporated. FC (cyclohexane/AcOEt 5:1) gave **16** (D-*allo*/L-*talo* 1:1; 793 mg, 51%).

*6-{[(*tert*-Butyl)diphenylsilyloxy]methyl}-1-[5,6,7-trideoxy-2,3*-O-*isopropylidene-7*-C-*(triethylsilyl)-β*-D-ribo-*hept-6-ynofuranosyl]uracil* (**17**). A soln. of **16** (D-*allo*/L-*talo* 1:1; 400 mg, 0.5 mmol) in dry CH_2Cl_2 (15 ml) was treated with (thiocarbonyl)diimidazole (180 mg, 1.0 mmol), stirred for 30 h, and evaporated. FC (cyclohexane/AcOEt 2:1) gave a mixture of epimeric imidazoyl thiocarbamates (296 mg). Their soln. in dry toluene (6.5 ml) was treated with *α,α*-azoisobutyronitrile (AIBN; 9 mg, 0.056 mmol) and Bu_3SnH (0.2 ml, 0.76 mmol), stirred for 1.5 h at 80°, and evaporated. FC (cyclohexane/AcOEt 3:1) gave **17** (200 mg, 59%). White foam. R_f (cyclohexane/AcOEt 8:1) 0.16. $[\alpha]_D^{25} = -4.4$ ($c = 1.0$, $CHCl_3$). IR ($CHCl_3$): 3389*w*, 3018*s*, 2957*w*, 2875*w*, 2175*w*, 1697*s*, 1456*w*, 1428*w*, 1383*m*, 1158*w*, 1113*m*, 1005*w*, 877*w*, 839*w*. ^{1}H-NMR (300 MHz, $CDCl_3$): see *Table 10*; additionally, 10.35 (*d, J* = 1.8, NH); 7.71–7.66 (*m*, 4 arom. H); 7.49–7.40 (*m*, 6 arom. H); 1.50, 1.32 (2*s*, Me_2C); 1.09 (*s*, ^{t}Bu); 0.98 (*t*, *J* = 7.8, $(MeCH_2)_3Si$); 0.058 (*q*, *J* = 7.8, $(MeCH_2)_3Si$). ^{13}C-NMR (75 MHz, $CDCl_3$): see *Table 11*; additionally, 135.38 (4*d*); 131.75, 131.71 (2*s*); 130.19 (2*d*); 127.95 (2*d*); 127.90 (2*d*); 113.33 (*s*, Me_2C); 27.11, 25.13 (2*q*, Me_2C); 26.63 (*q*, Me_3C); 19.26 (*s*, Me_3C); 7.50 (*q*, $(MeCH_2)_3Si$); 4.53 (*t*, $(MeCH_2)_3Si$). HR-MALDI-MS: 697.3090 ($[M+Na]^+$, $C_{37}H_{50}N_2NaO_6Si_2^+$; calc. 697.3105).

*6-{[(*tert*-Butyl)diphenylsilyloxy]methyl}-1-(5,6,7-trideoxy-2,3*-O-*isopropylidene-β*-D-ribo-*hept-6-ynofuranosyl)uracil* (**18**). A soln. of **17** (94 mg, 0.21 mmol) in THF (3 ml) was treated with $Bu_4NF \cdot 3\,H_2O$ (100 mg, 0.31 mmol), stirred for 2 h at 25°, and evaporated. FC (cyclohexane/AcOEt 1:1) gave 67 mg of the didesilylated product. Its soln. in CH_2Cl_2 (6 ml) was treated with 1*H*-imidazole (27 mg, 0.4 mmol), DMAP (9 mg), and ^{t}BuPh$_2$SiCl (0.1 ml, 0.4 mmol), stirred for 12 h at 25°, and evaporated. FC (cyclohexane/AcOEt 3:1) gave **18** (106 mg, 88%). White solid. R_f (cyclohexane/AcOEt 1:2) 0.54. M.p. 139–141°. $[\alpha]_D^{25} = -3.3$ ($c = 1.0$, $CHCl_3$). UV ($CHCl_3$): 260 (14700). IR ($CHCl_3$): 3389*w*, 3309*w*, 3018*s*, 2933*w*, 2860*w*, 2100*w*, 1697*s*, 1455*w*, 1428*w*, 1384*m*, 1158*w*, 1113*m*, 1072*w*, 877*w*, 839*w*. ^{1}H-NMR (300 MHz, $CDCl_3$): see *Table 10*; additionally, 9.83 (br. *s*, NH); 7.70–7.65 (*m*, 4 arom. H); 7.49–7.26 (*m*, 6 arom. H); 1.52, 1.34 (2*s*, Me_2C); 1.08 (*s*, ^{t}Bu). ^{13}C-NMR (75 MHz, $CDCl_3$): see *Table 11*; additionally, 135.41 (4*d*); 131.72 (2*s*); 130.22 (2*d*); 127.96 (2*d*); 127.91 (2*d*); 113.70 (*s*, Me_2C); 27.21, 25.32 (2*q*, Me_2C); 26.66 (*q*, Me_3C); 19.29 (*s*, Me_3C). HR-MALDI-MS: 583.2226 ($[M+Na]^+$, $C_{31}H_{36}N_2NaO_6Si^+$; calc. 583.2240). Anal. calc. for $C_{31}H_{36}N_2O_6Si$ (560.72): C 66.40, H 6.47, N 5.00; found: C 66.47, H 6.57, N 4.90.

N^6-*Benzoyl-5′*-O-*[(*tert*-butyl)diphenylsilyl]-2′,3′*-O-*isopropylideneadenosine* (**20**). A soln. of **19** [15] (3.63 g, 8.82 mmol), 1*H*-imidazole (0.66 g, 9.7 mmol) in DMF (15 ml) was treated with ^{t}BuPh$_2$SiCl (3.5 ml, 13.2 mmol), stirred for 6 h at 25°, diluted with $CHCl_3$ (150 ml), washed with H_2O (2×50 ml) and brine (30 ml), dried (Na_2SO_4), and evaporated. FC (cyclohexane/AcOEt 1:1) gave **20** (5.0 g, 87%). White foam. R_f (cyclohexane/AcOEt 1:1) 0.28. $[\alpha]_D^{25} = -19.4$ ($c = 0.5$, $CHCl_3$). IR ($CHCl_3$): 3408*w*, 3009*m*, 2933*w*, 2860*w*, 1708*m*, 1612*s*, 1585*m*, 1454*s*, 1385*w*, 1252*m*, 1156*w*, 1088*s*, 861*w*, 823*w*. ^{1}H-NMR (300 MHz, $CDCl_3$): see *Table 12*; additionally, 9.00 (br. *s*, NH); 8.03–8.00 (*m*, 2 arom. H); 7.64–7.50 (*m*, 8 arom. H); 7.44–7.27 (*m*, 5 arom. H); 1.64, 1.40 (2*s*, Me_2C); 1.01 (*s*, ^{t}Bu). ^{13}C-NMR (75 MHz, $CDCl_3$): see *Table 13*; additionally, 164.25 (*s*, C=O); 135.42 (2*d*); 135.37 (2*d*); 133.60 (*s*); 132.71 (*d*); 132.55 (2*s*); 129.85 (2*d*); 128.83 (2*d*); 127.73 (2*d*); 127.69 (4*d*); 114.31 (*s*, Me_2C); 27.28, 25.43 (2*q*, Me_2C); 26.92 (*q*, Me_3C); 19.28 (*s*, Me_3C). HR-MALDI-MS: 672.2602 ($[M+Na]^+$, $C_{36}H_{39}N_5NaO_5Si^+$; calc. 672.2720).

N^6-*Benzoyl-5′*-O-*[(*tert*-butyl)dimethylsilyl]-2′,3′*-O-*isopropylideneadenosine* (**22**). A soln. of **19** (5 g, 12.2 mmol), 1*H*-imidazole (1 g, 14.7 mmol), and DMAP (0.15 g, 1.2 mmol), in CH_2Cl_2 (60 ml) was treated

Table 11. *Selected ^{13}C-NMR Chemical Shifts* [ppm] *of the Uridine Monomers* **3**, **5**–**10**, **12**–**15**, **17**, and **18** *in $CDCl_3$, and* **2** *in CD_3OD*

	2	**3**	**9**	**10**	**7**	**8**	**5**	**6**	**17**	**18**	**12**	**13**	**14**	**15**
C(2)	151.89	149.99	150.67	151.02	151.33	151.34	149.94	149.69	150.39	150.48	150.00	150.19	150.24	151.07
C(4)	166.03	163.17	163.76	162.79	163.50	162.39	163.35	162.87	163.85	163.32	163.19	163.42	162.73	162.57
C(5)	102.37	102.33	100.68	102.19	101.37	102.45	102.79	102.53	101.60	101.87	102.23	101.52	101.62	102.12
C(6)	144.14	140.93	156.06	153.41	155.27	153.37	140.77	141.71	153.88	153.64	140.45	154.99	153.83	153.48
CH_2–C(6)	–	–	59.95	62.17	60.01	62.17	–	–	62.04	62.17	–	60.87	62.10	62.12
C(1′)	95.31	92.41	91.74	92.14	91.83	92.48	91.89	93.65	91.74	91.67	91.89	91.20	91.38	91.85
C(2′)	85.57	84.20	83.49	83.58	81.82	82.37	83.27	84.52	84.35	84.78	85.36	84.21	84.29	83.30
C(3′)	82.80	80.78	81.60	81.03	80.33	80.42	82.38	82.79	84.31	84.20	80.28	81.59	81.92	80.36
C(4′)	90.65	88.41	90.83	90.09	88.42	88.91	84.40	84.58	87.47	87.49	86.68	89.38	89.54	87.49
C(5′)	63.40	63.61	63.09	62.79	62.64	62.34	24.43	23.13	24.73	23.29	63.40	64.17	64.31	62.81
C(6′)	82.74	82.16	103.76	81.48	103.34	81.13	102.52	79.77	103.73	80.37	–	–	–	–
C(7′)	75.80	74.76	88.77	74.10	88.72	74.45	85.14	70.88	83.64	69.96	–	–	–	–

Table 12. *Selected ^{1}H-NMR Chemical Shifts* [ppm] *and Coupling Constants* [Hz] *of the Adenosine Monomers* **20**, **22**, **25**, **26**, **29**–**37** *in $CDCl_3$, and* **24** *and* **28** *in $CDCl_3/CD_3OD$*

	20	**22**	**24**	**25**	**26**	**29**	**30**	**31**	**28**	**33**	**35**	**32**	**34**	**36**	**37**
H–C(2)	8.74	8.84	8.13	8.00	8.21	8.76	8.79	8.76	8.26	8.78	8.24	8.75	8.25	8.79	8.30
H–C(8)	8.16	8.24	–	–	–	–	–	–	7.84	–	–	–	–	–	–
CH_a–C(8)	–	–	–	–	–	4.99	5.06	5.03	–	5.07	4.95	5.04	4.98	5.05	4.99
CH_b–C(8)	–	–	–	–	–	4.92	4.98	4.95	–	5.00	4.88	4.95	4.85	4.97	4.89
H–C(1′)	6.18	6.23	5.97	6.08	6.09	6.33	6.60	6.53	5.90	6.53	6.48	6.54	6.48	6.60	6.60
H–C(2′)	5.36	5.29	5.23	5.76	5.85	5.60	5.80	5.26	5.13	5.23	5.25	5.18	5.18	5.78	5.70
H–C(3′)	4.98	4.95	5.02	5.20	5.20	5.07	5.16	5.16	5.01	5.06	5.11	5.22	5.23	5.13	5.18
H–C(4′)	4.44	4.47	4.49	4.41	4.34	4.24	4.27	4.51	4.56	4.51	4.52	4.80	4.78	4.35	4.34
H_a–C(5′)	3.92	3.89	3.90	3.83	3.81	3.82	3.79	4.03	4.60	4.67	4.71	4.56	4.45	2.74	2.70
H_b–C(5′)	3.79	3.77	3.73	3.69	3.68	3.70	3.67	3.83	–	–	–	–	–	2.54	2.50
HO–C(5′)	–	–	–	–	–	–	–	5.81	–	6.35	7.46–7.31	7.22	7.77	–	–
H–C(7′)	–	–	–	–	–	–	–	–	2.41	–	2.43	–	2.57	–	2.02
$J(H_a,H_b)$	–	–	–	–	–	14.4	13.2	13.5	–	13.2	13.2	13.5	12.9	13.2	12.9
J(1′,2′)	3.0	3.0	5.1	1.8	1.8	2.4	2.1	4.8	5.1	5.1	4.5	5.7	5.4	2.1	1.5
J(2′,3′)	6.3	6.3	5.7	6.3	6.3	6.6	6.6	6.0	6.0	6.0	6.0	6.0	6.0	6.6	6.6
J(3′,4′)	3.0	2.4	0.9	3.6	3.0	4.2	3.6	1.8	1.2	1.8	2.1	0.9	1.5	3.3	3.3
J(4′,5′a)	4.5	3.6	1.5	6.6	6.9	6.3	6.3	<1.0	2.1	2.1	2.1	1.8	1.5	6.9	8.1
J(4′,5′b)	5.1	3.9	1.5	6.6	6.0	6.3	6.3	1.8	–	–	–	–	–	7.2	6.3
J(5′a,5′b)	11.4	11.1	12.9	10.5	10.2	10.8	10.8	12.6	–	–	–	–	–	16.8	16.5
J(5′,OH)	–	–	–	–	–	–	–	[a])	–	11.1	10.5	1.5	1.5	–	–
^4J(5′,7′)	–	–	–	–	–	–	–	–	2.1	–	2.4	–	2.4	–	2.7, 2.4

[a]) J(5′a,OH) < 1.5, J(5′b,OH) $= 10.5$ Hz.

Table 13. *Selected* ^{13}*C-NMR Chemical Shifts* [ppm] *of the Adenosine Monomers* **20**, **22**, **25**, **26**, **29**–**37** *in* $CDCl_3$, **24** *in* $CDCl_3/CD_3OD$, *and* **28** *in* CD_3OD

	20	**22**	**24**	**25**	**26**	**29**	**30**	**31**	**28**	**33**	**35**	**32**	**34**	**36**	**37**
C(2)	152.70	152.73	154.26	152.40	152.52	152.49	152.32	152.01	152.42	152.04	151.09	151.86	151.98	152.32	152.55
C(4)	149.33	149.31	149.26	150.08	150.26	148.85	149.07	149.65	147.94	149.57	149.28[a])	149.80	149.17[a])	149.16	149.80[a])
C(5)	123.30	123.17	122.88	122.63	122.78	121.27	121.62	122.25	120.40	122.13	118.84	122.26	118.87	121.81	118.60
C(6)	150.96	151.02	152.08	154.01	153.85	152.38[a])	151.91[a])	151.47[a])	155.71	151.34[a])	155.40	151.10[a])	155.78	151.98[a])	155.24
C(8)	141.58	141.43	99.31	100.26	100.81	152.49[a])	152.62[a])	151.98[a])	139.88	151.86[a])	149.49[a])	152.98[a])	149.23[a])	152.56[a])	150.27[a])
CH_2–C(8)	–	–	–	–	–	58.17	59.97	59.89	–	59.92	59.71	59.92	59.70	60.03	59.89
C(1′)	91.46	91.89	95.62	93.31	93.75	89.78	90.20	92.27	94.19	92.16	92.17	92.85	92.68	90.40	90.08
C(2′)	84.32	84.99	82.18	82.88	82.72	83.78	83.23	82.85	82.67	82.54	82.91	82.07	82.32	84.13	84.22
C(3′)	81.38	81.46	81.48	82.21	82.51	80.57	81.98	81.37	81.61	81.62	81.51	80.72	80.49	83.31	83.91
C(4′)	87.09	87.41	85.38	88.11	88.43	86.86	87.77	85.60	87.13	86.86	87.33	86.97	87.24	85.47	85.89
C(5′)	63.88	63.55	63.09	63.79	63.35	62.79	63.27	63.26	62.90	63.69	62.93	63.62	62.94	24.63	23.25
C(6′)	–	–	–	–	–	–	–	–	81.61	101.21	82.22	101.37	80.43	101.93	79.98
C(7′)	–	–	–	–	–	–	–	–	73.22	89.65	72.95	91.88	74.50	86.82	70.23

[a]) Assignments may be interchanged.

with a soln. of ^{t}BuMe$_2$SiCl (3.68 g, 24.4 mmol) in CH_2Cl_2 (10 ml), stirred for 5 h at 25°, washed with H_2O (40 ml) and brine (30 ml), dried (Na_2SO_4), and evaporated. FC (cyclohexane/AcOEt 1:1) gave **22** (5.64 g, 88%). White foam. R_f (cyclohexane/AcOEt 1:2) 0.40. $[\alpha]_D^{25} = -58.8$ ($c = 0.5$, $CHCl_3$). UV ($CHCl_3$): 281 (22900). IR ($CHCl_3$): 3406*w*, 2998*m*, 2954*m*, 2931*m*, 2858*w*, 1707*m*, 1611*s*, 1584*m*, 1455*s*, 1385*w*, 1292*w*, 1220*s*, 1130*w*, 1090*s*, 968*w*, 838*m*. ^{1}H-NMR (300 MHz, $CDCl_3$): see *Table 12*; additionally, 9.11 (br. *s*, NH); 8.02–8.00 (*m*, 2 arom. H); 7.62–7.48 (*m*, 3 arom. H); 1.64, 1.41 (2*s*, Me_2C); 0.82 (*s*, ^{t}Bu); 0.01, 0.00 (2*s*, Me_2Si). ^{13}C-NMR (75 MHz, $CDCl_3$): see *Table 13*; additionally, 164.37 (*s*, C=O); 133.60 (*s*); 132.60 (*d*); 128.72 (2*d*); 127.71 (2*d*); 114.11 (*s*, Me_2C); 27.29, 25.43 (2*q*, Me_2C); 25.90 (*q*, Me_3C); 18.39 (*s*, Me_3C); −5.31, −5.41 (2*q*, Me_2Si). HR-MALDI-MS: 548.2238 ($[M+Na]^+$, $C_{26}H_{35}N_5NaO_5Si^+$; calc. 548.2407).

8-Iodo-2′,3′-O-*isopropylideneadenosine* (**24**). A soln of **23** [7] (384 mg, 0.71 mmol) in THF (16 ml) was treated with 8M $MeNH_2$ in EtOH (1.0 ml, 8.0 mmol), stirred for 2 h, and evaporated. FC (AcOEt/cyclohexane 1:1) gave **24** (261 mg, 84%). White solid. R_f (AcOEt/cyclohexane 1:1) 0.10. M.p. 205° (dec.). $[\alpha]_D^{25} = -87.8$ ($c = 0.5$, $CHCl_3$). UV ($CHCl_3$): 267 (38300). IR ($CHCl_3$): 3524*w*, 3411*w*, 3211*w*, 1634*s*, 1580*m*, 1444*w*, 1385*w*, 1288*m*, 1112*m*, 1084*m*, 997*w*, 851*w*. ^{1}H-NMR (300 MHz, $CDCl_3/CD_3OD$): see *Table 12*; additionally, 1.67, 1.35 (2*s*, Me_2C). ^{13}C-NMR (75 MHz, $CDCl_3/CD_3OD$): see *Table 13*; additionally, 113.97 (*s*, Me_2C); 27.70, 25.44 (2*q*, Me_2C). HR-MALDI-MS: 456.0130 ($[M+Na]^+$, $C_{13}H_{16}IN_5NaO_4^+$, calc. 456.0145).

5′-O-*[(*tert-*Butyl)diphenylsilyl]-8-iodo-2′,3′*-O-*isopropylideneadenosine* (**25**). A soln. of ^{i}Pr$_2$NH (2.6 ml, 18.9 mmol) in THF (80 ml) was cooled to −78°, treated dropwise with 1.6M BuLi in hexane (12.5 ml, 19.8 mmol), stirred for 15 min, warmed to 0° for 15 min, cooled to −78°, treated dropwise with a soln. of **20** (4 g, 6.2 mmol) in THF (75 ml), stirred for 2.5 h, treated dropwise with a soln. of *N*-iodosuccinimide (NIS; 4.1 g, 18.5 mmol) in THF (75 ml), stirred for 1.5 h, treated with AcOH (2 ml), and allowed to warm to 25°. After evaporation, a soln. of the residue in AcOEt (240 ml) was washed with cold sat. aq. $NaHCO_3$ soln. and brine, dried (Na_2SO_4), and evaporated. After filtration through a short pad of silica gel (AcOEt/cyclohexane 1:2) and evaporation, a soln. of the residue in THF (60 ml) was treated with 8M $MeNH_2$ in EtOH (4.9 ml, 39 mmol), stirred for 6 h, and evaporated. FC (AcOEt/cyclohexane 1:1) gave **25** (3.17 g, 77%). White foam. R_f (AcOEt/cyclohexane 2:1) 0.26. $[\alpha]_D^{25} = +7.7$ ($c = 1.0$, $CHCl_3$). IR ($CHCl_3$): 3412*w*, 3013*m*, 2933*w*, 2860*w*, 1632*s*, 1584*w*, 1442*w*, 1375*w*, 1288*w*, 1218*s*, 1157*w*, 1087*m*, 909*w*, 873*w*, 823*w*. ^{1}H-NMR (300 MHz, $CDCl_3$): see *Table 12*; additionally, 7.61–7.51 (*m*, 4 arom. H); 7.42–7.22 (*m*, 6 arom. H); 6.24 (br. *s*, NH_2); 1.64, 1.41 (2*s*, Me_2C); 1.01 (*s*, ^{t}Bu). ^{13}C-NMR (75 MHz, $CDCl_3$): see *Table 13*; additionally, 135.33 (2*d*); 135.29 (2*d*); 133.21, 132.90 (2*s*); 129.50, 129.45 (2*d*); 127.44 (2*d*); 127.36 (2*d*); 113.81 (*s*, Me_2C); 27.28, 25.54 (2*q*, Me_2C); 26.81 (*q*, Me_3C); 19.27 (*s*, Me_3C). HR-MALDI-MS: 694.1305 ($[M+Na]^+$, $C_{29}H_{34}IN_5NaO_4Si^+$; calc. 694.1425).

8-Iodo-2′,3′-O-*isopropylidene-5′*-O-*(triisopropylsilyl)adenosine* (**26**). Similarly to the preparation of **25**, **21** [9] (4.0 g, 7.0 mmol) was treated with LDA (50 mmol) and then with NIS (8.8 g, 39.6 mmol). After treating the mixture with AcOH and evaporating the solvent, a soln. of the residue in AcOEt was filtered through a short pad of silica gel (AcOEt/cyclohexane 1:2) and evaporated. A soln. of the residue in THF (55 ml) was treated with 8M $MeNH_2$ in EtOH (5.1 ml, 40.5 mmol), stirred for 4 h, and evaporated. FC (AcOEt/$CHCl_3$ 1:3) gave **26** (3.1 g, 76%). Light yellow foam. R_f (AcOEt/$CHCl_3$ 1:2) 0.20. $[\alpha]_D^{25} = -11.8$ ($c = 1.0$, $CHCl_3$). UV ($CHCl_3$): 267 (16300). IR ($CHCl_3$): 3412*m*, 2945*m*, 2867*m*, 1720*w*, 1632*s*, 1583*m*, 1442*m*, 1384*w*, 1287*m*, 1218*s*, 1157*m*, 1093*m*, 997*w*, 882*m*. ^{1}H-NMR (300 MHz, $CDCl_3$): see *Table 12*; additionally, 5.72 (br. *s*, NH_2); 1.63, 1.41 (2*s*, Me_2C); 0.97–0.95 (*m*, $(Me_2CH)_3$Si). ^{13}C-NMR (75 MHz, $CDCl_3$): see *Table 13*; additionally, 113.73 (*s*, Me_2C); 27.26, 25.53 (2*q*, Me_2C); 17.94 (*q*, $(Me_2CH)_3$Si); 11.96 (*d*, $(Me_2CH)_3$Si). HR-MALDI-MS: 612.1466 ($[M+Na]^+$, $C_{22}H_{36}IN_5NaO_4Si^+$; calc. 612.1576).

9-(6,7-Dideoxy-2,3-O-*isopropylidene-α*-L-talo-*hept-6-ynofuranosyl)adenine* (**28**). A soln. of **27** [7] (1.15 g, 2.26 mmol) in THF (16 ml) was cooled to 0°, treated with 8M $MeNH_2$ in EtOH (2 ml), stirred for 5 h at 25°, and evaporated. A soln. of the residue in THF (18 ml) was treated with $Bu_4NF \cdot 3\,H_2O$ (800 mg, 2.47 mmol), stirred for 2 h, and evaporated. FC ($CHCl_3$/MeOH 20:1) gave **28** (540 mg, 72%). White solid. R_f ($CHCl_3$/MeOH 30:1) 0.15. M.p. 229–231°. $[\alpha]_D^{25} = -41.9$ ($c = 0.25$, $CHCl_3$). UV ($CHCl_3$): 259 (10900). IR ($CHCl_3$): 3413*w*, 3306*w*, 3015*s*, 2260*w*, 1633*s*, 1591*w*, 1475*w*, 1427*w*, 1376*w*, 1335*w*, 1271*w*, 1121*m*, 1083*m*, 1046*w*, 930*w*, 846*w*. ^{1}H-NMR (300 MHz, $CDCl_3/CD_3OD$): see *Table 12*;

additionally, 1.62, 1.35 (2*s*, Me_2C). ^{13}C-NMR (75 MHz, $CDCl_3/CD_3OD$): see *Table 13*; additionally, 114.33 (*s*, $Me_2\mathit{C}$); 27.55, 25.23 (2*q*, Me_2C). HR-MALDI-MS: 354.1178 ($[M+Na]^+$, $C_{15}H_{17}N_5NaO_4^+$; calc. 354.1178). Anal. calc. for $C_{15}H_{17}N_5O_4$ (331.33): C 54.38, H 5.17, N 21.14; found: C 54.40, H 5.27, N 21.23.

N^6-*Benzoyl-5′*-O-*[(*tert-*butyl)dimethylsilyl]-8-(hydroxymethyl)-2′,3′*-O-*isopropylideneadenosine* (**29**). A soln. of ^{i}Pr$_2$NH (6.65 ml, 47.1 mmol) in THF (26 ml) was cooled to −76°, treated dropwise with 1.6M BuLi in hexane (29.5 ml, 47 mmol), stirred for 20 min, warmed to 0°, stirred for 15 min, cooled to −76°, treated dropwise with a soln. of **22** (4 g, 7.61 mmol) in THF (36 ml), stirred for 3 h, treated dropwise with DMF (18.2 ml) and stirred for 3 h. The soln. was treated with AcOH (6.7 ml), allowed to reach 27°, diluted with EtOH (72 ml), treated portionwise with $NaBH_4$ (1.2 g, 31.7 mmol), stirred for 3 h, cooled to 0°, treated with sat. aq. NH_4Cl soln. (40 ml), and evaporated. A soln. of the residue in CH_2Cl_2 (250 ml) was washed with H_2O (2×50 ml) and brine (40 ml), dried (Na_2SO_4), and evaporated. FC (cyclohexane/AcOEt 1:1) gave **29** (3.54 g, 83%). White solid. R_f (cyclohexane/AcOEt 1:1) 0.14. M.p. 147–148°. $[\alpha]_D^{25} = -20.4$ ($c = 0.5$, $CHCl_3$). UV ($CHCl_3$): 282 (29800). IR ($CHCl_3$): 3406*w*, 2998*w*, 2956*w*, 2932*w*, 2859*w*, 1707*m*, 1614*s*, 1590*m*, 1473*m*, 1428*m*, 1356*w*, 1257*s*, 1221*m*, 1209*s*, 1157*w*, 1087*s*, 972*w*, 897*w*, 838*m*. ^{1}H-NMR (300 MHz, $CDCl_3$): see *Table 12*; additionally, 9.16 (br. *s*, NH); 8.04–8.01 (*m*, 2 arom. H); 7.63–7.48 (*m*, 3 arom. H); 4.59 (br. *s*, *H*OCH_2–C(8)); 1.63, 1.41 (2*s*, Me_2C); 0.86 (*s*, ^{t}Bu); 0.013, 0.006 (2*s*, Me_2Si). ^{13}C-NMR (75 MHz, $CDCl_3$): see *Table 13*; additionally, 164.51 (*s*, C=O); 133.53 (*s*); 132.65 (*d*); 128.74 (2*d*); 127.76 (2*d*); 114.75 (*s*, $Me_2\mathit{C}$); 27.29, 25.49 (2*q*, Me_2C); 25.97 (*q*, Me_3C); 18.56 (*s*, $Me_3\mathit{C}$); −5.31 (2*q*, Me_2Si). HR-MALDI-MS: 578.2398 ($[M+Na]^+$, $C_{27}H_{37}N_5NaO_6Si^+$; calc. 578.2411). Anal. calc. for $C_{27}H_{37}N_5O_6Si$ (555.70): C 58.36, H 6.71, N 12.60; found: C 58.22, H 6.85, N 12.52.

N^6-*Benzoyl-5′*-O-*[(*tert-*butyl)dimethylsilyl]-8-{[(*tert-*butyl)diphenylsilyloxy]methyl}-2′,3′*-O-*isopropylideneadenosine* (**30**). A soln. of **29** (2.98 g, 5.36 mmol), 1*H*-imidazole (0.44 g, 6.43 mmol), and DMAP (66 mg, 0.54 mmol) in CH_2Cl_2 (76 ml) was treated dropwise with ^{t}BuPh$_2$SiCl (2.78 ml, 10.76 mmol), stirred at 27° for 9 h, washed with H_2O (2×30 ml) and brine (30 ml), dried (Na_2SO_4), filtered, and evaporated. FC (cyclohexane/AcOEt 2:1) gave **30** (3.78 g, 89%). White foam. R_f (cyclohexane/AcOEt 1:1) 0.59. $[\alpha]_D^{25} = -10.8$ ($c = 1.0$, $CHCl_3$). UV ($CHCl_3$): 283 (24000). IR ($CHCl_3$): 3408*w*, 3017*s*, 2933*w*, 2859*w*, 1708*m*, 1615*s*, 1588*m*, 1472*m*, 1462*m*, 1428*m*, 1360*w*, 1258*m*, 1087*s*. ^{1}H-NMR (300 MHz, $CDCl_3$): see *Table 12*; additionally, 8.91 (br. *s*, NH); 8.00–7.97 (*m*, 2 arom. H); 7.72–7.32 (*m*, 13 arom. H); 1.62, 1.42 (2*s*, Me_2C); 1.09, 0.84 (2*s*, 2 ^{t}Bu); −0.046, −0.051 (2*s*, Me_2Si). ^{13}C-NMR (75 MHz, $CDCl_3$): see *Table 13*; additionally, 164.14 (*s*, C=O); 135.58 (2*d*); 135.53 (2*d*); 133.73 (*s*); 132.58 (*d*); 132.09, 132.04 (2*s*); 129.90, 129.84 (2*d*); 128.75 (2*d*); 127.71 (2*d*); 127.63 (2*d*); 127.61 (2*d*); 113.97 (*s*, $Me_2\mathit{C}$); 27.32, 25.60 (2*q*, Me_2C); 26.79, 25.93 (2*q*, 2 Me_3C); 19.32, 18.45 (2*s*, 2 $Me_3\mathit{C}$); −5.22 (*s*, Me_2Si). MALDI-MS: 816.0 ($[M+Na]^+$, $C_{43}H_{55}N_5NaO_6Si_2^+$). Anal. calc. for $C_{43}H_{55}N_5O_6Si_2$ (794.11): C 65.04, H 6.98, N 8.82; found: C 64.76, H 6.81, N 8.88.

N^6-*Benzoyl-8-{[(*tert-*butyl)diphenylsilyloxy]methyl}-2′,3′*-O-*isopropylideneadenosine* (**31**). A soln. of **30** (80.5 mg, 0.1 mmol) in MeCN/^{t}BuOH 9:1 (1.0 ml) was treated with 20–25% H_2SiF_6 soln. in H_2O (15.4 µl), stirred for 12 h at 27°, treated with aq. Na_2CO_3 soln. (2 ml), and extracted with AcOEt (3×4 ml). The combined org. layers were washed with H_2O (2×3 ml) and brine (3 ml), dried (Na_2SO_4), filtered, and evaporated. FC (cyclohexane/AcOEt 1:1) gave **30** (13 mg, 16%) and **31** (54 mg, 79%). White solid. R_f (cyclohexane/AcOEt 1:1) 0.13. M.p. 179–180°. $[\alpha]_D^{25} = -47.2$ ($c = 1.0$, $CHCl_3$). UV ($CHCl_3$): 284 (24600). IR ($CHCl_3$): 3407*w*, 3015*m*, 2975*w*, 1710*m*, 1614*s*, 1591*m*, 1428*s*, 1360*m*, 1255*s*, 1172*w*, 1114*m*, 1083*m*, 1047*m*, 877*w*, 854*w*, 824*w*. ^{1}H-NMR (300 MHz, $CDCl_3$): see *Table 12*; additionally, 8.95 (br. *s*, NH); 7.99–7.96 (*m*, 2 arom. H); 7.72–7.57 (*m*, 5 arom. H); 7.45–7.28 (*m*, 8 arom. H); 1.58, 1.37 (2*s*, Me_2C); 1.09 (*s*, ^{t}Bu). ^{13}C-NMR (75 MHz, $CDCl_3$): see *Table 13*; additionally, 135.51 (2*d*); 135.44 (2*d*); 133.48 (*s*); 132.68 (*d*); 132.05, 131.86 (2*s*); 129.94, 129.85 (2*d*); 128.75 (2*d*); 127.74 (2*d*); 127.63 (2*d*); 127.59 (2*d*); 114.06 (*s*, $Me_2\mathit{C}$); 27.62, 25.39 (2*q*, Me_2C); 26.73 (*q*, Me_3C); 19.29 (*s*, $Me_3\mathit{C}$). HR-MALDI-MS: 702.2726 ($[M+Na]^+$, $C_{37}H_{41}N_5NaO_6Si^+$; calc. 702.2724). Anal. calc. for $C_{37}H_{41}N_5O_6Si$ (679.85): C 65.37, H 6.08, N 10.30; found: C 65.47, H 6.17, N 10.19.

Transformation of **31** *to* **32** *and* **33**. A soln. of **31** (1.62 g, 2.38 mmol) and DCC (1.48 g, 7.14 mmol) in dry DMSO (9.5 ml) was cooled to 15°, treated dropwise with $CHCl_2CO_2H$ (97.6 µl, 1.18 mmol), stirred for 15 min, warmed to 26°, stirred for 3 h, and filtered (washing of the residue with 6 ml of DMSO).

The combined filtrates and washings were extracted with hexane (4×100 ml). The DMSO layer was diluted with $CHCl_3$ (300 ml), washed with H_2O (2×150 ml), dried (Na_2SO_4), and evaporated affording the crude aldehyde (1.45 g).

A soln. of EtMgBr (7.26 mmol) in THF (12 ml) was cooled to 0°, treated dropwise with (trimethylsilyl)acetylene (1.01 ml, 7.21 mmol), stirred for 20 min, warmed to 26°, stirred for 40 min, cooled to 0°, treated with a soln. of the crude aldehyde in dry THF (30 ml), and stirred for 3 h. The mixture was treated with sat. aq. NH_4Cl soln. (36 ml) and allowed to warm to 26°. The layers were separated, and the aq. layer was extracted with AcOEt (2×60 ml). The combined org. layers were washed with H_2O and brine, dried (Na_2SO_4), and evaporated. FC (cyclohexane/AcOEt 1:2) gave **32** (772 mg, 42%) and **33** (386 mg, 21%).

Data of N^6-*Benzoyl-8-{[(*tert-*butyl)diphenylsilyloxy]methyl}-9-[6,7-dideoxy-2,3-*O-*isopropylidene-7-*C-*(trimethylsilyl)-β-*D-allo-*hept-6-ynofuranosyl]adenine* (**32**). White solid. R_f (cyclohexane/AcOEt 1:2) 0.36. M.p. 129–131°. $[\alpha]_D^{25} = -65.0$ ($c = 0.25$, $CHCl_3$). UV ($CHCl_3$): 284 (24600). IR ($CHCl_3$): 3480*w*, 3017*s*, 2200*w*, 1710*w*, 1615*w*, 1428*w*, 1252*w*, 1209*s*, 1088*w*, 1046*w*, 931*w*, 845*w*. ^{1}H-NMR (300 MHz, $CDCl_3$): see *Table 12*; additionally, 8.91 (br. *s*, NH); 7.99–7.96 (*m*, 2 arom. H); 7.72–7.29 (*m*, 13 arom. H); 1.59, 1.40 (2*s*, Me_2C); 1.08 (*s*, ^{t}Bu); 0.22 (*s*, Me_3Si). ^{13}C-NMR (75 MHz, $CDCl_3$): see *Table 13*; additionally, 135.51 (2*d*); 135.44 (2*d*); 133.46 (*s*); 132.77 (*d*); 132.02, 131.80 (2*s*); 130.01, 129.87 (2*d*); 128.81 (2*d*); 127.81 (2*d*); 127.66 (2*d*); 127.60 (2*d*); 114.04 (*s*, Me_2C); 27.69, 25.43 (2*q*, Me_2C); 26.70 (*q*, Me_3C); 19.30 (*s*, Me_3C); −0.07 (*q*, Me_3Si). HR-MALDI-MS: 798.3123 ($[M+Na]^+$, $C_{42}H_{49}N_5NaO_6Si_2^+$; calc. 798.3119). Anal. calc. for $C_{42}H_{49}N_5O_6Si_2$ (776.05): C 65.00, H 6.36, N 9.02; found: C 64.94, H 6.41, N 8.83.

Data of N^6-*Benzoyl-8-{[(*tert-*butyl)diphenylsilyloxy]methyl}-9-[6,7-dideoxy-2,3-*O-*isopropylidene-7-*C-*(trimethylsilyl)-α-*L-talo-*hept-6-ynofuranosyl]adenine* (**33**). White solid. R_f (cyclohexane/AcOEt 1:2) 0.23. M.p. 99–101°. $[\alpha]_D^{25} = +28.3$ ($c = 1.0$, $CHCl_3$). UV ($CHCl_3$): 285 (15600). IR ($CHCl_3$): 3450*w*, 3018*m*, 2860*w*, 2180*w*, 1710*w*, 1615*w*, 1592*w*, 1428*w*, 1359*w*, 1252*w*, 1221*s*, 1217*w*, 1213*s*, 1209*s*, 1089*w*, 1047*w*, 930*w*, 846*w*. ^{1}H-NMR (300 MHz, $CDCl_3$): see *Table 12*; additionally, 8.92 (br. *s*, NH); 7.99–7.96 (*m*, 2 arom. H); 7.72–7.37 (*m*, 12 arom. H); 7.24–7.19 (*m*, 1 arom. H); 1.61, 1.36 (2*s*, Me_2C); 1.08 (*s*, ^{t}Bu); 0.10 (*s*, Me_3Si). ^{13}C-NMR (75 MHz, $CDCl_3$): see *Table 13*; additionally, 164.01 (*s*, C=O); 135.64 (2*d*); 135.48 (2*d*); 133.50 (*s*); 132.72 (*d*); 131.93, 131.88 (2*s*); 129.89, 129.68 (2*d*); 128.79 (2*d*); 127.78 (2*d*); 127.69 (2*d*); 127.42 (2*d*); 114.39 (*s*, Me_2C); 27.69, 25.43 (2*q*, Me_2C); 26.70 (*q*, Me_3C); 19.30 (*s*, Me_3C); −0.07 (*q*, Me_3Si). HR-MALDI-MS: 798.3103 ($[M+Na]^+$, $C_{42}H_{49}N_5NaO_6Si_2^+$; calc. 798.3119). Anal. calc. for $C_{42}H_{49}N_5O_6Si_2$ (776.05): C 65.00, H 6.36, N 9.02; found: C 64.88, H 6.62, N 8.78.

*8-{[(*tert-*Butyl)diphenylsilyloxy]methyl}-9-[6,7-dideoxy-2,3-*O-*isopropylidene-β-*D-allo-hept-6-ynofuranosyl]adenine* (**34**). A soln. of **32** (887 mg, 1.14 mmol) in MeOH (17.5 ml) was cooled to 0°, treated with sat. K_2CO_3 soln. in MeOH (12 ml), stirred for 6 h, diluted with aq. NH_4Cl soln. and H_2O, and extracted with $CHCl_3$ (3×25 ml). The combined org. layers were washed with H_2O (30 ml) and brine (30 ml), dried (Na_2SO_4), and evaporated. A soln. of the residue in THF (24 ml) was treated with 8M $MeNH_2$ in EtOH (1.1 ml), stirred for 6 h, and evaporated. FC (cyclohexane/AcOEt 1:2) gave **34** (491 mg, 72%). White solid. R_f (cyclohexane/AcOEt 1:2) 0.13. M.p. 199–201°. $[\alpha]_D^{25} = -1.0$ ($c = 0.25$, $CHCl_3$). UV ($CHCl_3$): 240.0 (16400). IR ($CHCl_3$): 3468*w*, 3270*w*, 3017*s*, 2270*w*, 1660*m*, 1579*w*, 1528*w*, 1486*w*, 1415*w*, 1282*w*, 1221*s*, 1213*s*, 1209*s*, 1046*w*, 930*w*, 876*w*. ^{1}H-NMR (300 MHz, $CDCl_3$): see *Table 12*; additionally, 7.72–7.69 (*m*, 2 arom. H); 7.64–7.61 (*m*, 2 arom. H); 7.45–7.29 (*m*, 6 arom. H); 5.98 (br. *s*, NH_2); 1.58, 1.39 (2*s*, Me_2C); 1.07 (*s*, ^{t}Bu). ^{13}C-NMR (75 MHz, $CDCl_3$): see *Table 13*; additionally, 135.40 (2*d*); 135.35 (2*d*); 132.13, 131.84 (2*s*); 129.91, 129.85 (2*d*); 127.73 (2*d*); 127.61 (2*d*); 114.02 (*s*, Me_2C); 27.62, 25.43 (2*q*, Me_2C); 26.67 (*q*, Me_3C); 19.30 (*s*, Me_3C). HR-MALDI-MS: 622.2460 ($[M+Na]^+$, $C_{32}H_{37}N_5NaO_5Si^+$; calc. 622.2462).

*8-{[(*tert-*Butyl)diphenylsilyloxy]methyl}-9-(6,7-dideoxy-2,3-*O-*isopropylidene-α-*L-talo-*hept-6-ynofuranosyl)adenine* (**35**). A soln. of **33** (183 mg, 0.236 mmol) was cooled to −20°, treated with sat. K_2CO_3 soln. in MeOH (3 ml), stirred for 5 h, diluted with aq. NH_4Cl soln. and H_2O, and extracted with $CHCl_3$ (3×20 ml). The combined org. layers were washed with H_2O (20 ml) and brine (20 ml), dried (Na_2SO_4), and evaporated. A soln. of the residue in THF (6 ml) was treated with 8M $MeNH_2$ in EtOH (0.2 ml), stirred for 18 h, and evaporated. FC (cyclohexane/AcOEt 1:2) gave **35** (113 mg, 80%). White solid. R_f (cyclohexane/AcOEt 1:2) 0.11. M.p. 208–210°. $[\alpha]_D^{25} = -5.2$ ($c = 1.0$, $CHCl_3$). UV ($CHCl_3$): 265 (15600). IR ($CHCl_3$): 3412*w*, 3307*w*, 3018*m*, 2860*w*, 2250*w*, 1638*m*, 1590*w*, 1455*w*, 1428*w*, 1376*w*, 1333*w*, 1221*s*, 1217*s*, 1213*s*, 1209*s*, 1114*w*, 1085*w*, 1047*w*, 856*w*, 824*w*. ^{1}H-NMR (300 MHz, $CDCl_3$): see *Table 12*; additionally,

7.71–7.66 (*m*, 4 arom. H); 7.46–7.31 (*m*, 6 arom. H, HO–C(5′)); 5.87 (br. *s*, NH_2); 1.57, 1.36 (2*s*, Me_2C); 1.08 (*s*, ^{t}Bu). ^{13}C-NMR (75 MHz, $CDCl_3$): see *Table 13*; additionally, 135.52 (2*d*); 135.49 (2*d*); 132.13, 132.02 (2*s*); 129.88, 129.82 (2*d*); 127.72 (2*d*); 127.65 (2*d*); 114.17 (*s*, Me_2C); 27.54, 25.41 (2*q*, *Me*$_2$C); 26.81 (*q*, *Me*$_3$C); 19.32 (*s*, Me_3C). HR-MALDI-MS: 622.2463 ($[M+Na]^+$, $C_{32}H_{37}N_5NaO_5Si^+$; calc. 622.2462).

N^6-*Benzoyl-8-[[(*tert*-butyl)diphenylsilyloxy]methyl]-9-[5,6,7-trideoxy-2,3*-O-*isopropylidene-7*-C-*(trimethylsilyl)-β*-D-ribo-*hept-6-ynofuranosyl]adenine* (**36**). A soln. of **32**/**33** *ca.* 2:1 (1.253 g, 1.615 mmol) in dry CH_2Cl_2 (30 ml) was treated with (thiocarbonyl)diimidazole (576 mg, 3.23 mmol), stirred for 20 h at 26°, and evaporated. FC (cyclohexane/AcOEt 1:1) gave the imidazolyl thiocarbamate (1.2 g). Its soln. in dry toluene (22 ml) was treated with AIBN (32 mg, 0.2 mmol) and Bu_3SnH (0.69 ml, 2.61 mmol), and stirred for 1.5 h at 80°. Evaporation and FC (cyclohexane/AcOEt 2:1) gave **36** (795 mg, 65%). White foam. R_f (cyclohexane/AcOEt 1:1) 0.56. M.p. 107–109°. $[\alpha]_D^{25} = -17.7$ ($c = 1.0$, $CHCl_3$). UV ($CHCl_3$): 284 (30000). IR ($CHCl_3$): 3408*w*, 2998*w*, 2960*w*, 2860*w*, 2176*w*, 1708*s*, 1615*s*, 1589*s*, 1461*m*, 1428*s*, 1356*m*, 1253*s*, 1168*w*, 1094*s*. ^{1}H-NMR (300 MHz, $CDCl_3$): see *Table 12*; additionally, 8.96 (br. *s*, NH); 8.00–7.97 (*m*, 2 arom. H); 7.72–7.32 (*m,* 13 arom. H); 1.62, 1.42 (2*s*, Me_2C); 1.09 (*s*, ^{t}Bu); 0.14 (*s*, Me_3Si). ^{13}C-NMR (75 MHz, $CDCl_3$): see *Table 13*; additionally, 164.22 (*s*, C=O); 135.59 (2*d*); 135.54 (2*d*); 133.70 (*s*); 132.57 (*d*); 132.09, 132.02 (2*s*); 129.90, 129.85 (2*d*); 128.73 (2*d*); 127.71 (2*d*); 127.67 (4*d*); 114.10 (*s*, Me_2C); 27.04, 25.52 (2*q*, *Me*$_2$C); 26.81 (*q*, *Me*$_3$C); 19.32 (*s*, Me_3C); 0.16 (*q*, Me_3Si). MALDI-MS: 782.0 ($[M+Na]^+$, $C_{42}H_{49}N_5NaO_5Si_2^+$). Anal. calc. for $C_{42}H_{49}N_5O_5Si_2$ (760.05): C 66.37, H 6.50, N 9.21; found: C 66.43, H 6.35, N 9.04.

*8-[[(*tert*-Butyl)diphenylsilyloxy]methyl]-9-(5,6,7-trideoxy-2,3*-O-*isopropylidene-β*-D-ribo-*hept-6-ynofuranosyl)adenine* (**37**). A soln. of **36** (231 mg, 0.3 mmol) in THF (30 ml) was cooled to 0°, treated with $Bu_4NF \cdot 3\ H_2O$ (107 mg, 0.33 mmol), stirred for 3 h, and evaporated. FC (cyclohexane/AcOEt 2:1) gave the terminal acetylene (163 mg). Its soln. in THF (6 ml) was treated with 8M $MeNH_2$ in EtOH (0.3 ml, 2.4 mmol), stirred for 9 h at 25°, and evaporated. FC (cyclohexane/AcOEt 1:1) gave **37** (134 mg, 77%). White solid. R_f (cyclohexane/AcOEt 1:1) 0.31. M.p. 160–161°. $[\alpha]_D^{25} = -28.0$ ($c = 1.0$, $CHCl_3$). UV ($CHCl_3$): 264.0 (11400). IR ($CHCl_3$): 3412*w*, 3309*w*, 3018*s*, 2860*w*, 2100*w*, 1635*s*, 1591*w*, 1428*w*, 1374*m*, 1329*w*, 1157*w*, 1082*s*, 1007*w*. ^{1}H-NMR (300 MHz, $CDCl_3$): see *Table 12*; additionally, 7.70–7.60 (*m*, 4 arom. H); 7.50–7.30 (*m*, 6 arom. H); 5.90 (br. *s*, NH_2); 1.62, 1.41 (2*s*, Me_2C); 1.08 (*s*, ^{t}Bu). ^{13}C-NMR (75 MHz, $CDCl_3$): see *Table 13*; additionally, 135.56 (2*d*); 135.51 (2*d*); 132.15 (2*s*); 129.89, 129.82 (2*d*); 127.73 (2*d*); 127.65 (2*d*); 114.00 (*s*, Me_2C); 27.02, 25.54 (2*q*, *Me*$_2$C); 26.80 (*q*, *Me*$_3$C); 19.30 (*s*, Me_3C). HR-MALDI-MS: 606.2513 ($[M+Na]^+$, $C_{32}H_{37}N_5NaO_4Si^+$; calc. 606.2512). Anal. calc. for $C_{32}H_{37}N_5O_4Si$ (583.75): C 65.84, H 6.39, N 12.00; found: C 66.10, H 6.44, N 11.74.

2,3-O-*Isopropylidene-5′*-O-*(triisopropylsilyl)uridin-6-yl-(6 → 7′*-C*)-9-(6,7-dideoxy-2,3*-O-*isopropylidene-β*-D-allo-*hept-6-ynofuranosyl)adenine* (**41**). A soln. of **38** [2] (363 mg, 0.64 mmol), **39** [6] (183 mg, 0.55 mmol), $[Pd_2(dba)_3]$ (25 mg, 0.028 mmol), CuI (12 mg, 0.056 mmol), and $P(fur)_3$ (12 mg, 0.045 mmol) in degassed Et_3N/toluene 1:1 (11 ml) was stirred for 16 h at 25°. Evaporation and FC ($CHCl_3$/MeOH 20:1) gave **41** (300 mg, 70%). Pale yellow solid. R_f ($CHCl_3$/MeOH 20:1) 0.14. M.p. 171–173°. $[\alpha]_D^{25} = -88.0$ ($c = 1.0$, $CHCl_3$). UV ($CHCl_3$): 265 (15500). IR ($CHCl_3$): 3411*w*, 3017*s*, 2944*m*, 2867*m*, 2250*w*, 1697*s*, 1634*m*, 1595*m*, 1432*w*, 1376*m*, 1338*w*, 1303*w*, 1271*w*, 1253*w*, 1209*s*, 1155*w*, 1091*s*, 997*w*, 930*w*, 882*w*. ^{1}H-NMR (300 MHz, $CDCl_3$): see *Table 14*; additionally, 10.13 (br. *s*, NH); 6.14 (br. *s*, NH_2); 1.66, 1.57, 1.42, 1.37 (4*s*, 2 Me_2C); 1.08–1.03 (*m*, $(Me_2CH)_3Si$). ^{13}C-NMR (75 MHz, $CDCl_3$): see *Table 15*; additionally, 114.46, 113.64 (2*s*, 2 Me_2C); 27.72, 27.33, 25.53, 25.41 (4*q*, 2 *Me*$_2$C); 18.03 (*q*, $(Me_2CH)_3Si$); 12.05 (*d*, $(Me_2CH)_3Si$). MALDI-MS: 792.3 ($[M+Na]^+$, $C_{36}H_{51}N_7NaO_{10}Si^+$). Anal. calc. for $C_{36}H_{51}N_7O_{10}Si$ (769.93): C 56.16, H 6.68, N 12.73; found: C 55.92, H 6.77, N 12.64.

2′,3′-O-*Isopropylidene-5′*-O-*(triisopropylsilyl)uridin-6-yl-(6 → 7′*-C*)-9-[6,7-dideoxy-2,3*-O-*isopropylidene-5*-O-*(triisopropylsilyl)-β*-D-allo-*hept-6-ynofuranosyl]adenine* (**42**). A soln. of **38** (183 mg, 0.32 mmol), **40** [1] (131 mg, 0.27 mmol), $[Pd_2(dba)_3]$ (12.8 mg, 0.014 mmol), CuI (5.3 mg, 0.028 mmol), and $P(fur)_3$ (5.2 mg, 0.022 mmol) in degassed Et_3N/toluene 1:1 (8 ml) was stirred for 16 h at 25°. Evaporation and FC ($CHCl_3$/MeOH 80:1) gave **42** (175 mg, 70%). Pale yellow solid. R_f ($CHCl_3$/MeOH 50:1) 0.08. M.p. 142–144°. $[\alpha]_D^{25} = +62.1$ ($c = 1.0$, $CHCl_3$). UV ($CHCl_3$): 264 (16400). IR ($CHCl_3$): 3485*w*, 3412*w*, 3330*w*, 2945*s*, 2868*s*, 2233*w*, 1697*s*, 1636*s*, 1596*m*, 1465*m*, 1434*w*, 1384*s*, 1330*m*, 1296*w*, 1252*m*, 1157*m*, 1088*s*, 997*m*, 882*m*. ^{1}H-NMR (300 MHz, $CDCl_3$): see *Table 14*; additionally, 13.39 (br. *s*, NH); 6.85 (br.

Table 14. *Selected ^{1}H-NMR Chemical Shifts* [ppm] *and Coupling Constants* [Hz] *of the U*[c$_y$]A$^{(*)}$ Dimers* **41**–**45**, **47**, *and* **48** *in CDCl$_3$*[a])

	41	**42**	**43**[b])	**44**	**45**[b])	**47**[b])	**48**[c])
Uridine unit (II)							
H–C(5)	6.02	5.53	6.01	5.79	5.78	5.54	5.22
H–C(1′)	6.24	5.96	6.25	6.16	6.20	6.16	6.23
H–C(2′)	5.24	5.27	5.25–5.18	5.18–5.14	5.07	5.33	5.42
H–C(3′)	4.88	4.81	4.85	4.87–4.81	4.80	4.85	4.89
H–C(4′)	4.22	4.14	4.21	4.06	4.14	4.20	4.20
2 H–C(5′)	3.88	3.83	3.87	3.80	3.81	3.85	3.84
^4J(5,NH)	0	1.5	2.1	1.5	1.8	0	0.9
J(1′,2′)	1.5	<1.0	1.2	0.9	1.9	<1.0	0
J(2′,3′)	6.6	6.3	6.6	[c])	6.2	6.2	6.3
J(3′,4′)	4.5	4.5	4.5	4.5	4.2	4.2	3.9
J(4′,5′)	6.9	6.3	6.3	6.6	6.2	6.3	6.3
Adenosine unit (I)							
H–C(2)	8.33	8.29	8.32	8.33	8.31	8.35	8.29
H–C(8)	7.91	8.08	–	7.92	–	8.06	–
CH$_a$–C(8)	–	–	5.06	–	5.02	–	5.04
CH$_b$–C(8)	–	–	4.89	–	4.93	–	4.96
H–C(1′)	5.89	6.16	6.52	5.89	6.50	6.15	6.57
H–C(2′)	5.16	5.97	5.25–5.18	5.18–5.14	5.21	5.92	5.97
H–C(3′)	5.21	5.09	5.25–5.18	5.06	5.14	5.17	5.33
H–C(4′)	4.63	4.45	4.60	4.65	4.58	4.46	4.26
H$_a$–C(5′)	5.01	4.96	5.06	4.87–4.81	4.94	3.03	2.95
H$_b$–C(5′)	–	–	–	–	–	2.93	2.87
HO–C(5′)	8.15	–	8.07	8.28	7.88	–	–
J(H$_a$,H$_b$)	–	–	12.9	–	13.3	–	13.2
J(1′,2′)	3.9	1.2	4.8	4.8	4.4	1.5	<1.5
J(2′,3′)	6.0	6.3	[d])	6.0	6.0	6.2	6.0
J(3′,4′)	0	3.9	0	0	2.0	4.0	5.1
J(4′,5′a)	1.2	4.5	<1.0	<1.0	1.5	4.5	5.1
J(4′,5′b)	–	–	–	–	–	4.2	4.2
J(5′a,5′b)	–	–	–	–	–	17.4	17.4
J(5′a,OH)	<1.0	–	<1.0	11.4	10.4	–	–

[a]) Assignments based on selective homodecoupling experiments. Concentration: 60 mM (**41**: 10 mM). [b]) Assignments based on a DQF-COSY and a HSQC spectrum. [c]) Assignments based on a HMBC spectrum. [d]) Not determined.

s, NH$_2$); 1.63, 1.54, 1.44, 1.42 (4*s*, 2 Me$_2$C); 1.15–0.97 (*m*, 2 (Me$_2$CH)$_3$Si). ^{13}C-NMR (75 MHz, CDCl$_3$): see *Table 15*; additionally, 114.30, 113.30 (2*s*, 2 Me$_2$*C*); 27.53, 27.22, 25.72, 25.58 (4*q*, 2 *Me*$_2$C); 17.98 (*q*, 2 (*Me*$_2$CH)$_3$Si); 12.25, 12.05 (2*d*, 2 (Me$_2$*C*H)$_3$Si). HR-MALDI-MS: 948.4651 ([*M*+Na]$^+$, $C_{45}H_{71}N_7NaO_{10}Si_2^+$; calc. 948.4699). Anal. calc. for $C_{45}H_{71}N_7O_{10}Si_2$ (926.27): C 58.35, H 7.73, N 10.59; found: C 58.20, H 7.93, N 10.38.

2′,3′-O-*Isopropylidene-5′*-O-*(triisopropylsilyl)uridin-6-yl-(6 → 7′*-C*)-8-{[*(tert-*butyl)diphenylsilyloxy]-methyl}-9-(6,7-dideoxy-2,3*-O-*isopropylidene-β*-D-allo-*hept-6-ynofuranosyl)adenine* (**43**). Similarly to the preparation of **41**, treatment of **38** (404 mg, 0.712 mmol) with **34** (360 mg, 0.584 mmol) gave **43** (412 mg, 68%). Light yellow solid. R_f (AcOEt/cyclohexane 2:1) 0.20. M.p. 153–155°. $[\alpha]_D^{25} = -49.1$ (c=2.0, $CHCl_3$). UV ($CHCl_3$): 268 (16100). IR ($CHCl_3$): 3410*w*, 3017*m*, 2943*m*, 2866*w*, 2240*w*, 1697*m*, 1638*m*, 1596*w*, 1454*w*, 1428*w*, 1376*m*, 1335*w*, 1302*w*, 1269*w*, 1218*s*, 1215*s*, 1210*s*, 1156*w*, 1088*m*, 908*w*, 882*w*. ^{1}H-

Table 15. *Selected* ^{13}*C-NMR Chemical Shifts* [ppm] *of the U*[c$_y$]A$^{(*)}$ Dimers* **41**–**45**, **47**, *and* **48** *in* $CDCl_3$

	41	**42**	**43**[a])	**44**	**45**[a])	**47**[a])	**48**[b])
Uridine unit (II)							
C(2)	149.57	150.13	149.59[b])	150.10	149.91[b])	150.55	149.96
C(4)	161.95	163.70	162.30	162.95	162.78	164.04	163.86
C(5)	108.78	108.57	108.74	108.32	108.19	108.43	107.86
C(6)	137.22	136.61	137.28	137.41	137.66	137.36	137.45
C(1′)	94.76	93.87	94.08	94.67	94.11	93.96	94.34
C(2′)	83.95	84.25	83.95	83.98	84.00	84.29	83.99
C(3′)	82.19	82.25	82.19	82.12	82.28	82.41	82.54
C(4′)	89.32	89.83	89.32	89.14	89.36	89.75	89.38
C(5′)	64.19	64.46[c])	64.24	64.04	64.19	64.37	64.18
Adenosine unit (I)							
C(2)	152.36	152.40	152.07	152.41	152.31	152.83	152.87
C(4)	147.75	148.82	149.19[c])	147.69	149.44[c])	149.13	150.20
C(5)	120.76	119.87	118.90	120.28	118.80	119.68	118.28
C(6)	155.97	155.75	155.74	156.16	155.97	155.96	155.54
C(8)	140.18	140.41	149.53[c])	140.01	149.52[c])	139.89	150.01
CH_2–C(8)	–	–	59.66	–	59.48	–	59.96
C(1′)	94.12	91.25	92.67	93.88	92.40	90.59	88.53
C(2′)	82.72	83.18	82.72	82.71	83.16	83.69	83.55
C(3′)	80.60	81.37	80.39	81.64	81.33	82.71	82.54
C(4′)	87.26	89.69	86.87	86.53	86.73	84.05	83.99
C(5′)	63.80	64.56[c])	63.75	63.83	63.77	24.19	23.88
C(6′)	98.98	99.23	99.19	100.63	101.35	98.55	99.09
C(7′)	76.58	76.58	76.39	75.34	75.03	73.69	73.33

[a]) Assignments based on a HSQC spectrum. [b]) Assignments based on a HMBC spectrum. [c]) Assignments may be interchanged.

NMR (500 MHz, $CDCl_3$): see *Table 14*; additionally, 10.89 (br. *s*, NH); 7.71–7.62 (*m*, 4 arom. H); 7.47–7.31 (*m*, 6 arom. H); 6.31 (br. *s*, NH_2); 1.59, 1.58, 1.41, 1.36 (4*s*, 2 Me_2C); 1.08 (*s*, ^{t}Bu); 1.08–1.02 (*m*, $(Me_2CH)_3Si$). ^{13}C-NMR (125 MHz, $CDCl_3$): see *Table 15*; additionally, 135.48 (2*d*); 135.46 (2*d*); 132.22, 131.98 (2*s*); 129.94, 129.87 (2*d*); 127.76 (2*d*); 127.66 (2*d*); 114.36, 113.62 (2*s*, 2 Me_2C); 27.67, 27.35, 25.55 (3*q*, 2 Me_2C); 26.76 (*q*, Me_3C); 19.31 (*s*, Me_3C); 18.03 (*q*, $(Me_2CH)_3Si$); 12.06 (*d*, $(Me_2CH)_3Si$). HR-MALDI-MS: 1060.465 ($[M+Na]^+$, $C_{53}H_{71}N_7NaO_{11}Si_2^+$; calc. 1060.465). Anal. calc. for $C_{53}H_{71}N_7O_{11}Si_2$ (1038.36): C 61.38, H 6.89, N 9.44; found: C 61.10, H 6.72, N 9.50.

2′,3′-O-*Isopropylidene-5′*-O-*(triisopropylsilyl)uridin-6-yl-(6 → 7′*-C*)-9-(6,7-dideoxy-2,3*-O-*isopropylidene-α*-L-talo-*hept-6-ynofuranosyl)adenine* (**44**). Similarly to the preparation of **41**, treatment of **38** (170 mg, 0.32 mmol) with **28** (85 mg, 0.26 mmol) gave **44** (168 mg, 84%). White solid. R_f ($CHCl_3$/MeOH 20:1) 0.11. M.p. 168–170°. $[\alpha]_D^{25} = +52.3$ (*c* = 2.0, $CHCl_3$). UV ($CHCl_3$): 265 (23500). IR ($CHCl_3$): 3412*w*, 3014*m*, 2944*m*, 2867*m*, 2219*w*, 1696*s*, 1634*s*, 1595*m*, 1431*m*, 1376*m*, 1337*w*, 1270*w*, 1241*w*, 1156*m*, 1123*m*, 1083*s*, 997*w*, 881*m*. ^{1}H-NMR (300 MHz, $CDCl_3$): see *Table 14*; additionally, 12.14 (br. *s*, NH); 6.75 (br. *s*, NH_2); 1.64, 1.54, 1.37, 1.31 (4*s*, 2 Me_2C); 1.03–0.98 (*m*, $(Me_2CH)_3Si$). ^{13}C-NMR (75 MHz, $CDCl_3$): see *Table 15*; additionally, 114.40, 113.43 (2*s*, 2 Me_2C); 27.68, 27.26, 25.45, 25.32 (4*q*, 2 Me_2C); 18.00 (*q*, $(Me_2CH)_3Si$); 12.02 (*d*, $(Me_2CH)_3Si$). MALDI-MS: 792.3 ($[M+Na]^+$, $C_{36}H_{51}N_7NaO_{10}Si^+$). Anal. calc. for $C_{36}H_{51}N_7O_{10}Si$ (769.93): C 56.16, H 6.68, N 12.73; found: C 56.06, H 6.67, N 12.60.

2′,3′-O-*Isopropylidene-5′*-O-*(triisopropylsilyl)uridin-6-yl-(6 → 7′*-C*)-8-{[(*tert*-butyl)diphenylsilyloxy]-methyl}-9-(6,7-dideoxy-2,3*-O-*isopropylidene-α*-L-*talo-*hept-6-ynofuranosyl)adenine* (**45**). Similarly to the preparation of **41**, treatment of **38** (107 mg, 0.19 mmol) with **35** (95 mg, 0.158 mmol) gave **45** (147 mg, 90%). Light yellow solid. R_f (AcOEt/cyclohexane 3:1) 0.25. M.p. 154–156°. $[\alpha]_D^{25} = +27.6$ (*c* = 2.0,

$CHCl_3$). UV ($CHCl_3$): 267 (31400). IR ($CHCl_3$): 3411*w*, 3017*s*, 2943*m*, 2866*m*, 2210*w*, 1694*s*, 1638*m*, 1595*w*, 1454*m*, 1428*m*, 1334*w*, 1156*w*, 1122*s*, 1084*s*, 882*m*, 824*w*. ^{1}H-NMR (500 MHz, $CDCl_3$): see *Table 14*; additionally, 11.11 (br. *s*, NH); 7.67–7.64 (*m*, 4 arom. H); 7.40–7.29 (*m*, 6 arom. H); 6.39 (br. *s*, NH_2); 1.59, 1.54, 1.37, 1.32 (4*s*, 2 Me_2C); 1.06 (*s*, ^{t}Bu); 1.02–0.96 (*m*, $(Me_2CH)_3Si$). ^{13}C-NMR (125 MHz, $CDCl_3$): see *Table 15*; additionally, 135.63 (2*d*); 135.61 (2*d*); 132.40, 132.22 (2*s*); 129.96, 129.94 (2*d*); 127.77 (4*d*); 114.53, 113.53 (2*s*, 2 Me_2C); 27.52, 27.23, 25.47, 25.36 (4*q*, 2 Me_2C); 26.71 (*q*, Me_3C); 19.23 (*s*, Me_3C); 17.93, 17.91 (*q*, $(Me_2CH)_3Si$); 11.96 (*d*, $(Me_2CH)_3Si$). HR-MALDI-MS: 1060.465 ($[M+Na]^+$, $C_{53}H_{71}N_7NaO_{11}Si_2^+$; calc. 1060.465). Anal. calc. for $C_{53}H_{71}N_7O_{11}Si_2$ (1038.36): C 61.38, H 6.89, N 9.44; found: C 61.35, H 6.95, N 9.32.

2′,3′-O-*Isopropylidene-5′*-O-*(triisopropylsilyl)uridin-6-yl-(6 → 7′*-C*)-9-(5,6,7-trideoxy-2,3*-O-*isopropylidene-β*-D-ribo-*hept-6-ynofuranosyl)adenine* (**47**). Similarly to the preparation of **41**, treatment of **38** (209 mg, 0.37 mmol) with **46** [3] (100 mg, 0.32 mmol) gave **47** (184 mg, 76%). Light yellow solid. R_f ($CHCl_3$/MeOH 40:1) 0.13. M.p. 148–150°. $[\alpha]_D^{25} = +51.8$ ($c = 1.0$, $CHCl_3$). UV ($CHCl_3$): 265 (18400). IR ($CHCl_3$): 3411*w*, 3018*w*, 2943*m*, 2867*w*, 2230*w*, 1698*m*, 1653*w*, 1597*m*, 1433*w*, 1384*w*, 1330*w*, 1219*s*, 1217*s*, 1213*s*, 1157*w*, 1089*w*, 909*m*, 882*w*. ^{1}H-NMR (500 MHz, $CDCl_3$): see *Table 14*; additionally, 13.40 (br. *s*, NH); 6.93 (br. *s*, NH_2); 1.63, 1.54, 1.44, 1.40 (4*s*, 2 Me_2C); 1.02–0.97 (*m*, $(Me_2CH)_3Si$). ^{13}C-NMR (125 MHz, $CDCl_3$): see *Table 15*; additionally, 114.58, 113.43 (2*s*, 2 Me_2C); 27.40, 27.24, 25.64, 25.52 (4*q*, 2 Me_2C); 17.89 (*q*, $(Me_2CH)_3Si$); 11.92 (*d*, $(Me_2CH)_3Si$). MALDI-MS: 776.0 ($[M+Na]^+$, $C_{36}H_{51}N_7NaO_9Si^+$). Anal. calc. for $C_{36}H_{51}N_7O_9Si$ (753.93): C 57.35, H 6.82, N 13.00; found: C 57.34, H 6.85, N 13.00.

2′,3′-O-*Isopropylidene-5′*-O-*(triisopropylsilyl)uridin-6-yl-(6 → 7′*-C*)-8-[[(*tert-*butyl)diphenylsilyloxy]-methyl]-9-(5,6,7-trideoxy-2,3*-O-*isopropylidene-β*-D-ribo-*hept-6-ynofuranosyl)adenine* (**48**). Similarly to the preparation of **41**, treatment of **38** (107 mg, 0.19 mmol) with **37** (92 mg, 0.16 mmol) gave **48** (120 mg, 73%). White solid. R_f ($CHCl_3$/MeOH 20:1) 0.30. M.p. 181–183°. $[\alpha]_D^{25} = +21.9$ ($c = 1.0$, $CHCl_3$). UV ($CHCl_3$): 267 (7680). IR ($CHCl_3$): 3388*w*, 3010*w*, 2942*m*, 2866*m*, 2230*w*, 1696*s*, 1611*m*, 1499*m*, 1462*m*, 1427*s*, 1384*m*, 1157*w*, 1087*s*, 999*w*, 882*w*. ^{1}H-NMR (300 MHz, $CDCl_3$; assignments based on a HMBC spectrum): see *Table 14*; additionally, 12.93 (br. *s*, NH); 7.74–7.64 (*m*, 4 arom. H); 7.48–7.31 (*m*, 6 arom. H); 6.58 (br. *s*, NH_2); 1.63, 1.45 (2*s*, Me_2C/I); 1.59, 1.45 (2*s*, Me_2C/II); 1.09 (*s*, ^{t}Bu); 1.04–1.01 (*m*, $(Me_2CH)_3Si$). ^{13}C-NMR (75 MHz, $CDCl_3$; assignments based on a HMBC spectrum): see *Table 15*; additionally, 135.59 (2*d*); 135.52 (2*d*); 132.25 (2*s*); 129.89, 129.78 (2*d*); 127.73 (2*d*); 127.60 (2*d*); 114.09 (*s*, Me_2C/I); 113.28 (*s*, Me_2C/II); 27.64, 27.51, 25.99, 25.73 (4*q*, 2 Me_2C); 26.83 (*q*, Me_3C); 19.33 (*s*, Me_3C); 18.00 (*q*, $(Me_2CH)_3Si$); 12.02 (*d*, $(Me_2CH)_3Si$). MALDI-MS: 1060.5 ($[M+Na]^+$, $C_{53}H_{71}N_7NaO_{10}Si_2^+$). Anal. calc. for $C_{53}H_{71}N_7O_{10}Si_2$ (1022.36): C 62.27, H 7.00, N 9.59; found: C 62.39, H 7.00, N 9.43.

2′,3′-O-*Isopropylidene-5′*-O-*(triisopropylsilyl)adenosin-8-yl-(8 → 7′*-C*)-1-(6,7-dideoxy-2,3*-O-*isopropylidene-β*-D-allo-*hept-6-ynofuranosyl)uracil* (**51**). A soln. of **26** (200 mg, 0.35 mmol), **49** [2] (90 mg, 0.3 mmol), $[Pd_2(dba)_3]$ (13 mg, 0.016 mmol), CuI (6.6 mg, 0.031 mmol), and $P(fur)_3$ (6 mg, 0.023 mmol) in degassed Et_3N/toluene 1:1 (6 ml) was stirred for 16 h at 26°. Evaporation and FC ($CHCl_3$/MeOH 20:1) gave **51** (215 mg, 92%). Light-yellow solid. R_f ($CHCl_3$/MeOH 20:1) 0.09. M.p. 209–211°. $[\alpha]_D^{25} = +8.5$ ($c = 1.0$, $CHCl_3$). UV ($CHCl_3$): 268 (18600), 296 (20400). IR ($CHCl_3$): 3326*w*, 3199*w*, 3016*m*, 2944*m*, 2867*m*, 2210*w*, 1696*s*, 1602*w*, 1456*m*, 1384*m*, 1328*m*, 1271*m*, 1157*m*, 1092*s*, 880*m*, 808*w*. ^{1}H-NMR (300 MHz, (D_6)DMSO): see *Table 16*; additionally, 11.49 (br. *s*, NH); 7.62 (br. *s*, NH_2); 1.56, 1.54, 1.35 (3*s*, 2 Me_2C); 0.94 (br. *s*, $(Me_2CH)_3Si$). ^{13}C-NMR (75 MHz, $CDCl_3$/CD_3OD): see *Table 17*; additionally, 114.07, 113.50 (2*s*, 2 Me_2C); 26.88, 26.76, 25.02, 24.94 (4*q*, 2 Me_2C); 17.54, 17.52 (2*q*, $(Me_2CH)_3Si$); 11.65 (*d*, $(Me_2CH)_3Si$). MALDI-MS: 792.3 ($[M+Na]^+$, $C_{36}H_{51}N_7NaO_{10}Si^+$). Anal. calc. for $C_{36}H_{51}N_7O_{10}Si$ (769.93): C 56.16, H 6.68, N 12.73; found: C 56.23, H 6.70, N 12.66.

2′,3′-O-*Isopropylidene-5′*-O-*(triisopropylsilyl)adenosin-8-yl-(8 → 7′*-C*)-1-[6,7-dideoxy-2,3*-O-*isopropylidene-5-(triisopropylsilyl)-β*-D-allo-*hept-6-ynofuranosyl]uracil* (**52**). A soln. of **26** (58 mg, 0.1 mmol), **50** [2] (42 mg, 0.09 mmol), $[Pd_2(dba)_3]$ (4.1 mg, 0.0045 mmol), CuI (2 mg, 0.009 mmol), and $P(fur)_3$ (2 mg, 0.004 mmol) in degassed Et_3N/toluene 1:1 (3 ml) was stirred for 16 h at 26°. Evaporation and FC ($CHCl_3$/MeOH 80:1) gave **52** (72 mg, 86%). Light-yellow solid. R_f ($CHCl_3$/MeOH 50:1) 0.11. M.p. 145–147°. $[\alpha]_D^{25} = -70.5$ ($c = 1.0$, $CHCl_3$). UV ($CHCl_3$): 269 (15300), 297 (16000). IR ($CHCl_3$): 3409*w*, 3198*w*, 2946*s*, 2868*m*, 2250*w*, 1696*s*, 1633*s*, 1600*w*, 1461*m*, 1384*m*, 1327*m*, 1271*m*, 1157*m*, 1095*s*, 1014*w*, 997*w*, 882*m*, 809*w*. ^{1}H-NMR (300 MHz, $CDCl_3$): see *Table 18*; additionally, 11.25 (br. *s*, NH); 6.98 (br.

Table 16. *Selected ^{1}H-NMR Chemical Shifts* [ppm] *and Coupling Constants* [Hz] *of the A*[c_y]U$^{(*)}$ Dimers* **51**, **55**, *and* **60** *in (D$_6$)DMSO*

	51	**55**[a])	**60**[a])		**51**	**55**[a])	**60**[a])
Adenosine unit (II)				Uridine unit (I)			
H–C(2)	8.19	8.16	8.16	H–C(5)	5.67[b])	5.51	5.54
H–C(1′)	6.22	6.09	6.12	CH_a–C(6)	–	4.70	4.69
H–C(2′)	5.67	5.46	5.48	CH_b–C(6)	–	4.47	4.47
H–C(3′)	5.13	4.972	4.99	H–C(1′)	5.92	5.90	5.93
H–C(4′)	4.18	4.11	4.145	H–C(2′)	5.06	5.25	5.26
H_a–C(5′)	3.82	3.56	3.56	H–C(3′)	4.99	4.975	4.84
H_b–C(5′)	3.72	3.48	3.47	H–C(4′)	4.18	4.01	4.21
HO–C(5′)	–	5.26	5.27	H–C(5′)	4.85	4.67	3.02, 2.93
J(1′,2′)	1.8	3.6	3.3	HO–C(5′)	6.59	6.38	–
J(2′,3′)	6.5	6.0	6.3	*J*(H_a,H_b)	–	13.8	13.8
J(3′,4′)	3.1	2.7	2.7	*J*(1′,2′)	2.4	<1.5	<1.5
J(4′,5′a)	6.3	5.1	5.4	*J*(2′,3′)	6.2	6.3	6.6
J(4′,5′b)	7.2	5.7	5.7	*J*(3′,4′)	3.3	3.3	3.6
J(5′a,5′b)	10.6	11.1	11.7	*J*(4′,5′)	6.6	9.3	6.9, 7.2
J(5′a,OH)	–	6.0	5.4	*J*(5′,OH)	6.2	6.9	–
J(5′b,OH)	–	6.3	6.3				

[a]) Assignments based on selective homodecoupling experiments. [b]) δ(H–C(6)) = 7.82 ppm, *J*(5,6) = 8.1 Hz.

s, NH_2); 1.60, 1.57, 1.39, 1.37 (4*s*, 2 Me_2C); 1.12–1.15 (*m*, $(Me_2CH)_3Si$); 0.94–0.96 (*m*, $(Me_2CH)_3Si$). ^{13}C-NMR (75 MHz, $CDCl_3$): see *Table 17*; additionally, 114.10, 113.55 (2*s*, 2 Me_2*C*); 27.22, 27.12, 25.34, 25.27 (4*q*, 2 *Me*$_2$C); 18.07, 18.03, 17.93, 17.90 (4*q*, 2 (*Me*$_2$CH)$_3$Si); 12.41, 11.96 (2*d*, 2 (Me_2*C*H)$_3$Si). HR-MALDI-MS: 948.4636 ($[M+Na]^+$, $C_{45}H_{71}N_7NaO_{10}Si_2^+$; calc. 948.4699). Anal. calc. for $C_{45}H_{71}N_7O_{10}Si_2$ (926.27): C 58.35, H 7.73, N 10.59; found: C 58.18, H 7.59, N 10.44.

2′,3′-O-*Isopropylidene-5′*-O-*(triisopropylsilyl)adenosin-8-yl-(8 → 7′*-C*)-6-{[(*tert-*butyl)diphenylsilyl-oxy]methyl}-1-(6,7-dideoxy-2,3*-O-*isopropylidene-β*-D-allo-*hept-6-ynofuranosyl)uracil* (**53**). Similarly to the preparation of **51**, treatment of **26** (133 mg, 0.23 mmol) with **8** (115 mg, 0.20 mmol) gave **53** (184 mg, 89%). Light yellow solid. R_f ($CHCl_3$/MeOH 20:1) 0.26. M.p. 157–159°. $[\alpha]_D^{25} = -4.2$ ($c = 0.5$, $CHCl_3$). UV ($CHCl_3$): 295 (15300). IR ($CHCl_3$): 3410*w*, 3019*s*, 2944*m*, 2866*w*, 2220*w*, 1698*m*, 1633*m*, 1463*w*, 1384*m*, 1220*s*, 1215*s*, 1210*s*, 1105*m*, 878*w*. ^{1}H-NMR (500 MHz, $CDCl_3$): see *Table 18*; additionally, 11.60 (br. *s*, NH); 7.68–7.63 (*m*, 4 arom. H); 7.48–7.37 (*m*, 6 arom. H); 6.93 (br. *s*, NH_2); 1.62, 1.53, 1.44, 1.36 (4*s*, 2 Me_2C); 1.07 (*s*, ^{t}Bu); 0.96 (br. *s*, $(Me_2CH)_3Si$). ^{13}C-NMR (125 MHz, $CDCl_3$): see *Table 17*; additionally, 135.54 (2*d*); 135.53 (2*d*); 131.87, 131.83 (2*s*); 130.37, 130.33 (2*d*); 128.07 (2*d*); 128.01 (2*d*); 113.63 (*s*, 2 Me_2*C*); 27.44, 27.24, 25.56, 25.49 (4*q*, 2 *Me*$_2$C); 26.60 (*q*, *Me*$_3$C); 19.20 (*s*, Me_3*C*); 17.85 (*q*, $(Me_2CH)_3$-Si); 11.85 (*d*, $(Me_2CH)_3Si$). HR-MALDI-MS: 1060.465 ($[M+Na]^+$, $C_{53}H_{71}N_7NaO_{11}Si_2^+$; calc. 1060.465). Anal. calc. for $C_{53}H_{71}N_7O_{11}Si_2$ (1038.36): C 61.38, H 6.89, N 9.44; found: C 61.20, H 7.11, N 9.22.

2′,3′-O-*Isopropylidene-5′*-O-*[(*tert-*butyl)diphenylsilyl]adenosin-8-yl-(8 → 7′*-C*)-1-(6,7-dideoxy-2,3*-O-*isopropylidene-β*-D-allo-*hept-6-ynofuranosyl)uracil* (**54**). Similarly to the preparation of **51**, treatment of **25** (156 mg, 0.232 mmol) with **49** (61 mg, 0.2 mmol) gave **24** (153 mg, 90%). White solid. R_f ($CHCl_3$/MeOH 30:1) 0.13. M.p. 163–165°. $[\alpha]_D^{25} = +30.6$ ($c = 0.5$, $CHCl_3$). UV ($CHCl_3$): 267 (15200). IR ($CHCl_3$): 3396*w*, 3014*m*, 2260*w*, 1696*s*, 1634*m*, 1602*w*, 1455*w*, 1384*m*, 1328*m*, 1270*m*, 1157*w*, 1085*s*, 875*w*, 808*w*. ^{1}H-NMR (300 MHz, $CDCl_3$/CD_3OD): see *Table 18*; additionally, 7.55–7.45 (*m*, 4 arom. H); 7.35–7.17 (*m*, 6 arom. H); 1.585 (br., 6 H), 1.39, 1.35 (3*s*, 2 Me_2C); 0.96 (*s*, ^{t}Bu). ^{13}C-NMR (125 MHz, $CDCl_3$/CD_3OD): see *Table 17*; additionally, 135.25 (2*d*); 135.21 (2*d*); 129.48 (2*s*); 129.41 (2*d*); 127.41 (2*d*); 127.29 (2*d*); 114.25, 113.71 (*s*, 2 Me_2*C*); 27.20, 25.38 (2*q*, *Me*$_2$C); 26.73 (*q*, *Me*$_3$C); 19.18 (*s*, Me_3*C*). HR-MALDI-MS: 874.3187 ($[M+Na]^+$, $C_{43}H_{49}N_7NaO_{10}Si^+$; calc. 874.3310). Anal. calc. for $C_{43}H_{49}N_7O_{10}Si$ (851.99): C 60.62, H 5.80, N 11.51; found: C 60.83, H 5.94, N 11.34.

Table 17. *Selected* ^{13}*C-NMR Chemical Shifts* [ppm] *of the A*[c$_y$]U$^{(*)}$ Dimers* **52**, **53**, and **55**–**60** *in* $CDCl_3$, *and of* **51** *and* **54** *in* $CDCl_3/CD_3OD$ *10:1*

	51	**52**	**53**[a])	**54**	**55**[b])	**56**	**57**	**58**[a])	**59**	**60**[b])
Adenosine unit (II)										
C(2)	153.23	153.60	153.18	153.24	153.27	150.89	153.32	153.34	153.21	152.65
C(4)	148.16	148.44	148.44	148.22	147.03	148.87	148.57	148.46	148.20	147.66
C(5)	118.74	119.63	119.06	118.90	118.61	119.19	119.26	119.22	118.89	119.46
C(6)	155.05	155.67	155.31	155.18	154.77	155.53	155.70	155.66	155.53	155.79
C(8)	133.68	133.23	134.37	133.60	133.89	133.92	134.13	134.68	134.90	134.18
C(1′)	90.31	90.58	90.72	90.24	92.78	90.64	91.50	90.62	90.62	92.90
C(2′)	82.87	83.37	83.13	83.30	81.67	83.22	83.15	83.24	83.22	82.69
C(3′)	82.14	82.54	82.65	82.20	82.25	82.54	82.59	82.66	82.90	81.85
C(4′)	87.70	88.71	88.23	88.27	85.00	88.60	88.37	85.14	85.21	85.02
C(5′)	63.25	63.67	63.46	63.97	63.42	63.48	64.72	63.48	63.46	63.38
Uridine unit (I)										
C(2)	150.32	150.37	151.41	150.15	151.31	153.63	153.20[c])	150.80	151.62	152.36
C(4)	164.30	164.88	163.67	164.82	162.16	163.96	163.21	164.16	163.78	163.04
C(5)	102.03	102.30	102.61	101.65	102.82	102.69	102.54	102.75	101.97	102.89
C(6)	141.60	141.76	153.48	142.27	152.13	142.81	153.58[c])	142.97	153.21	152.74
CH_2–C(6)	–	–	62.41	–	62.54	–	62.10	–	63.46	62.32
C(1′)	93.15	95.24	91.34	93.95	89.96	94.40	92.32	95.44	91.04	91.65
C(2′)	84.19	85.13	83.74	84.46	83.97	83.99	84.31	84.63	84.88	85.56
C(3′)	80.25	82.54	80.79	80.37	80.13	80.78	82.17	82.14	82.73	83.46
C(4′)	88.39	89.98	88.80	88.47	87.34	88.90	90.57	88.64	88.70	85.76
C(5′)	62.02	64.12	63.05	62.50	63.19	63.20	63.41	24.58	24.16	24.66
C(6′)	94.25	93.60	94.46	94.10	93.94	95.54	94.56	93.48	93.55	94.30
C(7′)	74.10	75.37	74.65	74.73	74.44	74.43	74.53	71.62	71.84	71.57

[a]) Assignments based on a HSQC spectrum. [b]) Assignments based on a HMBC spectrum. [c]) Assignments may be interchanged.

X-Ray Analysis of **54**·*MeOH*[10]). Crystallisation of **54** from MeOH gave crystals of (**54**·MeOH)$_2$ suitable for X-ray analysis: $C_{88}H_{106}N_{14}O_{22}Si_2$ (1768.05); orthorhombic $P2_12_12_1$; $a=17.2059(2)$, $b=17.4366(2)$, $c=32.1057(7)$ Å. $V=9632.1(2)$ Å^3; $Z=4$; $D_{calc.}=1.219$ Mg/m^3. Intensities were measured on an *KCCD* diffractometer with MoK_α radiation (graphite monochromator, $\lambda=0.7107$ Å) at 233 K, Θ range 1.33–21.96°. Of the 11512 total collected reflections, 11512 independent reflections were observed. The crystals contain highly disordered molecules of MeOH. $R=0.0624$, $R_w=0.1611$. The structure was solved by direct methods and refined by full-matrix least-squares analysis (SHELXL-97 program) including an isotropic extinction correction. All heavy atoms were refined anisotropically, except C(4) of a Ph group. The position of the H-atoms is based on stereochemical considerations and refined isotropically.

2′,3′-O-*Isopropylideneadenosin-8-yl-(8 → 7′*-C*)-6-{[(*tert*-*butyl)diphenylsilyloxy]methyl}-1-(6,7-dideoxy-2,3*-O-*isopropylidene-β*-D-allo-*hept-6-ynofuranosyl)uracil* (**55**). Similarly to the preparation of **51**, treatment of **24** (53 mg, 0.12 mmol) with **8** (58 mg, 0.1 mmol) gave **55** (73 mg, 83%). Light yellow solid. R_f ($CHCl_3$/MeOH 20:1) 0.29. M.p. 158–160°. $[\alpha]_D^{25}=+161.5$ ($c=1.0$, $CHCl_3$). UV ($CHCl_3$): 270 (19300), 294 (19700), 306 (17200). IR ($CHCl_3$): 3417*w*, 3326*w*, 3215*w*, 2934*w*, 2861*w*, 2260*w*, 1712*s*, 1649*m*, 1455*w*, 1384*m*, 1332*m*, 1299*w*, 1155*w*, 1112*s*, 1082*s*, 998*w*, 878*w*. ^{1}H-NMR (300 MHz, $CDCl_3$; assignments based on a HMBC spectrum): see *Table 18*; additionally, 11.90 (br. *s*, NH); 7.62–7.56 (*m*, 4 arom. H); 7.46–7.31 (*m*, 6 arom. H); 1.72, 1.51 (2*s*, Me_2C/II); 1.53, 1.33 (2*s*, Me_2C/I); 1.02 (*s*, ^{t}Bu). ^{1}H-NMR (300 MHz, (D_6)DMSO): see *Table 16*; additionally, 11.57 (br. *s*, NH); 7.68–7.55 (*m*, 4 arom. H, NH_2); 7.52–7.46 (*m*, 6 arom. H); 1.51, 1.44, 1.29, 1.275 (4*s*, 2 Me_2C); 0.98 (*s*, ^{t}Bu). ^{13}C-NMR (75 MHz, $CDCl_3$; assignments based on a HMBC spectrum): see *Table 17*; additionally, 135.39 (2*d*);

Table 18. *Selected ^{1}H-NMR Chemical Shifts* [ppm] *and Coupling Constants* [Hz] *of the A*[c_y]U$^{(*)}$ Dimers* **52**, **53**, **55**–**60** *in $CDCl_3$, and* **54** *in $CDCl_3$/CD_3OD 10:1*[a])

	52	**53**[b])	**54**	**55**[c])[d])	**56**	**57**	**58**[b])	**59**	**60**[c])[e])
Adenosine unit (II)									
H–C(2)	8.29	8.13	8.04	7.99	8.31	8.20	8.30	8.21	8.30
H–C(1′)	6.16	6.32	6.24	6.29	6.29	6.32	6.30	6.32	6.24
H–C(2′)	5.62	5.76	5.62	5.84	5.71	5.73	5.74	5.79	5.27
H–C(3′)	5.14	5.19	5.15	5.09	5.19	5.20	5.21	5.22	5.05
H–C(4′)	4.26	4.30	4.36	4.57	4.31	4.31	4.33	4.37–4.29	4.50
H_a–C(5′)	3.80	3.82	3.76	3.95	3.78	3.78	3.81	3.74	3.96
H_b–C(5′)	3.69	3.67	3.64	3.77	3.68	3.66	3.68	3.61	3.76
J(1′,2′)	1.5	1.6	1.5	5.7	1.5	1.8	1.1	1.2	5.4
J(2′,3′)	6.3	6.2	6.0	5.4	6.3	6.3	6.1	6.0	5.7
J(3′,4′)	3.3	2.8	3.3	<1.0	3.0	3.0	2.9	3.0	<1.0
J(4′,5′a)	6.6	7.7	6.6	<1.0	7.2	7.8	7.4	7.8	<1.0
J(4′,5′b)	6.6	6.5	6.6	<1.0	6.6	6.6	6.6	6.6	<1.0
J(5′a,5′b)	10.5	10.1	10.5	12.6	10.2	10.5	10.2	10.2	12.6
Uridine unit (I)									
H–C(5)[f])	5.73	5.46	5.67	5.19	5.68	5.60	5.69	5.41	5.62
H–C(6)	7.79	–	7.68	–	7.54	–	7.46	–	–
CH_a–C(6)	–	4.58	–	4.46	–	4.63	–	4.68	4.60
CH_b–C(6)	–	4.34	–	4.11	–	4.44	–	4.42	4.40
H–C(1′)	5.87	5.97	5.87	5.97	5.85	6.04	5.67	6.01	5.98
H–C(2′)	5.00	5.31	4.95	5.28	5.07	5.31–5.25	5.17	5.35–5.29	5.33
H–C(3′)	4.94	5.22	5.08	4.94	5.12	5.31–5.25	5.05	5.35–5.29	5.33
H–C(4′)	4.56	4.30	4.47	4.15	4.47	4.46–4.41	4.43	4.37–4.29	4.35
H_a–C(5′)	5.02	4.94	4.92	4.77	4.95	5.03	3.10	3.14	3.06
H_b–C(5′)	–	–	–	–	–	–	3.06	3.06	2.99
HO–C(5′)	–	5.11[g])	–	5.34[g])	5.05[g])	4.46–4.41	–	–	–
J(5, 6)	8.1	–	8.1	–	8.1	–	8.1	–	–
J(H_a,H_b)	–	13.7	–	13.2	–	14.1	–	13.8	13.5
J(1′,2′)	1.8	1.0	2.1	<1.0	2.4	<1.0	<1.0	<1.0	1.5
J(2′,3′)	6.3	6.3	6.3	6.6	6.3	[h])	6.1	[h])	[h])
J(3′,4′)	2.4	4.8	3.0	6.0	3.3	[h])	4.2	[h])	<2.0
J(4′,5′a)	5.1	5.7	3.6	6.6	3.3	5.4	5.6	4.8	6.9
J(4′,5′b)	–	–	–	–	–	–	6.3	5.4	6.3

[a]) Assignments based on selective homodecoupling experiments. Concentration: 60 mM for **52**, **53**, and **57**–**59**, 50 mM for **55** and **60**, 30 mM for **56**, and 4 mM for **54**. [b]) Assignments based on a DQF-COSY and a HSQC spectrum. [c]) Assignments based on a HMBC spectrum. [d]) δ(HO–C(5/II)) = 6.77 ppm; *J*(5′a,OH) < 1.5, *J*(5′b,OH) = 11.4 Hz. [e]) δ(HO–C(5/II)) = 6.51 ppm; *J*(5′a,OH) < 1.5, *J*(5′b,OH) = 9.9 Hz. [f]) ^4J(5,NH) ≤ 1.5 Hz. [g]) br. *s*; *J*(5′,OH) not determined. [h]) Not determined.

135.30 (2*d*); 131.62, 131.50 (2*s*); 130.32, 130.21 (2*d*); 127.94 (2*d*); 127.88 (2*d*); 114.61 (*s*, Me_2C/I); 113.64 (*s*, Me_2C/II); 28.09, 27.64, 26.10, 25.63 (4*q*, 2 Me_2C); 26.61 (*q*, Me_3C); 19.24 (*s*, Me_3C). HR-MALDI-MS: 904.3352 ([*M* + Na]$^+$, $C_{44}H_{51}N_7NaO_{11}Si^+$; calc. 904.3314).

2′,3′-O-*Isopropylidene*-5′-O-*(triisopropylsilyl)adenosin-8-yl-(8 → 7′*-C)-*1-(6,7-dideoxy-2,3*-O-*isopropylidene*-α-L-talo-*hept-6-ynofuranosyl)uracil* (**56**). A soln. of **26** (200 mg, 0.35 mmol), **2** (90 mg, 0.3 mmol), [Pd_2(dba)$_3$] (13 mg, 0.016 mmol), CuI (6.6 mg, 0.031 mmol), and P(fur)$_3$ (6 mg, 0.023 mmol) in degassed Et_3N/toluene 1:1 (6 ml) was stirred for 18 h at 26°. Evaporation and FC ($CHCl_3$/MeOH 25:1) gave **56** (226 mg, 99%). Light-yellow solid. R_f ($CHCl_3$/MeOH 16:1) 0.23. M.p. 168–170°.

$[\alpha]_D^{25} = -27.6$ ($c = 1.0$, $CHCl_3$). UV ($CHCl_3$): 295 (13800). IR ($CHCl_3$): 3407*w*, 3017*s*, 2944*w*, 2867*w*, 2220*w*, 1697*s*, 1635*m*, 1600*w*, 1456*w*, 1384*m*, 1328*w*, 1270*w*, 1221*s*, 1209*s*, 1157*w*, 1087*m*, 930*w*, 881*w*, 809*w*. ^{1}H-NMR (300 MHz, $CDCl_3$): see *Table 18*; additionally, 11.71 (br. *s*, NH); 7.6–6.8 (br. *s*, NH_2); 1.60, 1.59, 1.40, 1.37 (4*s*, 2 Me_2C); 0.97–0.95 (*m*, $(Me_2CH)_3Si$). ^{13}C-NMR (75 MHz, $CDCl_3$): see *Table 17*; additionally, 114.58, 113.63 (2*s*, 2 Me_2C); 27.23, 25.44 (2*q*, 2 Me_2C); 17.93 (*q*, $(Me_2CH)_3Si$); 11.94 (*d*, $(Me_2CH)_3Si$). MALDI-MS: 792.3 ($[M+Na]^+$, $C_{36}H_{51}N_7NaO_{10}Si^+$). Anal. calc. for $C_{36}H_{51}N_7O_{10}Si$ (769.93): C 56.16, H 6.68, N 12.73; found: C 56.23, H 6.73, N 12.62.

2′,3′-O-*Isopropylidene-5′*-O-*(triisopropylsilyl)adenosin-8-yl-(8 → 7′-C)-6-{[(*tert-*butyl)diphenylsilyloxy]methyl}-1-(6,7-dideoxy-2,3*-O-*isopropylidene-α*-L-talo-*hept-6-ynofuranosyl)uracil* (**57**). Similarly to the preparation of **51**, treatment of **26** (231 mg, 0.4 mmol) with **10** (200 mg, 0.346 mmol) gave **57** (348 mg, 98%). Light yellow solid. R_f ($CHCl_3$/MeOH 50:1) 0.30. M.p. 169–171°. $[\alpha]_D^{25} = -119.0$ ($c = 1.0$, $CHCl_3$). UV ($CHCl_3$): 295 (15200). IR ($CHCl_3$): 3381*w*, 3199*w*, 3018*m*, 2944*w*, 2866*w*, 2220*w*, 1699*s*, 1654*w*, 1463*w*, 1384*m*, 1328*w*, 1299*w*, 1222*s*, 1216*s*, 1212*s*, 1158*w*, 1113*m*, 877*w*. ^{1}H-NMR (300 MHz, $CDCl_3$): see *Table 18*; additionally, 12.03 (br. *s*, NH); 7.70–7.60 (*m*, 4 arom. H); 7.50–7.33 (*m*, 6 arom. H); 1.62, 1.50, 1.41, 1.35 (4*s*, 2 Me_2C); 1.07 (*s*, ^{t}Bu); 0.96 (br. *s*, $(Me_2CH)_3Si$). ^{13}C-NMR (75 MHz, $CDCl_3$): see *Table 17*; additionally, 135.50 (2*d*); 135.39 (2*d*); 131.76 (2*s*); 130.30, 130.23 (2*d*); 128.03 (2*d*); 127.93 (2*d*); 114.00, 113.61 (2*s*, 2 Me_2C); 27.15, 25.40 (2*q*, 2 Me_2C); 26.55 (*q*, Me_3C); 19.16 (*s*, Me_3C); 17.82 (*q*, $(Me_2CH)_3Si$); 11.81 (*d*, $(Me_2CH)_3Si$). HR-MALDI-MS: 1060.460 ($[M+Na]^+$, $C_{53}H_{71}N_7NaO_{11}Si_2^+$; calc. 1060.465). Anal. calc. for $C_{53}H_{71}N_7O_{11}Si_2$ (1038.36): C 61.38, H 6.89, N 9.44; found: C 61.31, H 6.94, N 9.47.

2′,3′-O-*Isopropylidene-5′*-O-*(triisopropylsilyl)adenosin-8-yl-(8 → 7′*-C*)-1-(5,6,7-trideoxy-2,3*-O-*isopropylidene-β*-D-ribo-*hept-6-ynofuranosyl)uracil* (**58**). Similarly to the preparation of **51**, treatment of **26** (200 mg, 0.348 mmol) with **6** (87 mg, 0.3 mmol) gave **58** (209 mg, 91%). Light-yellow solid. R_f ($CHCl_3$/MeOH 20:1) 0.30. M.p. 152–154°. $[\alpha]_D^{25} = -62.2$ ($c = 2.0$, $CHCl_3$). UV ($CHCl_3$): 293 (16000). IR ($CHCl_3$): 3409*w*, 3199*w*, 3017*m*, 2974*m*, 2944*m*, 2867*w*, 2245*w*, 1697*s*, 1633*m*, 1602*w*, 1455*w*, 1384*m*, 1328*w*, 1221*s*, 1217*s*, 1213*s*, 1209*s*, 1157*w*, 1090*m*, 880*w*, 808*w*. ^{1}H-NMR (500 MHz, $CDCl_3$): see *Table 18*; additionally, 11.86 (br. *s*, NH); 7.34 (br. *s*, NH_2); 1.62, 1.58, 1.42, 1.38 (4*s*, 2 Me_2C); 0.96 (br. *s*, $(Me_2CH)_3Si$). ^{13}C-NMR (125 MHz, $CDCl_3$): see *Table 17*; additionally, 114.47, 113.55 (2*s*, 2 Me_2C); 27.40, 27.10, 25.50, 25.33 (4*q*, 2 Me_2C); 17.78, 17.76 (2*q*, $(Me_2CH)_3Si$); 11.80 (*d*, $(Me_2CH)_3Si$). HR-MALDI-MS: 776.3421 ($[M+Na]^+$, $C_{36}H_{51}N_7NaO_9Si^+$; calc. 776.3415). Anal. calc. for $C_{36}H_{51}N_7O_9Si$ (753.93): C 57.35, H 6.82, N 13.00; found: C 57.27, H 6.80, N 12.96.

2′,3′-O-*Isopropylidene-5′*-O-*(triisopropylsilyl)adenosin-8-yl-(8 → 7′*-C*)-6-{[(*tert-*butyl)diphenylsilyloxy]methyl}-1-(5,6,7-trideoxy-2,3*-O-*isopropylidene-β*-D-ribo-*hept-6-ynofuranosyl)uracil* (**59**). Similarly to the preparation of **51**, treatment of **26** (136 mg, 0.23 mmol) with **18** (106 mg, 0.184 mmol) gave **59** (150 mg, 80%). Light yellow solid. R_f ($CHCl_3$/MeOH 30:1) 0.26. M.p. 136–138°. $[\alpha]_D^{25} = -81.9$ ($c = 2.0$, $CHCl_3$). UV ($CHCl_3$): 292 (9980). IR ($CHCl_3$): 3410*w*, 3196*w*, 3017*m*, 2943*m*, 2866*w*, 2244*w*, 1700*m*, 1651*m*, 1602*w*, 1463*w*, 1428*w*, 1384*m*, 1329*w*, 1298*w*, 1261*w*, 1217*s*, 1211*s*, 1157*w*, 1093*m*, 879*w*. ^{1}H-NMR (300 MHz, $CDCl_3$): see *Table 18*; additionally, 12.50 (br. *s*, NH); 7.71–7.66 (*m*, 4 arom. H); 7.49–7.37 (*m*, 6 arom. H); 1.64, 1.54, 1.44, 1.36 (4*s*, 2 Me_2C); 1.09 (*s*, ^{t}Bu); 0.94 (br. *s*, $(Me_2CH)_3Si$). ^{13}C-NMR (75 MHz, $CDCl_3$): see *Table 17*; additionally, 135.37 (4*d*); 131.84, 131.76 (2*s*); 130.17 (2*d*); 127.94 (2*d*); 127.86 (2*d*); 113.66, 113.32 (2*s*, 2 Me_2C); 27.40, 27.27, 25.54 (2 C) (3*q*, 2 Me_2C); 26.64 (*q*, Me_3C); 19.29 (*s*, Me_3C); 17.90 (*q*, $(Me_2CH)_3Si$); 11.91 (*d*, $(Me_2CH)_3Si$). HR-MALDI-MS: 1044.471 ($[M+Na]^+$, $C_{53}H_{71}N_7NaO_{10}Si_2^+$; calc. 1044.470). Anal. calc. for $C_{53}H_{71}N_7O_{10}Si_2$ (1022.36): C 62.27, H 7.00, N 9.59; found: C 62.24, H 6.88, N 9.70.

2′,3′-O-*Isopropylideneadenosin-8-yl-(8 → 7′*-C*)-6-{[(*tert-*butyl)diphenylsilyloxy]methyl}-1-(5,6,7-trideoxy-2,3*-O-*isopropylidene-β*-D-ribo-*hept-6-ynofuranosyl)uracil* (**60**). Similarly to the preparation of **51**, treatment of **24** (25 mg, 0.055 mmol) with **18** (26 mg, 0.046 mmol) gave **60** (32 mg, 80%). Light yellow solid. R_f ($CHCl_3$/MeOH 20:1) 0.36. M.p. 184–186°. $[\alpha]_D^{25} = -154.7$ ($c = 1.0$, $CHCl_3$). UV ($CHCl_3$): 270 (15100), 293 (16400), 304 (11600). IR ($CHCl_3$): 3325*w*, 3193*w*, 3013*m*, 2934*m*, 2861*w*, 2245*w*, 1702*s*, 1658*m*, 1633*m*, 1454*w*, 1384*m*, 1331*m*, 1231*w*, 1156*w*, 1112*s*, 1084*s*, 998*w*, 880*w*. ^{1}H-NMR (300 MHz, $CDCl_3$; assignments based on a HMBC spectrum): see *Table 18*; additionally, 12.80 (br. *s*, NH); 7.87 (br. *s*, NH_2); 7.71–7.64 (*m*, 4 arom. H); 7.52–7.37 (*m*, 6 arom. H); 1.66, 1.39 (2*s*, Me_2C/II); 1.51, 1.36 (2*s*, Me_2C/I); 1.08 (*s*, ^{t}Bu). ^{1}H-NMR (300 MHz, (D_6)DMSO): see *Table 16*; additionally, 11.56 (br. *s*,

NH); 7.70–7.60 (*m*, 4 arom. H); 7.58 (br. *s*, NH_2); 7.50–7.39 (*m*, 6 arom. H); 1.52, 1.445, 1.29 (6 H) (3*s*, 2 Me_2C); 1.01 (*s*, ^{t}Bu). ^{13}C-NMR (75 MHz, $CDCl_3$; assignments based on a HMBC spectrum): see *Table 17*; additionally, 135.39 (4*d*); 131.75 (2*s*); 130.19 (2*d*); 127.95 (2*d*); 127.87 (2*d*); 113.64 (*s*, Me_2C/II); 113.38 (*s*, Me_2C/I); 27.91, 27.32, 25.73, 25.60 (4*q*, 2 Me_2C); 26.66 (*q*, Me_3C); 19.30 (*s*, Me_3C). HR-MALDI-MS: 888.3334 ($[M+Na]^+$, $C_{44}H_{51}N_7NaO_{10}Si^+$; calc. 888.3364).

REFERENCES

[1] S. Eppacher, P. K. Bhardwaj, B. Bernet, J. L. B. Gala, T. Knöpfel, A. Vasella, *Helv. Chim. Acta* **2004**, *87*, 2969.
[2] S. Eppacher, N. Solladié, B. Bernet, A. Vasella, *Helv. Chim. Acta* **2000**, *83*, 1311.
[3] H. Gunji, A. Vasella, *Helv. Chim. Acta* **2000**, *83*, 2975.
[4] H. Gunji, A. Vasella, *Helv. Chim. Acta* **2000**, *83*, 3229.
[5] S. Eppacher, N. Solladié, A. Vasella, *Helv. Chim. Acta* **2004**, *87*, 2926.
[6] P. K. Bhardwaj, A. Vasella, *Helv. Chim. Acta* **2002**, *85*, 699.
[7] H. Gunji, A. Vasella, *Helv. Chim. Acta* **2000**, *83*, 1331.
[8] A. Vasella, *Chimia* **2005**, *59*, 785.
[9] A. J. Matthews, P. K. Bhardwaj, A. Vasella, *Chem. Commun.* **2003**, 950; A. J. Matthews, P. K. Bhardwaj, A. Vasella, *Helv. Chim. Acta* **2004**, *87*, 2273.
[10] D. H. R. Barton, S. W. McCombie, *J. Chem. Soc., Perkin Trans. 1* **1975**, 1574.
[11] P. A. Levene, R. S. Tipson, *J. Biol. Chem.* **1934**, *106*, 113.
[12] A. S. Pilcher, P. Desong, *J. Org. Chem.* **1993**, *58*, 5130.
[13] A. R. Maguire, W. Meng, S. M. Roberts, A. J. Willetts, *J. Chem. Soc., Perkin Trans. 1* **1993**, 1795.
[14] D. E. Frantz, R. Fässler, E. M. Carreira, *J. Am. Chem. Soc.* **2000**, *122*, 1806.
[15] S. Chladek, J. Smrt, *Collect. Czech. Chem. Commun.* **1964**, *29*, 214.
[16] S. Fuji, T. Fujiwara, K. Tomita, *Nucleic Acids Res.* **1976**, *3*, 1985.
[17] B. Bernet, A. Vasella, *Helv. Chim. Acta* **2000**, *83*, 995; B. Bernet, A. Vasella, *Helv. Chim. Acta* **2000**, *83*, 2055.
[18] O. F. Schall, G. W. Gokel, *J. Am. Chem. Soc.* **1994**, *116*, 6089.
[19] K. Pervushin, A. Ono, C. Fernández, T. Szyperski, M. Kainosho, K. Wüthrich, *Proc. Natl. Acad. Sci. U. S. A.* **1998**, *95*, 14147.
[20] A. Dunger, H. H. Limbach, K. Weisz, *J. Am. Chem. Soc.* **2000**, *122*, 10109.
[21] S. Nakano, Y. Uotani, K. Uenishi, M. Fujii, N. Sugimoto, *Nucleic Acids Res.* **2005**, *33*, 7111.
[22] K. J. Fettes, N. Howard, D. T. Hickman, S. Adah, M. R. Player, P. F. Torrence, J. Micklefield, *J. Chem. Soc., Perkin Trans 1* **2002**, 485.
[23] P. S. Miller, K. N. Fang, N. S. Kondo, P. O. P. Ts'o, *J. Am. Chem. Soc.* **1971**, *93*, 6657.
[24] C. R. Cantor, M. M. Warshaw, H. Shapiro, *Biopolymers* **1970**, *9*, 1059.
[25] J. S. Chen, R. B. Shirts, *J. Phys. Chem.* **1985**, *89*, 1643.
[26] B. Peterson, Ph.D. Thesis, University of California at Los Angeles, 1994.
[27] J. D. Dunitz, *Chem. Biol.* **1995**, *2*, 709.
[28] E. Grunwald, L. L. Comeford, *Protein-Solvent Interact.* **1995**, 421.
[29] Y. Inoue, Y. Liu, L. H. Tong, B. J. Shen, D. S. Jin, *J. Am. Chem. Soc.* **1993**, *115*, 10637.
[30] E. A. Meyer, R. K. Castellano, F. Diederich, *Angew. Chem., Int. Ed.* **2003**, *115*, 1244.
[31] E. Grunwald, C. Steel, *J. Am. Chem. Soc.* **1995**, *117*, 5687.
[32] M. S. Searle, M. S. Westwell, D. H. Williams, *J. Chem. Soc., Perkin Trans. 2* **1995**, 141.
[33] G. A. Weiland, K. P. Minneman, P. B. Molinoff, *Nature* **1979**, *281*, 114.
[34] M. S. Searle, D. H. Williams, *Nucleic Acids Res.* **1993**, *21*, 2051.
[35] K. N. Houk, A. G. Leach, S. P. Kim, X. Y. Zhang, *Angew. Chem., Int. Ed.* **2003**, *42*, 4872.
[36] F. Mohamadi, N. G. J. Richards, W. C. Guida, R. Liskamp, C. Caufield, M. Lipton, G. Chang, T. Hendrickson, W. C. Still, *J. Comput. Chem.* **1990**, *11*, 440.
[37] N. Foloppe, B. Hartmann, L. Nilsson, A. D. MacKerell Jr., *Biophys. J.* **2002**, *82*, 1554.
[38] S. N. Rao, V. Sasisekharan, *Int. J. Biol. Macromol.* **1983**, *5*, 83.

[39] D. L. Miles, D. W. Miles, H. Eyring, *Biochim. Biophys. Acta* **1978**, *518*, 17; D. L. Miles, D. W. Miles, P. Redington, H. Eyring, *Proc. Natl. Acad. Sci. U. S. A.* **1976**, *73*, 4257.
[40] K. S. Vijayaiakshmi, N. Yathindra, *Biochim. Biophys. Acta* **1980**, *607*, 171.
[41] M. Goto, H. Kanno, E. Sugaya, Y. Osa, H. Takayangi, *X-Ray Struct. Anal. Online* **2004**, *20*, x39; T. Ma, S. B. Pai, Y. L. Zhu, J. S. Lin, K. Shanmuganathan, J. Du, C. Wang, H. Kim, M. G. Newton, Y. C. Cheng, C. K. Chu, *J. Med. Chem.* **1996**, *39*, 2835; G. R. Revankar, N. B. Hanna, K. Ramasamy, S. B. Larson, D. F. Smee, R. A. Finch, T. L. Avery, R. K. Robins, *J. Heterocycl. Chem.* **1990**, *27*, 909; C. Tamura, M. Yoshikawa, S. Sato, T. Hata, *Chem. Lett.* **1973**, *11*, 1221; A. R. I. Munns, P. Tollin, H. R. Wilson, D. W. Young, *Acta Crystallogr., Sect. B* **1970**, *26*, 1114.
[42] A. Kumar, R. T. Walker, *Tetrahedron* **1990**, *46*, 3101; R. N. Hunston, M. Jehangir, A. S. Jones, R. T. Walker, *Tetrahedron* **1980**, *36*, 2337.
[43] M. J. Camarasa, P. Fernández-Resa, M. T. Garcia-López, F. G. De las Heras, P. P. Méndez-Castrillón, B. Alarcón, L. Carrasco, *J. Med. Chem.* **1985**, *28*, 40.
[44] C. Crey-Desbiolles, D.-R. Ahn, C. J. Leumann, *Nucleic Acids Res.* **2005**, *33*, e77.
[45] R. E. A. Kelly, Y. J. Lee, L. N. Kantorovich, *J. Phys. Chem. B* **2005**, *109*, 11933.
[46] N. B. Leontis, E. Westhof, *RNA* **2001**, *7*, 499.

Received August 18, 2006